Earth-Science Reviews 235 (2022) 104239

Contents lists available at ScienceDirect

Earth-Science Reviews

journal homepage: www.elsevier.com/locate/earscirev

Review Article

Review of satellite radar interferometry for subsidence analysis

Federico Raspini *, Francesco Caleca, Matteo Del Soldato, Davide Festa, Pierluigi Confuorto, Silvia Bianchini

Earth Sciences Department of the University of Firenze – DST UNIFI, Via Giorgio La Pira n.4, Firenze, Italy

ARTICLE INFO

Keywords:
Subsidence
SAR
DInSAR
Mapping
Monitoring
Characterization
Modeling

ABSTRACT

This paper includes a critical review of the existing literature on the use of satellite SAR imagery for subsidence analysis. Land subsidence, related to multiple natural and human-induced processes, is observed globally in an increasing number of areas. Potentially leading to severe impacts on economics and the environment, subsidence has attracted growing scientific attention and, over the last decades, new tools and methods have been developed for accurately measuring the spatial and temporal evolution of surface deformations associated with subsidence phenomena. The collection of the existing scientific literature on the satellite InSAR for subsidence analysis was conducted in January 2022 exploiting the WoS's freely accessible web search engine. An extensive database of 1059 scientific contributions was compiled, covering the period 1997–2021. The content of each record in the literature database has been critically examined to collect and store information regarding the study area location, microwave band adopted, satellite used, processing approach, subsidence cause, application type, field evidence and strategies to validate and compare InSAR data.

Analysis of temporal distribution revealed a substantial growth in scientific production and an increasing interest of geoscientists, with a mean value of 21 articles per year from 1997 to 2014, rising to about 100 articles per year between 2015 and 2021. All continents include at least a study area, with Asia and Europe having the largest number of case studies, with 586 and 281 analyses in their territory, respectively, and revealing a clear geographical bias in subsidence study locations. Graphical visualizations and syntheses of current applications are presented. The large availability of different acquisition bands, the increasing imaging capabilities, refinement of processing approaches, and growing expertise in data interpretation allowed InSAR data to be used at different scales of analysis, for different purposes and subsidence types, in a wide range of physiographic settings.

This review highlights that satellite InSAR has moved from being a niche topic to an operative tool with a major role in subsidence studies. Despite more than 25 years of progress and advancements, technical and operational challenges remain to be faced. Leveraging on the analysis of the literature review and authors' experience, recommendations and perspectives are provided for a more effective use of InSAR data.

Abbreviation: A-DInSAR, Differential Synthetic Aperture Radar Interferometry; ASI, Italian Space Agency; CALM, Circumpolar Active-Layer Monitoring; CONAE, *Comision Nacional de Actividades Espaciales of Argentina*; CPT, Coherent Pixel Technique; CSK SG, COSMO-SkyMed Second Generation; DEM, Digital Elevation Models; ECMWF, European Centre for Medium-Range Weather Forecasts; EGMS, European Ground Motion Service; EO, Earth Observation; ESA, European Space Agency; ETM, Enhanced Thematic Mapper; FEM, Finite Element Models; GEE, Google Earth Engine; GEOS-ATSA, Advance Time Series Analysis of GEOS Department - University of New South Wales; GEP, Geohazard Exploitation Platform; GNSS, Global Navigation Satellite System; GPD, Gross Domestic Product; G-POD, Grid-Processing On Demand; GPR, Ground Penetrating Radar; GPS, Global Positioning System; GRACE, Gravity Recovery and Climate Experiment; InSAR, Synthetic Aperture Radar Interferometry; IPTA, Interferometric Point Target Analysis; JAXA, Japan Aerospace Exploration Agency; KARI, Korea Aerospace Research Institute; LiDAR, Light Detection And Ranging; LOS, Lin Of Sight; MERIS, Medium Resolution Imaging Spectrometer; MODIS, Moderate Resolution Imaging Spectroradiometer; MT-InSAR, Multi-Temporal Synthetic Aperture Radar Interferometry; PSI, Persistent Scatterers Interferometry; PSIC, Persistent Scatterer Interferometry Codes Cross Comparison and Certification; PSInSAR, Permanent Scatterer Synthetic Aperture Radar Interferometry; PSP-DIFSAR, Persistent Scatterer Pairs Differential Synthetic Aperture Radar Interferometry; SAR, Synthetic Aperture Radar; SBAS, Small BAseline Subset; SNAP, Sentinel Application Platform; StaMPS, Stanford Method for Persistent Scatterers; TWS, Terrestrial Water Storage; UAV, Unmanned Aerial Vehicle; WoS, Web of Science.

* Corresponding author.
E-mail address: federico.raspini@unifi.it (F. Raspini).

https://doi.org/10.1016/j.earscirev.2022.104239
Received 8 August 2022; Received in revised form 27 October 2022; Accepted 27 October 2022
Available online 2 November 2022
0012-8252/

1. Introduction

Land subsidence is defined as a downward vertical movement of the Earth's surface referred to both as a slow and graduate lowering and sudden sinking of the ground. Subsidence can be caused by single or multiple natural or anthropogenic triggering processes or by a combination of both. Overall, natural subsidence is generally caused by geological factors that account for tectonic motions and compaction of sedimentary deposits under the pressure of overlying sediments.

Subsidence induced and/or accelerated by anthropogenic causes mainly results from the extraction of natural resources like groundwater, salt, oil or gas from a basin, an aquifer or a subsurface reservoir faster than the natural or artificial recharge can replace them (Galloway and Burbey, 2011) or from land reclamation. In recent decades, natural compaction processes of normally consolidated fine-grained sediments have been locally aggravated by loading human action (Solari et al., 2016), especially where soft clay or organic soils are present, reaching magnitudes greater than those of natural origin. Ground subsidence also results from underground mining activity, usually referred to as "mine subsidence" (Gueguen et al., 2009).

Considerable ground displacements have been reported in several cities around the world, such as Morelia in Mexico (Cigna et al., 2012), Rome in Italy (Stramondo et al., 2008), coastal mega-cities in Asia such as Bangkok in Thailandia (Aobpaet et al., 2013), Ho Chi Minh City in Vietnam (Minh et al., 2015) and Shanghai in China (Liu et al., 2008) or New Orleans in the USA (Dixon et al., 2006).

Impacts of ground subsidence should be accounted for both long- and short-time scales. Natural subsidence is estimated to be a few millimetres per year; therefore, its consequences are relatively modest, occurring mostly in a very long time. Even when subsidence rates are slow, the cumulative effect over decades may dramatically increase the exposure of populations to flooding in alluvial areas and coastal lowlands, especially when combined with sea-level rise (Melet et al., 2021) and extreme weather events (windstorms, heavy rainfall and related river discharges). Conversely, subsidence due to anthropogenic factors can reach values from ten to over a hundred times higher than the natural subsiding phenomenon and its effects are manifested in a relatively short time. High-magnitude subsidence can have an impact on the natural environment (increased susceptibility to flooding, seawater intrusion, ground fissuring) and can determine serious consequences on human activities with structural damage to underground utility and linear infrastructures, settlements of buildings and flood-control structures.

Land subsidence is observed worldwide and, as a global, ubiquitous, and long-standing geological problem, it has attracted scientific attention. A global model recently proposed by Herrera-García et al. (2021) indicates that potential subsidence threatens 12 million km^2 (8%) of the Earth surface with a probability greater than 50% (medium-high to very high). Focusing only on areas where the potential subsidence probability is high or very high, subsidence model indicates a potentially threatened area of 2.2 million km^2, with 1.2 billion inhabitants (19% of the global population) and an exposed GDP of US$ 8.19 trillion.

Many studies all over the world pay attention to the causes of land subsidence, monitoring techniques, disaster assessments, and governance measures. Given the distribution of land subsidence worldwide and its severe consequence on the environment and economy, land subsidence has been one of the challenging topics needing research and technology transfer and further investigation and monitoring at the international level (Hu et al., 2004). Historically, land subsidence has been monitored by using different *in situ* methodologies such as high-precision geometric leveling, extensometers, GNSS or GPS networks, which permit the retrieval of accurate measures on specific benchmarks. These techniques require intensive time-consuming fieldwork and merely provide spatially limited point measurements of deformation.

More recently, satellite InSAR techniques rapidly developed and became a useful well-established EO approach to detect and monitor slow-moving ground displacements, *e.g.*, subsidence, thanks to millimetre accuracy, wide-area coverage, frequent data sampling, the possibility of tracking the history of deformations, and the higher benefit/cost ratio with respect of targeted ground-based monitoring campaigns. The key role and success of EO techniques for the investigation of geohazards are tackled in recent scientific research papers, *e.g.*, Tomás and Li (2017), and Cigna (2018).

Satellite EO gave a meaningful contribution to subsidence monitoring. The last 25 years have witnessed large exploitation of satellite InSAR data for subsidence investigations. Some papers well highlight the effectiveness of interferometric technologies for monitoring land subsidence (Raucoules et al., 2007; Wang and Sun, 2014) and underline the benefits deriving from their synergic use with *in situ* conventional technologies. Reviews on ground subsidence analyses have been produced at the national level: Solari et al. (2018) summarized the subsidence phenomenon analysed with InSAR methods in Italy, Tomás et al. (2014) reviewed ground subsidence case studies in Spain, Maleki and McKenzie (2021) presented a review on conventional and satellite-based methods for monitoring land subsidence in the USA and Suresh and Yarrakula (2018) for the coal mining scenario in India.

This review's contribution aims to illustrate the role of satellite radar interferometry for subsidence analysis at a global level over the last 25 years, by highlighting current applications and future perspectives. Subsidence as considered in this paper refers to the hydro-geological facet of the phenomenon caused by different processes such as natural terrain compaction, settlement of compressible soils, thaw subsidence due to permafrost warming, fluid withdrawal (*e.g.*, petroleum and groundwater pumping or geothermal exploitation), mining activities, land reclamation, load imposition, urban sprawl and engineering constructions. This review considers neither subsidence referred to pure tectonics movements, volcanic deformations (*e.g.*, due to magma and lava flow, pyroclastic flow, magma cooling), or induced by seismic activity.

This review encompasses all the possible scientific contributions, gathered by means of the freely accessible web search engine WoS's (Clarivate, 2019), presenting research studies on subsidence using satellite radar interferometric techniques. It is worth highlighting that this paper is neither intended to focus on technical aspects of satellite radar imagery elaboration nor to list advantages and limitations of different processing approaches.

Overall, this work offers an unprecedented systematic overview on the contribution of satellite InSAR technologies to subsidence analysis and investigation over time and at global scale.

2. Satellite radar interferometry

Satellite InSAR is a well-known and widely implemented technique capable of providing precise measurements of displacements occurring on the Earth's surface. The basic principle of InSAR is the exploitation of the phase difference of at least two complex SAR images acquired from different orbit positions and/or different times (Bamler and Hartl, 1998). Approaches based on the combination of two images (*i.e.*, DInSAR) were firstly oriented towards the detection and the analysis of single or short-lasting events, such as earthquakes (Massonnet and Feigl, 1995; Massonnet et al., 1993; Peltzer and Rosen, 1995) and volcanic eruptions/deformations (Briole et al., 1997; Lanari et al., 1998; Massonnet and Feigl, 1995). DInSAR approaches were also used for the detection and mapping of subsidence-induced displacements in mining areas (Massonnet and Feigl, 1998; Raymond and Rudant, 1997) or by groundwater extraction (Galloway et al., 1998; Hoffmann et al., 2003). However, conventional DInSAR may have constraints when discriminating between the effects of displacement and atmospheric signature, and it can be strongly affected by temporal and geometrical decorrelations.

To overcome these limitations, MT-InSAR techniques have been developed. Also known as PSI according to Crosetto et al. (2016) or A-

DInSAR (Herrera et al., 2007), such a family of algorithms uses large stacks of SAR images collected with the same sensor under the same geometry, allowing the removal of the phase contributions non-related to the displacement. In this way, multiple interferograms are generated, enhancing the use of long-time series of displacements.

In the last decade, several MT-InSAR approaches have been developed (Fig. 1). Two classes of multi-interferometric processing techniques - firstly, the PSInSAR (Ferretti et al., 2001) and secondly the SBAS technique (Berardino et al., 2002) - are used for processing long sequences of SAR imagery. The first is a pioneering approach that exploits

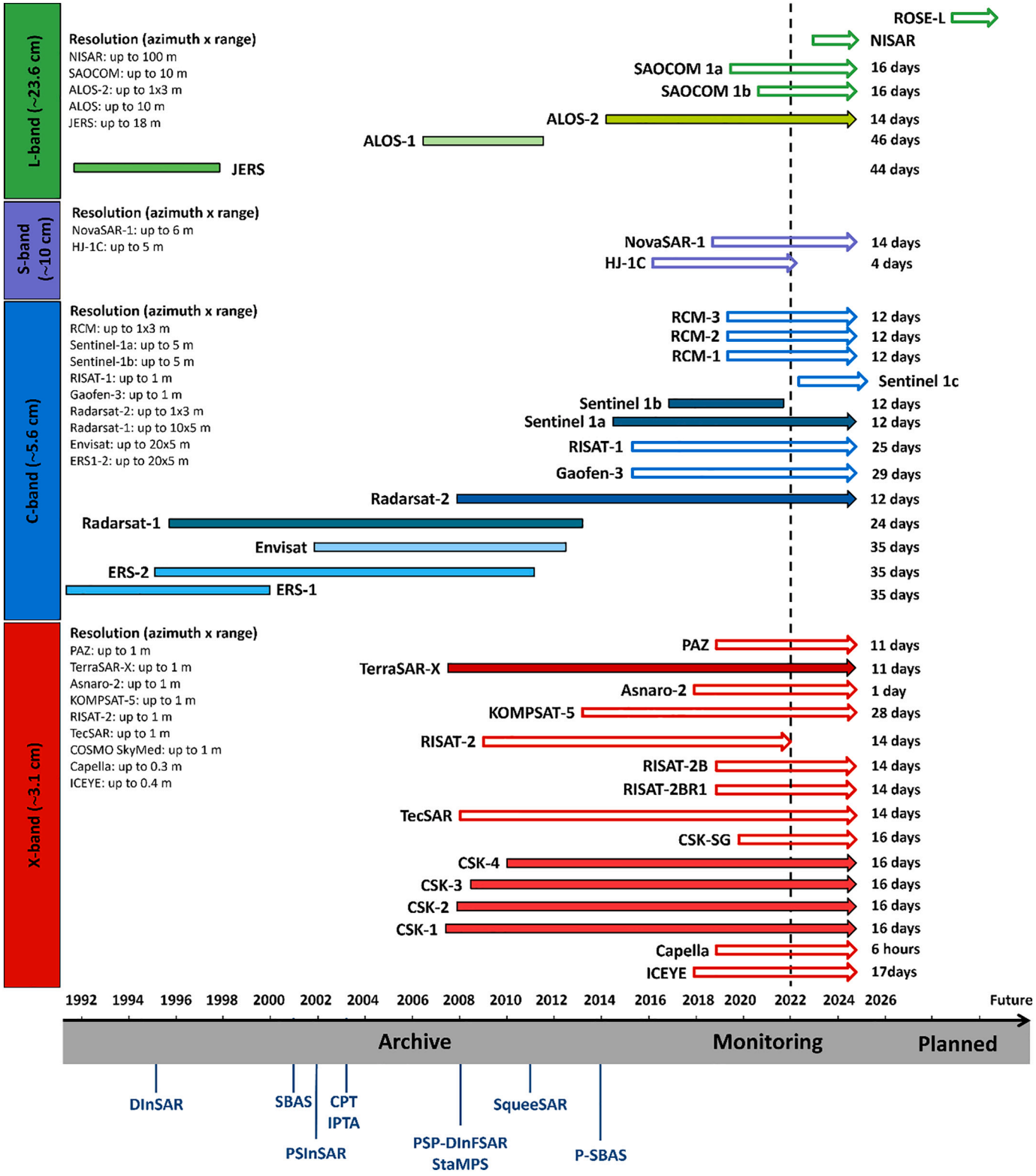

Fig. 1. Characteristics of past, present and future SAR satellites and constellations suitable for interferometric applications, grouped by the acquisition band. Timeline of some of the most significant processing approach is also included. Solid fill indicates satellite platforms that have been adopted for subsidence analysis within the collected database (1997–2021).

the concept of the permanent scatterers, *i.e.*, high coherence targets on the ground, overcoming the temporal and the geometrical decorrelation and estimating the deformation. The second is also a seminal algorithm, which uses reduced baselines (either spatial or temporal) to limit the decorrelation, and multi-looked data to reduce phase noise.

Another important contribution is the one proposed by Hooper et al. (2004), in which a novel method for PS selection has been advanced, based on the identification of low-amplitude natural targets with phase stability, along with a widely implemented package named StaMPS (Hooper, 2008). Other remarkable algorithms are, within the great variety in literature, the CPT (Mallorqui et al., 2003), the IPTA (Werner et al., 2003)) and the PSP-DIFSAR (Costantini et al., 2008). One of the latest innovations in the InSAR algorithm is the definition of the SqueeSAR algorithm (Ferretti et al., 2011), capable of joining PSs (pixel-like radar targets) and DSs (Distributed Scatterers), taking into account their statistical behaviour.

Analogous to the development of the algorithms, also several packages (open-source or commercial) were implemented over the last twenty-five years, such as SARPROZ (Perissin et al., 2011), SARscape (implemented by Sarmap), ROI_PAC (Rosen et al., 2004), DORIS (Kampes and Usai, 1999) and many others.

The flourishing of several MT-InSAR approaches has been fostered by the increasing availability of SAR data (Fig. 1), which is the main technical aspect driving the capability to sample deformation phenomena. Typically, a minimum of 15–20 images is needed to perform a reliable MT-InSAR analysis: the larger the number of images, the more precise and robust the results (Crosetto et al., 2016). At the time of writing this review, there are several active SAR missions, operating within different bands of the microwave domain: C-band (centre frequency 5.4 GHz, wavelength 5.6 cm), X-band (centre frequency 9.6 GHz, wavelength 3.1) and L-band (centre frequency 1.3 GHz, wavelength 23.5).

3. The literature database

3.1. Data collection

The collection of the existing scientific literature on different aspects of subsidence analysis using satellite interferometric approaches was conducted exploiting the WoS's freely accessible web search engine (Clarivate, 2019). The WoS for the Natural Sciences and Engineering is comparable to the Scopus search engine with similar biases despite Scopus's larger journal coverage (Mongeon and Paul-Hus, 2016) and both offer the best coverage of journals, articles and cited reference levels (Norris and Oppenheim, 2007). Generally, about 66% of the documents can be found in both databases and only 33% of the contributions reference is included, alternately, in one or the other (Vieira and Gomes, 2009).

Original papers published by international journals after peer review, book chapters and conference proceedings were gathered (Fig. 2a). The data collection involved all contributions referring to every country in the world, where the authors exploited the InSAR technique to study subsidence. The only requirement was the use of the English language.

On the WoS website, it is possible to make an advanced search, by setting different parameters to make more accurate research. More in detail, the data collection criteria are listed below:

- #1 "AK" (Author Keywords) - this command allows extracting the contributions setting words included in the list of the author keywords. In this field these words were used: (*i*) "SAR", (*ii*) "Interferometry", (*iii*) "InSAR"; (*iv*) "MT-InSAR"; (*v*) "DInSAR"; or (*vi*) "PS".

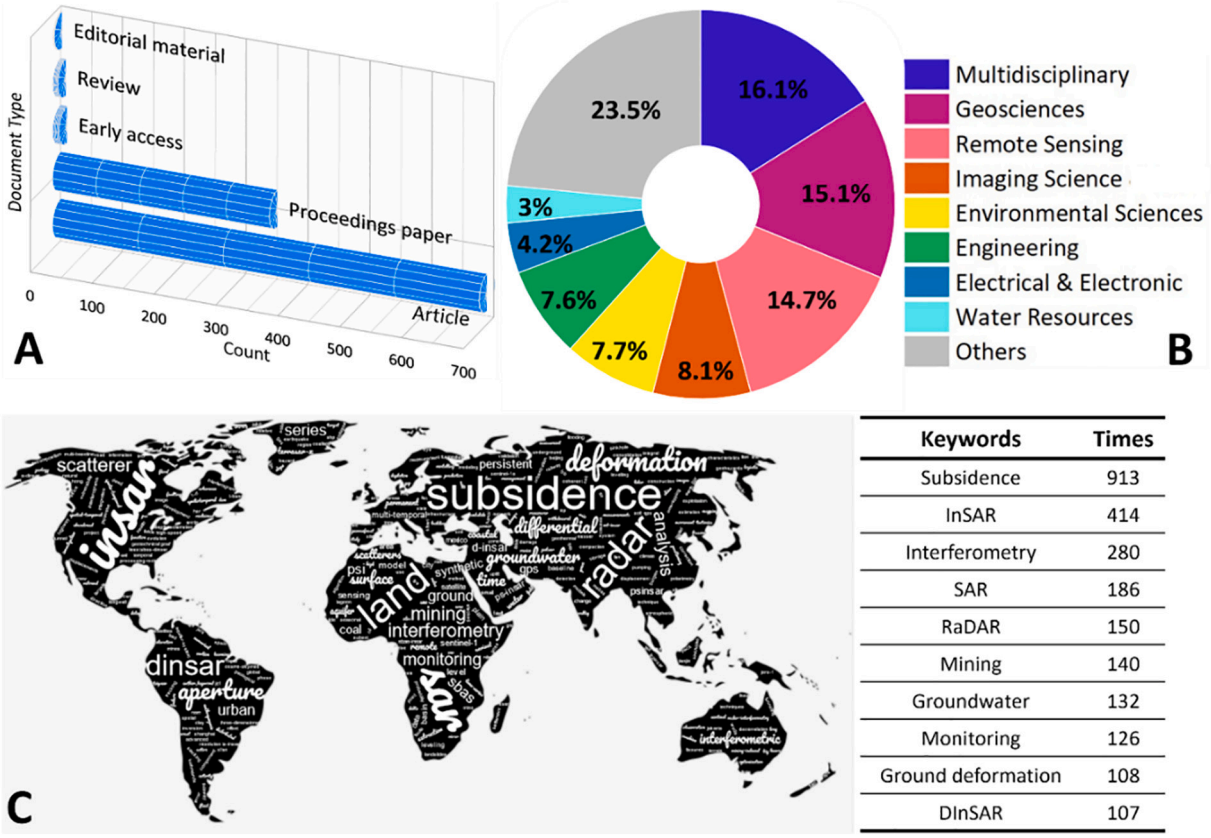

Keywords	Times
Subsidence	913
InSAR	414
Interferometry	280
SAR	186
RaDAR	150
Mining	140
Groundwater	132
Monitoring	126
Ground deformation	108
DInSAR	107

Fig. 2. A) Bar chart shows the number of different document types in the literature database. B) Pie chart reports the percentage of WoS categories. C) Word cloud (Created with www.wordclouds.com) of the list of keywords of the selected contributions. The size of the words reflects the number of times that were used (see also table on the bottom right).

All these words could be inserted in the same string of conditions separated by "OR".
- #2 "AK" - in this field the word "subsidence" was set.
- #3"TI" (Title words) - this condition allows for selecting contributions from words included in the title.

  In this field these words were used: (*i*) "SAR", (*ii*) "Interferometry", (*iii*) "InSAR"; (*iv*) "MT-InSAR"; (*v*) "DInSAR"; or (*vi*) "PS". All these words could be inserted in the same string of conditions separated by "OR".
- #4 "TI" - in the second condition of this field only "subsidence" was used.

Two Boolean operators, *i.e.*, AND (both) or OR (at least one), were used for combining different words in the same condition or more conditions, for extracting all the contributions respecting these requirements.

The conditions were combined in order to extract all the articles that satisfy the required parameters. For example, all the contributions that have, within the keywords list, "subsidence" (#2) and one of the words of #1 were collected by combining #1 and #2. Following this rationale three more criteria were set:

- #5 equal to #1 AND #2 - combination of the conditions set within the lists of keywords defined by authors.
- #6 equal to #3 AND #4 - combination of two conditions within the lists of title words.
- #7 equal to #5 OR #6 - combination lists complying with the conditions on the author keywords and title words.

The data collection was operated in January 2022. The retrieved collection, including a preliminary list of 1183 contributions, can be considered representative for the scientific literature on the use of SAR imagery for subsidence analysis in the 25-year period 1997–2021. The first conclusion that can be drawn is that, despite the lack of a global systematic review, the literature on the exploitation of SAR acquisitions for subsidence analysis turned out to be extensive. The high number of published studies witnesses the recognized need for subsidence analysis and the growing capabilities of SAR imagery to detect and map subsidence.

3.2. Database construction

Following the collection phase, 21 contributions were deleted from the list, because not written in English (16 in Chinese, 2 in Spanish, 1 in France, Polish, and Turkish). Now the database contains 1162 contributions. After this preliminary skimming, all the articles in the preliminary list were examined thoroughly, to identify and exclude those contributions not relevant for the review, even if, as they satisfied the criteria set with the advanced search. The removals were made according to the identifications of issues not strictly related to the subsidence phenomenon and hence considered not relevant for this review. Besides some contributions dealing with body subsidence in the field of clinical neurology and surgery (clearly unrelated to the topic), some authors used the word "subsidence" as a general term meaning a movement away from the satellite. These are the case of lowering related to volcanic systems (*e.g.*, magma cooling), earthquakes, or faults movements. In other cases, subsidence is used to indicate a landslide movement with a dominant vertical component. Moreover, some contributions were related to subsidence analysis with SAR sensors hosted on the airborne platforms and then discarded from further analysis.

In the end, the database was filled with the information extracted from 1059 contributions including original articles (708), conference proceedings (331), early access (10), reviews (8) and Editorial material (2) (Fig. 2a). Every record in the WoS collection is assigned to at least one subject category which reflects its source publication. Contributions of the literature database belong to a large variety of WoS categories (Fig. 2b), with Multidisciplinary (16.1%), Remote Sensing (15.1%) and Geosciences (14.7%) the most represented, in line with analysis conducted by Mondini et al. (2021) for landslide failures.

The contributions were stored in the form of a database, realized for collecting and cataloguing as much information as possible. The database was initially generated automatically by extracting from the WoS records a list file containing several general information about the selected contributions:

- Publication Type - a distinction between original papers in journals (J), book chapter (B), series (S) or extended abstract or proceeding of conferences (C).
- Authors - a record that contains the list of all authors (and related affiliations).
- Article Title.
- Journal.
- Author keywords - the list of keywords indicated by the authors and useful for the selection of the article with the conditions in the advanced search of the WoS search engine (Fig. 2b)
- Abstract
- Publication Year.

Then, to characterize the individual studies in our collection, each article was read and critically analysed, to identify and collect all the necessary information (Fig. 3).

Several new fields have been added to the database and then populated to catalogue each contribution and make a more detailed characterization:

- State corresponding - country that hosts the affiliation institute of the corresponding author.
- Continent corresponding - continent that hosts the affiliation institute of the corresponding author.
- State AoI - country where the study area (AoI, area of interest) investigated is located.
- Continent AoI - continent where the study area (AoI) investigated is located.
- SAR Satellite - the SAR satellite(s) used to perform the analysis in the contribution.
- Band satellite - the microwave band(s) adopted to perform the analysis.
- Cause - list of the cause(s) of the subsidence. The list of possible subsidence triggers was made before starting the literature analysis, considering the well-known categories (*e.g.*, groundwater pumping, mining, load imposition, *etc.*…). Literature analysis reveals that many other causes (*e.g.*, the karstification and landfill compaction) should be taken into account and, despite their lower representativeness, they should be considered to depict a complete scenario of major and minor causes.
- Processing Technique - the processing approach(es) used to elaborate satellite SAR data. For this field the same consideration made for the cause of subsidence is applicable, distinguishing widely consolidated techniques used worldwide and new algorithms recently flourished.
- Applications - each contribution was labelled according to the type of analysis, according to the following classes: (*i*) Mapping; (*ii*) Monitoring, (*iii*) Modeling, (*iv*) Characterization, (*v*) Technical paper, (*vi*) Review, and (*vii*) Simulated subsidence.
- Integration - the possible validation or comparison with other data was included in this field. In case of no integration the word "No" was inserted.
- Field evidence - the recording of damage on structures or ground. In case of no presence or reporting in the contribution, the word "No" was inserted.

Unlike the basic information of the selected contributions, this

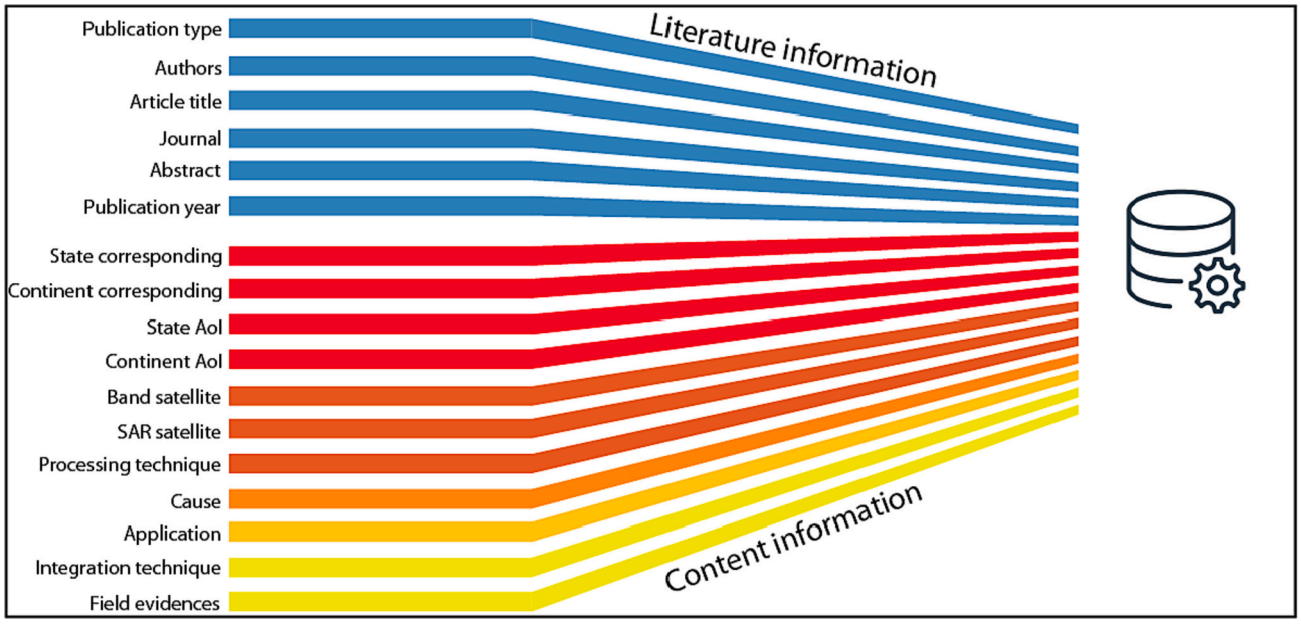

Fig. 3. Literature and content information used to populate the database created to summarize the information of the 1.059 selected contributions. In the upper part the automatic extraction by the WoS search engine, in the lower part the additional field to characterize and classify the information inside individual study.

second block of additional data was not available for all the studies, except for affiliation of the corresponding author. Both technical information on adopted processing approach and details on causes of subsidence provided in the contributions are sometimes scarce. Overall, information on the processing approaches is accurate on studies published in remote sensing journals, while it is more limited in Earth Science and multidisciplinary journals. Conversely, these latter contain studies with more and more accurate subsidence characterization, albeit at the expense of details on methods used to elaborate SAR imagery, which are commonly described by means of relevant references.

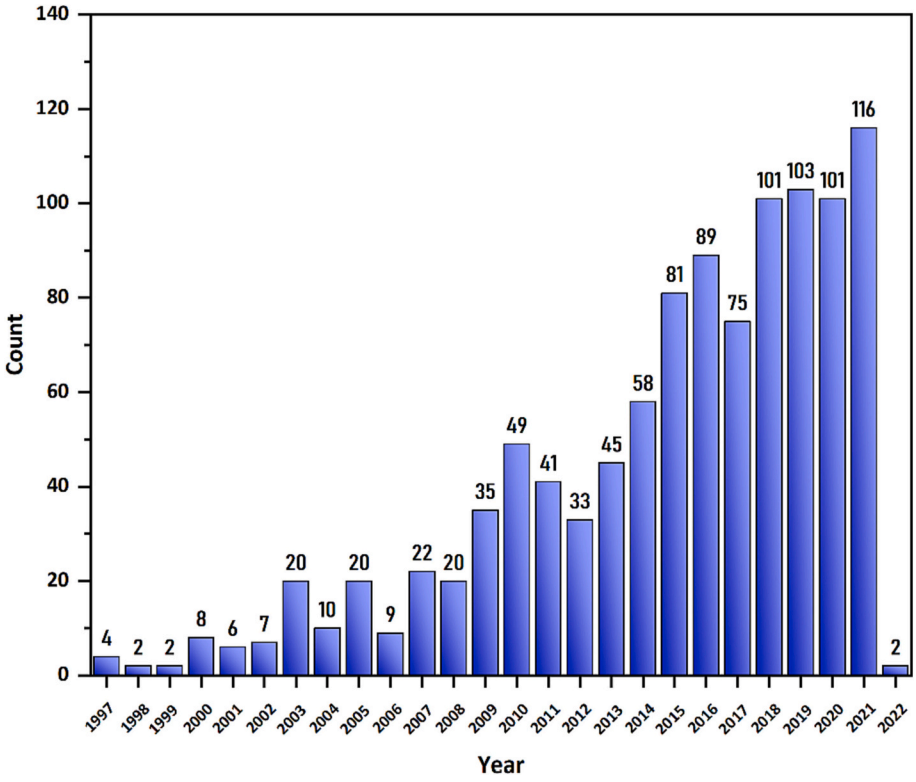

Fig. 4. Temporal distribution of the 1059 scientific contributions published per year from 1997 to January 2022. A growing trend is visible also in terms of absolute number of scientific contributions: from 2015 the sum of works is 666, which is approximately double compared to the amount produced between 1997 and 2014 (391).

4. Database review

4.1. Temporal evolution of the scientific production

A total of 1059 documents were collected and analysed for this review.

The first documents date back to early 1997, and the most recent ones were published in early January 2022 (the date of the articles' collection). The first contribution to this research field dates to April 1997 (Massonnet et al., 1997), with a DInSAR elaboration of ERS acquisitions to map the deformation field associated with the activity of the East Mesa geothermal plant (California, USA). Still, in 1997 the third "ERS Symposium on Space at the Service of Our Environment" was held in Florence, where pioneering works exploring the potential and limits of SAR interferometry applied to ERS acquisitions for mining subsidence detection were presented (Haynes et al., 1997; Raymond and Rudant, 1997; Stow and Wright, 1997).

The most recent records within the database include the exploitation of Sentinel-1 image for the analysis of the surface subsidence caused by underground coal mining in the Loess Plateau (Yang et al., 2022) and in the Anhui Province (Wang et al., 2022) in China, adopting a multi-temporal and a differential approach, respectively.

The average production is about 40 articles per year, though it is highly variable, with a general increasing trend, witnessing the continuous scientific interest in the study of subsidence by using satellite InSAR techniques. Fig. 4 shows that a substantial growth in scientific production on this topic starts in 2015. From this year, the yearly production ranges from 75 to 116, with a mean value of 95 contributions per year (2022 has not been considered, because it is still in progress), five times more than the average production (18) in the previous interval.

Certainly, this progressive growth can be largely related to the launch in April 2014 of the first satellite of the Sentinel-1 mission, which opened new possibilities for InSAR applications, thanks to the policy on data acquisition and availability (Showstack, 2014). The potential of the Sentinel-1 mission was already evident during its operation ramp-up phase, especially for its wide-area capability (Kalia et al., 2014). The first work based on the use of Sentinel-1 data was published in 2015 by Crosetto et al. (2015), who presented ground deformation maps and displacement time series obtained by applying a PSI method to a set of 10 Sentinel-1 images to map subsidence over the metropolitan area of the Federal District of Mexico City.

4.2. Geographic distribution of the InSAR applications

In this review, the spatial distribution of papers collected was evaluated through two parameters: the country of the corresponding author's organization ("*State corresponding*") and the country of the study area ("*State_AoI*").

The analysis of the affiliation of the corresponding author revealed that all continents (except Antarctica) are well represented; Asia is the area that provided the largest number of contributions, with more than 50% of the records (544) within the database. Europe is the second continent with 348 contributions, while the other continents are ordered as follows: North America (120 contributions), Oceania (34) and Africa (10). South America (3) is the less represented continent for what concerns affiliation of the corresponding author. More in detail, at the country level, China has the largest number of corresponding authors with 354 works (more than 33%), followed by Italy and the USA, with 122 and 89 contributions, respectively.

The spatial distribution of papers collected was also analysed through the location of study areas (Fig. 5).

Among the 1059 articles stored in our database, 1051 include a specific area of interest. Eight of these papers did not indicate any

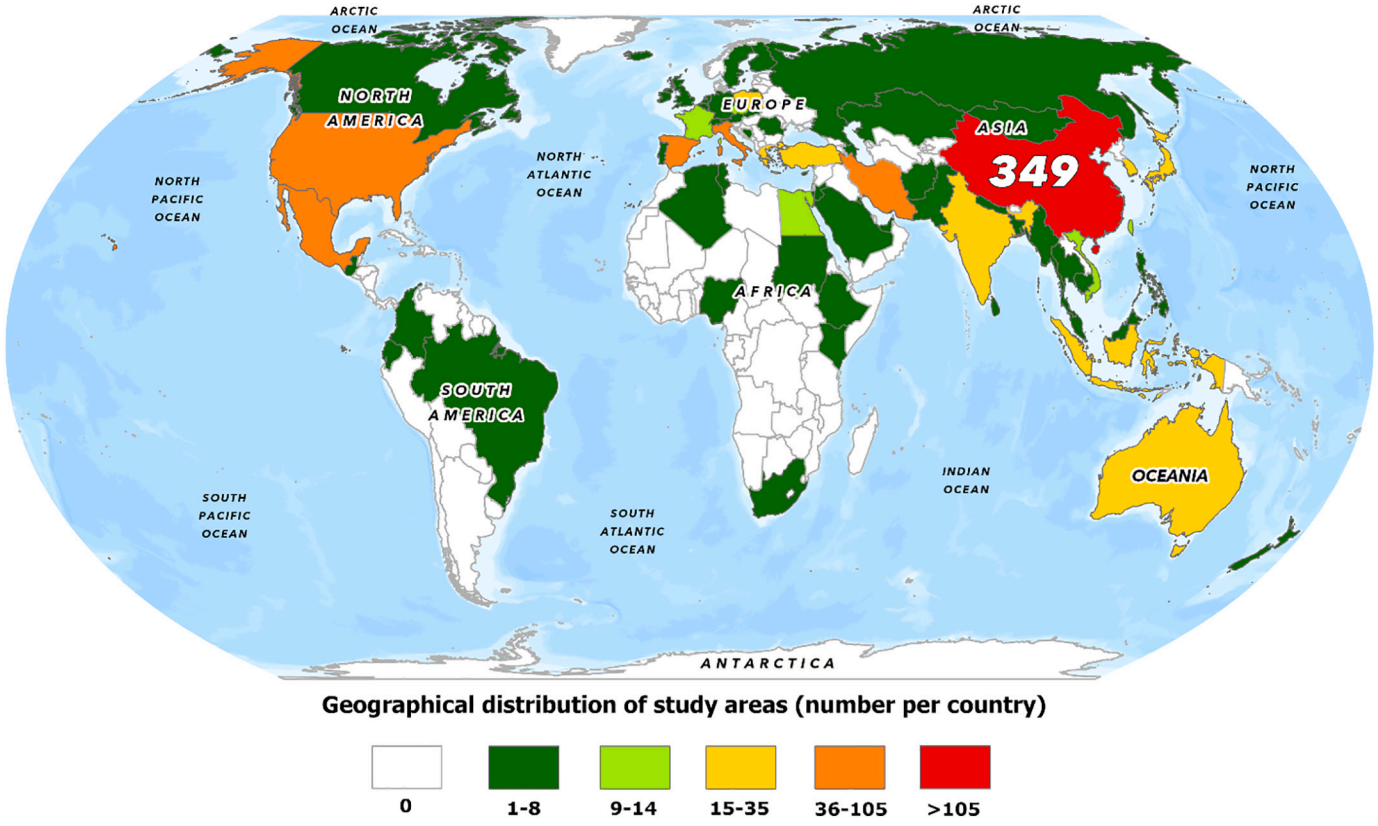

Fig. 5. Global map showing the geographical distribution of the InSAR applications for subsidence analysis (number of study areas per country). Countries coloured based on the number of studies.

specific area, as they were either more focused on the technical aspect of subsidence analysis *e.g.*, Xing et al. (2010) presented the advantage of Corner reflectors in InSAR processing or XunChun et al. (2011) discussed a general framework for the integration of DInSAR with prediction model, or provided an overview of literature contributions (Cigna, 2018; Tomás and Li, 2017). Review papers (Ishwar and Kumar, 2017), discussing the applications of satellite SAR interferometric techniques on a specific subsidence type, also do not include site-specific analysis.

Among the 1051 contributions presenting analysis for a specific study area, 1042 focus on a single continent, 7 on two continents and 2 have targeted three different continents, with a total amount of 1063 study areas (Fig. 5). This means that multiple countries can be the target of a single study (Bonì et al., 2017), with Cigna and Tapete (2020) who exploited the Parallel SBAS workflow integrated within ESA's G-POD platform to retrieve subsidence patterns in three different continents (Asia, South America and Africa). Semple et al. (2017) catalogued and classified more than 250 locations of deformation in the Western USA, Canada, and Mexico suspected to be caused by anthropogenic activities. Strozzi et al. (2018) exploited Sentinel-1 summer acquisitions to spot surface displacement in low-land permafrost regions over Alaska, Greenland, Siberia and Shetland Islands (counting four different countries). Ng and Ge (2007) and Ng et al. (2007) investigated urban subsidence due to groundwater extraction in cities in Australia and China.

Except for Antarctica, all continents include at least a study area: Asia has the largest number of case studies (586). China is by far the most investigated country with 349 subsidence cases analysed using satellite interferometry (Du et al., 2020; Ge et al., 2011; Liu et al., 2014b; Luo et al., 2018; Zhang et al., 2007). Iran (Ghazifard et al., 2016; Motagh et al., 2007; Ranjgar et al., 2021) and Indonesia (Bayuaji et al., 2010; Du et al., 2018b; Gumilar et al., 2011) also contributed to a large number of case studies in Asia, with 48 and 31 areas, respectively.

The second continent for number of study areas is Europe, with 281 applications. Italy and Spain are the countries that mostly contributed. Indeed, the study areas located in their territories are 55% of those of the entire continent: Italy has 101 applications focused on subsidence cases in its territory (*e.g.*, Bianchini et al., 2019; Bitelli et al., 2015; Del Soldato et al., 2018; Meisina et al., 2006; Solari et al., 2018), while Spain has 61 works (*e.g.*, Bru et al., 2017; Ruiz-Constan et al., 2017; Sanabria et al., 2014; Tomás et al., 2005).

North America is the third continent based on study areas, with 142 applications, 78 of which were focused on subsidence cases in the USA (Grzovic and Ghulam, 2015; Hoffmann and Zebker, 2003; Iwahana et al., 2016; Plattner et al., 2010; Schmidt and Bürgmann, 2003; Simmons and Wempen, 2021). Mexico (Avila-Olivera et al., 2007; Castellazzi et al., 2016a; Chaussard et al., 2014; Navarro-Hernandez et al., 2020) and Canada (Chen et al., 2018a; Samsonov et al., 2014) contributed to InSAR applications on subsidence studies in North America with 59 and 7 study areas, respectively.

The other continents presented the following data: (*i*) Africa has 26 applications focused on its territory (Baer et al., 2018; Koros and Agustin, 2017; Woppelmann et al., 2013); (*ii*) Oceania showed 20 sites where subsidence has been studied using satellite interferometry (Hole et al., 2007; Ng et al., 2009; Parker et al., 2017); (*iii*) South America provided 7 subsidence cases (Ammirati et al., 2020; Jacome et al., 2020; Ramos et al., 2014).

5. Database analysis

5.1. Satellite acquisition bands and processing approaches

Among the 1059 scientific records within the database, 1051 presented results of interferometric elaborations. For only 8 contributions (belonging to Review and Technical paper categories) authors didn't present any ground deformation data as they summarize the state of art of SAR applications (Review), or because they focus on technological aspects (Technical paper). For the remaining contributions the processed dataset is not available. It is worth highlighting that most of the contributions (728 among 1043, representing 69.3% of the total) used a single satellite platform to investigate land subsidence. The remaining part (*i.e.*, 30.7%) used different interferometric datasets in synergy, with multiple combinations of satellite platforms and bands, to extend understanding of the investigated phenomenon. Analysis of the literature database allowed us to spot 323 applications using multiple platforms (*i.e.*, from two to six). Considering all the aforementioned scientific contributions, whether they are articles, book chapters, or conference papers, a total of 1561 interferometric datasets have been processed, created and presented within 1051 contributions.

Considering the satellite wavelength, most of the paper shows a massive application of C-band images for InSAR-related subsidence analysis, with 71.1% of applications, followed by X-band and L-band, with 15.5% and 13.4% of analysed datasets, respectively. These percentages are quite consistent with those calculated by Del Soldato et al. (2021), which reviewed InSAR and GNSS integration over Europe and Solari et al. (2020) who analysed Italian literature on landslide analysis with satellite interferometry. In both works, the authors found that C-band is the most used (percentage in the order of 76–78%), followed by the X-band. L-band images are even less frequently used.

Analysing in further detail the satellite platforms (Fig. 6), the ESA C-band Envisat is the most widely adopted, being used 401 times (26.6% of the total), followed by ERS and Sentinel-1, that account for 282 (18.7%) and 279 (18.5%) applications, respectively. Regarding other satellites, minor use frequencies are registered, listed from high to low: ALOS-1 (11.4%), TerraSAR-X (8.8%), the RADARSAT 1/2 constellation (7.3%), COSMO-SkyMed (4.6%), JERS-1 (2.4%) and, finally, ALOS-2 (1.5%).

Takeuchi and Yamada (2002) proposed the first application of a multi-band approach with L-band JERS-1 and C-band ERS acquisitions, whose capabilities to measure subsidence in urban and rural areas were presented and discussed. The high-resolution X-band has been firstly exploited by Strozzi et al. (2009) who pointed out how the stability of backscatter intensity of Corner Reflectors in TerraSAR-X images would generate time series with the smallest noise level, highlighting the potential of X-band in monitoring land subsidence of the Venice lagoon in Italy. Zhu et al. (2013) combined C-, L- and X-bands interferometry to investigate spatial and temporal variations in deformation pattern over

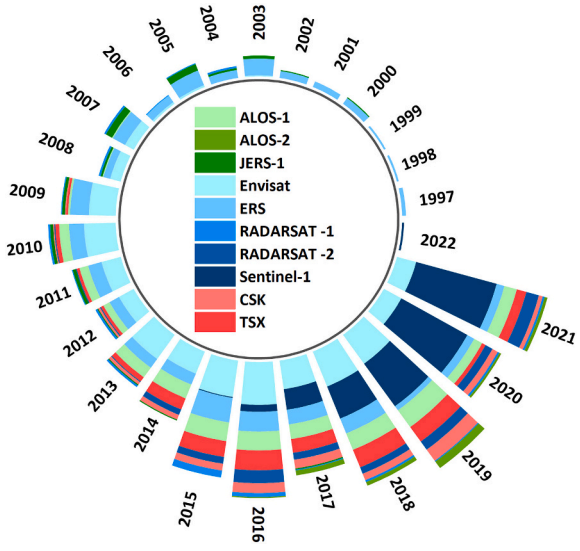

Fig. 6. Satellite platforms usage from 1997 to January 2022 for the subsidence analysis. In recent years the spreading of Sentinel-1 satellites is evident: being freely accessible, they provide the scientific community, as well as public and private companies, with consistent archives of openly available radar data acquired at global scale.

the Taiyuan basin (China); these authors cross-checked the multiband data and found consistent results, although some differences in terms of extension and rate of displacement were observed. Cigna et al. (2016a) exploited five data stacks to create a 25 five years-long satellite monitoring of land subsidence and coastline retreat in Capo Colonna (Southern Italy). Du et al. (2019) combined five SAR sensors with all the three bands (C-, X- and L-bands) for a long-term assessment of land subsidence in Mexico City. Scoular et al. (2020), leveraging five satellite missions as well, investigated patterns of deformation in East London during the construction of the Lee Tunnel.

Among the 1059 scientific records within the database, 1051 presented results of interferometric elaborations. For only 8 contributions (the same that did not indicate any specific area, falling in the Review and Technical paper categories), information on the processing approach is not available. A total of 1168 elaborations have been performed (Fig. 7), with several contributions adopting multiple approaches.

A total of 312elaborations (corresponding to 26.7%) exploit DInSAR-based approaches, with ROI_PAC (Rosen et al., 2004), GAMMA (Werner et al., 2000) and DORIS (Kampes and Usai, 1999) software largely used. The remaining 73.3% relied on one of the available MT-InSAR algorithms.

Forty different multi-temporal approaches have been used to process satellite acquisitions. The SBAS approach (Berardino et al., 2002), counted 235 times (20.1% of the total), is the most adopted technique, followed by PSInSAR (Ferretti et al., 2001) and IPTA (Werner et al., 2003), used 201 (17.2%) and 67 (5.8%) times, respectively. Other techniques are well represented, among which, CPT (Mora et al., 2002) with 33 (2.8%) applications, PSP-DIFSAR (Costantini et al., 2008) and SqueeSAR (Ferretti et al., 2011) used 15 and 14 times (1.3% and 1.2%), respectively. SPN (Arnaud et al., 2003) has been exploited 13 times, while GEOS-ATSA (Ge et al., 2014) 12 times.

It should be remarked that it is not possible to establish a precise number of times each approach was used, since, in some contributions, the processing algorithm was not clearly specified (in this case the label Generic MT-InSAR has been used, 64 times, *i.e.*, 5.5%) or only the software package is indicated (for 109 application, representing 9.4% of the total), including StaMPS (Hooper et al., 2012), SARPROZ (Perissin et al., 2011), and SARscape (implemented by Sarmap), since each one encompasses different processing algorithms.

A minor portion of investigators adopted other processing approaches, with 67 elaborations carried out with 22 different algorithms (most of one counted one or two times), witnessing the great vitality of the interferometric community and the recent flourishing of elaboration chains.

5.2. Subsidence types and triggers

It is well-known that land subsidence is a subtle and challenging phenomenon as it can be triggered by purely geological and anthropogenic factors. In some situations, surface lowering patterns reflect the combination of human-related and natural causes and overlapping of different sources of deformation can complicate the interpretation of the subsidence mechanism. For each of the 1059 contributions collected, the triggering force of the analysed subsidence has been identified, relying on information provided by the authors (Fig. 8). Considering all the scientific contributions, a total of 21 driving forces within 1037 contributions. The cause of subsidence is not available for 22 contributions, either belonging to the Review (6) and Technical paper (11) categories. In very few cases (5), the cause of subsidence is not clearly indicated, and it was not possible to directly infer it, being the focus more on the potential effects of ground lowering on infrastructure and thermal effects in time series (*e.g.*, Poreh et al. (2016)), rather than on subsidence interpretation.

Literature database analysis confirms that interpretation of subsidence mechanism is often a difficult task, as in several cases (267 contributions, *i.e.*, 25.7% of the total), measured deformation is related to multiple causes while in 770 contributions (corresponding to 74.3%)

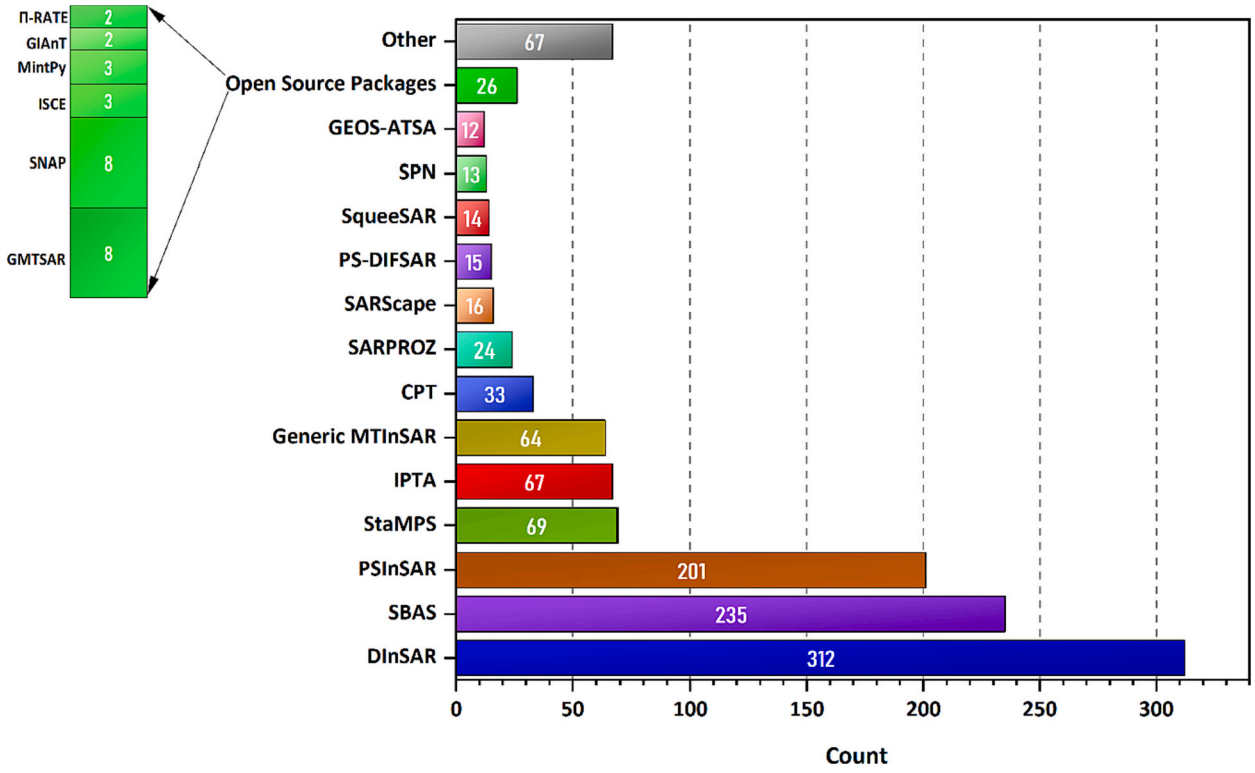

Fig. 7. Processing approaches, software packages and techniques used for subsidence analysis. Not surprisingly DInSAR, PSInSAR and SBAS approaches are the most adopted. It worth highlighting, the development, in recent years, of several open-source software packages.

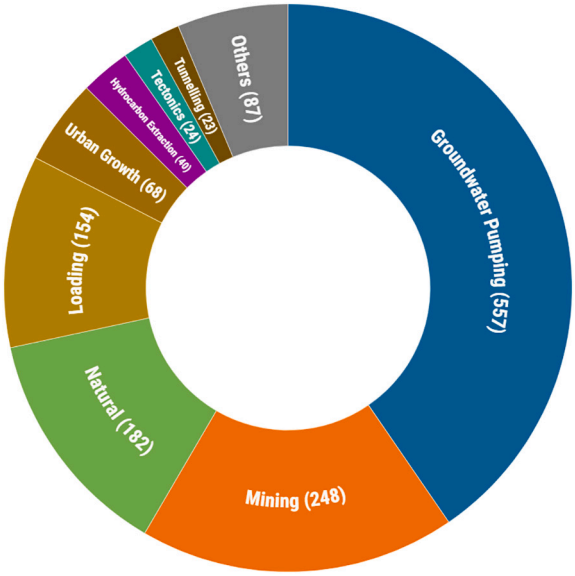

Fig. 8. Main driving forces (cause) of subsidence phenomena collected from literature analysis. Within parenthesis is reported the number of times each cause has been identified in database. Details of the class "Others" can be found in Fig. 9.

land lowering is directly attributed to a single driving force. Whatever the cause, both single-pair and multi-temporal InSAR analysis has been recognized as a valuable tool to track deformation phenomena, with a large spectrum of possible applications to ground-deformation assessment (Raucoules et al., 2007), both in the urban and natural environment.

5.2.1. Natural subsidence

Natural subsidence is the result of sediment consolidation and loss of interstitial fluids caused by lithostatic loading, compaction and tectonics. Many of the world's largest river deltas and coastal plains are experiencing long-term sinking due to natural subsidence. Higgins et al. (2014), analysing InSAR measurements, demonstrated that subsidence in the Ganges-Brahmaputra Delta (Bangladesh) is primarily controlled by local stratigraphy, with high-subsidence areas reflecting underlying geologic units. Becker and Sultan (2009), using ERS acquisitions, concluded that subsidence in the northeast part Nile Delta (Egypt) is heavily influenced by compaction of the most recent sediments and that the highest subsidence rates are correlated with the distribution of the youngest depositional centres (major deposition occurred between ~3500 yr BP and present). Woppelmann et al. (2013) focused on the western part of the Nile Delta with Envisat data, inferring that land subsidence in this area is primarily dominated by tectonic setting and sediment thickness and compaction degree. Yastika et al. (2019) investigated land subsidence in the coastal city of Semarang (Indonesia) with C- and L-band, founding a close correlation with marine and alluvium sediments that have the potential to subside due to natural consolidation. Fryksten and Nilfouroushan (2019) measured ground deformation in Uppsala (Sweden) and related it to the presence of thick layers of postglacial clays. The existence of a tectonic component overlapping the soil consolidation in Morelia is reported by Cabral-Cano et al. (2010).

A joint effect of anthropogenic and geological factors is widely reported in the literature (*e.g.*, Polcari et al. (2014)). Liu et al. (2016) described how the Yellow River Delta in China has been subsiding due to the combined effects of human and natural factors. Supported by InSAR data, the authors stated that natural sediment consolidation can only account for a few mm/year of subsidence, while a substantial amount may be attributable to the activity of the hydrocarbon exploration field. Analysis of two decades (1992–2010) of C-band data (Di Paola et al., 2021; Matano et al., 2018) supported the interpretation of the Volturno coastal plain (South Italy) land subsidence, where ground lowering can be considered an overlapping of natural process (compaction of the alluvial sediments infill under the lithostatic load) and anthropic influences (water pumping and urbanization). In some cases, despite the ubiquitous presence of Quaternary deposits highly susceptible to rapid vertical motion, human influence on subsidence is dominant (van der Horst et al., 2018). The surface subsidence of many areas is due either to natural or anthropogenic causes, among which the Po Plain in Italy (Stramondo et al., 2007), where a combination of a long-term natural movement and the surface effects of anthropogenic activity is documented, and Beijing in China (Zhou et al., 2016; Zhu et al., 2015) whose uneven subsidence pattern is strongly affected by the thickness variability of the compressible deposits and partially by the distribution of groundwater depression cones.

Human activities, such as groundwater extraction (Hung et al., 2011), land-use changes (Minderhoud et al., 2018), urban-induced loading (Solari et al., 2017) and reduced aggradation are recognized to exacerbate some situations, which may become critical along the coastal regions where land subsidence increases the exposure of population and assets to inundation and future sea-level related hazards (Anzidei et al., 2021; Aucelli et al., 2017).

5.2.2. Anthropogenic subsidence

Concerning anthropogenic causes, they can be identified primarily in fluid (hydrocarbon and groundwater) extraction, geothermal exploitation and mining activities. Moreover, in the last decades, the economic growth and population increase have led to large urban sprawl worldwide, with a corresponding rise of new building blocks (and related sediments compaction due to overload) and expansion of subsoil urban structures (*e.g.*, tunnelling), potentially triggering subsidence.

5.2.2.1. Groundwater overexploitation. Accounted 561 times, groundwater overexploitation represents the most common human-related cause of land subsidence, as compaction of susceptible aquifer systems, typically unconsolidated alluvial or basin-fill aquifer systems, can affect large agricultural and urbanized areas worldwide with increasing demand for freshwater. Examples of areas where the observed subsidence patterns largely reflect the spatial distribution of head declines include:

- Mexico City (Lopez-Quiroz et al., 2009; Osmanoglu et al., 2011), Toluca valley (Calderhead et al., 2011) and Morelia in Mexico (Cigna et al., 2012);
- the Los Angeles basin (Zhang et al., 2012), Las Vegas (Amelung et al., 1999), Phoenix (Miller and Shirzaei, 2015) and the Antelope valley (Hoffmann and Zebker, 2003) in the USA;
- the Segura River valley (Herrera et al., 2009a; Tomás et al., 2005) in Spain, Xi'an (Qu et al., 2014);
- Tianjin (Liu et al., 2010) and Beijing (Chen et al., 2016; Ng et al., 2012b) in China;
- the Rafsanjan plain (Motagh et al., 2017) in Iran, Calcutta (Chatterjee et al., 2006) in India, Yunlin County (Tung and Hu, 2012) in Taiwan and the Konya Plain (Calo et al., 2017) in Turkey;
- Sarno (Cascini et al., 2006), the Pistoia basin (Del Soldato et al., 2018) in Italy, the Gulf of Thessaloniki (Nikos et al., 2016) in Greece.

Many contributions underlined the strong relationship between *subsidence* due to *groundwater extraction and faulting* / pattern of structural faults buried by sediments. Schmidt and Bürgmann (2003) highlighted that uplift and subsidence patterns in Santa Clara Valley (California), an area with a long history of land deformation resulting from the excessive pumping of groundwater, is controlled by faults that can act as a hydrologic barrier to groundwater flow. Chaussard et al.

(2014) identified 21 areas in Central Mexico related to massive groundwater extraction, pointing out that subsiding areas are often bounded by high-velocity gradients that coincide with pre-existing faults and with transition in sediment types. Motagh et al. (2007) highlighted that the significant land subsidence in the Mashhad Valley (Iran), which resulted from extensive water table decline, is structurally controlled by the trends of Quaternary faults cutting the valley floor. Brunori et al. (2015) suggested that land subsidence processes and the associated ground fissuring affecting Ciudad Guzmán (Mexico) are driven by aquifer exploitation and controlled by the distribution and position of buried faults. Anderssohn et al. (2008) provide an example of how the deformation pattern and elongation of the subsidence bowl in the Kashmar Valley in northeast Iran are governed by faults of Cretaceous-to-Tertiary age beneath or within the sedimentary valley infill.

5.2.2.2. Load imposition. Loading imposition is another important factor triggering land subsidence, being identified 154 times. Different settlement patterns can be measured in areas interested by recent urbanization, as a result of the combination between the applied load (in terms of both magnitude and time of imposition) and the mechanical behaviour of the loaded soils over time, which is linked also to the fine soil thickness, hydraulic conductivity and drainage conditions.

Stramondo et al. (2008) provided a complete analysis of surface movements within the urban fabric of Rome, depicting the temporal behaviour of buildings and the infrastructures. Ciampalini et al. (2019) analysed, in a 26 year-long monitoring period, the freight terminal located along the coastal plain of Tuscany (Italy), in terms of subsidence rates and deformation time series at the building scale. Stramondo et al. (2008) and Ciampalini et al. (2019) inferred that the observed deformation rates decrease over time with respect to the age of the buildings. Subsidence pattern and displacement time series for both the alluvial network in the city of Rome and the Tuscan Freight Terminal follow a time-depended trend that can be explained by the theory of consolidation from Terzaghi et al. (1996). Kim et al. (2010) mapped surface deformation induced by soil consolidation in Mokpo city (Korea) primarily built on land reclaimed from the sea, adopting a time-varying model which successfully reproduces the slow deceleration of ground subsidence associated with soil consolidation. Yang et al. (2018) analysed the relationship between ground deformation and building characteristics in Beijing, founding a potential correlation between block construction age and building volume on one side and spatial unevenness of land subsidence on the other.

Solari et al. (2016) highlighted that significant heterogeneity of the subsidence at the local scale for the city of Pisa (Italy) can be connected to both the subsoil characteristics and load imposition, which is the trigger for the accelerated consolidation process of highly compressible and organic layers. Bock et al. (2012), Tosi et al. (2015) and Tosi et al. (2018) highlighted that the significant local-scale variability of the land displacements, superposed on the regional trend of land subsidence in the lagoon of Venice (Italy), can be related to human interventions (new built-up areas, restoration works and construction of the mobile barriers for lagoon protection).

5.2.2.3. Mining activity. Mine subsidence (identified 248 times in the literature analysis) is a serious engineering, economic and environmental issue. It includes both ground lowering and collapse of overlying strata into mine voids. Subsidence may be the inevitable consequence of underground mining activities due to the advance of the excavation fronts, the opening of new rooms, or the progressive abandonment or collapse of the extraction galleries and structures and it may occur time after mining has ceased. Open pit mining can trigger subsidence in an indirect way, *i.e.*, through the pumping of water to maintain low the water level within the boundary of the pit. Subsidence characteristics may be highly variable, in terms of affected areas and kinematics. It can be localized or extended over large areas, immediate or delayed for decades. The magnitude of the deformation itself depends on several factors, such as the depth of the mining galleries and the time elapsed since the beginning and/or the closure of the excavation.

Spatiotemporal analysis of surface subsidence over mining areas using SAR data have been conducted worldwide, including NW Turkey (Abdikan et al., 2014), China (Dong et al., 2015; Fan et al., 2015; Yang et al., 2017c), Australia (Du et al., 2016), USA (Grzovic and Ghulam, 2015; Plattner et al., 2010) and East Europe (Czikhardt et al., 2017; Malinowska et al., 2018).

Unlike ground subsidence induced by overexploitation of groundwater resources, subsidence associated with mining activities can be very localized, rapid and destructive, especially when associated with the collapse of underground cavities. Herrera et al. (2007) applied multitemporal DInSAR to study the deformation pattern in the city of La Unión in Spain, a site where mining activities started in the Roman Age and where, in May 1998, a fast and sudden collapse of several underground mining galleries led to the total failure of an industrial building and severe damage in the surrounding zone. Residual settlements were detected and monitored, along with identification of different unknown deformation processes affecting several locations, furtherly investigated by Herrera et al. (2010b). Samsonov et al. (2013) integrated multiple InSAR data sets for the computation of two-dimensional time series of ground deformation related to coal mining activities along the French-German border. Time series of vertical and horizontal east-west components of ground deformation for twenty selected sites of interest allowed authors to identify and monitor accelerations of ground subsidence, reversal uplift and motion towards the centre of the subsidence bowls. Multi-temporal DInSAR has been applied to ERS dataset to study ground displacement in the Ebro Basin in Spain (Castaneda et al., 2009; Yerro et al., 2014), where the presence of evaporite formations caused the occurrence of numerous cover collapse sinkholes and ground movements associated to underground mining activities linked to the exploitation of a salt dome. Przylucka et al. (2015) combined conventional and advanced DInSAR techniques to monitor fast evolving mining subsidence in the Upper Silesian Coal Basin (Poland). Li et al. (2015) retrieved the 3-D displacements field of a mining area in China from a single InSAR pair, exploiting the proportional relationship between the horizontal displacement and gradient of vertical displacements caused by underground mining. Changes in the groundwater levels due to the intensification of mine exploitation requiring dewatering operations (Bozzano et al., 2015) or underground coal fires in mining reserves (Zhou et al., 2013) can be the cause of long-term vertical ground displacement.

5.2.2.4. Urban sprawl and engineering constructions. In the last decades, many large cities in the world have experienced rapid urbanization and population increase. Land subsidence as a consequence of urban development (identified 68 times within the database) can potentially damage infrastructures in the city; therefore, it has to be closely monitored and analysed. Dang et al. (2014) quantified the spatial distribution of the land subsidence in the city of Hanoi (Vietnam), which experiences rapid urbanization from the beginning of the 1990s. They recognized that the spatial patterns of subsidence are related to a combination of the lateral variations of several factors such as Quaternary shallow geology, the piezometric level in the aquifer, and urban sprawl (*i.e.*, the density of built-up surfaces), and the types of foundation chosen for the constructions. Abidin et al. (2011) and Ng et al. (2012a) reported that the land subsidence in Jakarta (capital city of Indonesia with more than 10 million inhabitants), was the result of (*i*) over-extraction of groundwater, (*ii*) conversion of agricultural areas into the urban fabric, (*iii*) massive construction, besides natural consolidation of soil layers and tectonic movements. Wang et al. (2012) and Chen et al. (2012) associated the coastal subsidence of the Pearl River Delta (which, with a population of 60 million, is one of the most densely populated areas in

the world) with rapid urban development in recent years. Dong et al. (2014) detailed the land subsidence in Shanghai, unveiling that while groundwater withdrawal is thought to be the primary cause of the homogeneous land subsidence, rapid urbanization and economic development (construction of skyscrapers, metro lines and highways) contributed exacerbating the phenomenon at the local scale. Urban areas built over reclaimed land from the sea are subjected to significant subsidence (Kim et al., 2005a; Liu et al., 2018; Xu et al., 2016).

Mexico City (Yan et al., 2012), Xi'an (Zhang et al., 2009; Zhao et al., 2009a), Beijing (Chen et al., 2015a; Gao et al., 2016), Lanzhou New District (Chen et al., 2018b), Nansha District (Ao et al., 2015), Vancouver (Samsonov et al., 2014) are other places where InSAR results highlighted a strict correlation between urbanization and land subsidence. InSAR data can support the detection of a very localized subsidence pattern around a skyscraper (Aslan et al., 2018), which causes local ground surface settling due to the consolidation of the underlying soft soil deposits.

In urban areas underground public transport is an alternative method for relieving traffic pressures, but ground subsidence (Sillerico et al., 2015; Wnuk et al., 2019), during construction and operation, can be a serious threat as it may affect the safety of operation and the stability of nearby buildings. Tunnelling has been recognized as a cause of subsidence 24 times. Milillo et al. (2018) produced a time series of cumulative deformation over the city of London (UK), where the Crossrail twin tunnels were excavated. Kim et al. (2007) found that the subsidence pattern of Deokpo Subway Station in Busan (Korea) appears to be related to subway tunnelling, based on its linear shape and its N-S elongation, almost parallel to the subway line direction. Chen et al. (2017) monitored the influence of the construction and operation of the underground railway network of Beijing City on local subsidence. Wang et al. (2017) accurately mapped the surface deformation of the subway network in the city of Guangzhou, a deltaic area whose geological conditions make it prone to soil compaction processes under the pressure of engineering constructions.

5.2.2.5. Hydrocarbon extraction. Beside groundwater withdrawal, also hydrocarbon extraction (still a form of fluid withdrawal) is responsible for surface deformation following reservoir compaction at oil/gas production sites. It has been spotted 40 times in the literature database. Qu et al. (2015), analysing InSAR measurements unveiled spatial–temporal variations of land subsidence over Houston–Galveston in Texas, highlighting that while groundwater extraction is the main cause of land subsidence over wide areas, oil and gas exploration has also contributed to localized lowering. Persistent land subsidence in this area can increase flood severity, as reported by Miller and Shirzaei (2019), who found a clear correlation between 2017 Hurricane Harvey and pre-cyclone land subsidence rates. Fiaschi et al. (2017) showed the benefits of long-term monitoring activity of the land subsidence related to the exploitation of the on- and off-shore methane gas fields along the Ravenna coastline (Italy). Cigna et al. (2016a), Sun et al. (2017) and Liu et al. (2016) presented successful applications of InSAR analysis in areas where oil and gas extraction is an element to account for measured land subsidence. Using horizontal and vertical components derived from satellite InSAR, Fokker et al. (2016) estimated subsurface model parameters for the Bergermeer gas field in the Netherlands.

A protocol for geodetic monitoring (including satellite InSAR) of subsidence phenomena along onshore hydrocarbon reservoirs is presented by Montuori et al. (2018).

Jha et al. (2015) and Codegone et al. (2016) presented an InSAR analysis of surface movements (uplift and subsidence) of underground gas storage fields and around injection wells on Italian cases.

5.2.3. Other causes

Ground subsidence in utilized geothermal areas (counted 21 times, Fig. 9) is often attributed either to pressure decrease or temperature

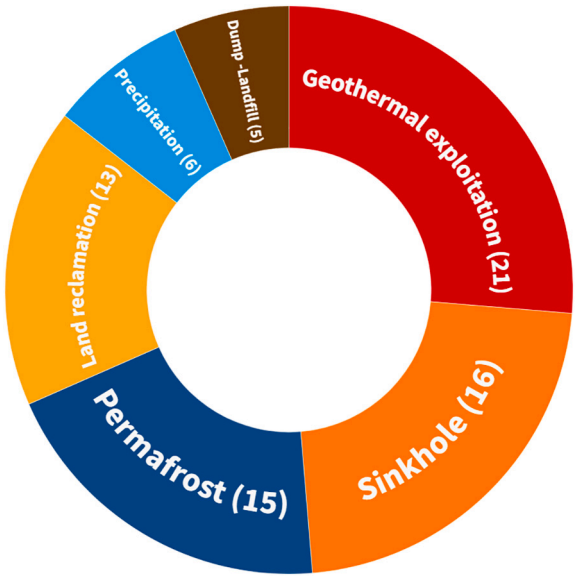

Fig. 9. Minor driving forces (cause) of subsidence phenomena collected from literature analysis. Within parenthesis is reported the number of times each cause has been identified in database.

decrease in the geothermal reservoir as a result of fluid extraction. The Trans-Mexican Volcanic Belt in central Mexico, including Los Humeros (Bekesi et al., 2019) and Cerro Prieto (Samsonov et al., 2017; Sarychikhina et al., 2011; Xu et al., 2017), Taupo in New Zealand (Hole et al., 2007), Reykjanes in Iceland (Keiding et al., 2010; Parks et al., 2020), Larderello in Italy (Rosi et al., 2016), Yangbajing in China (Li et al., 2016) and Olkaria in Kenia (Koros and Agustin, 2017) are geothermal fields where satellite InSAR has been applied to monitor related land subsidence.

Sinkholes are depressions occurring worldwide in many geological environments. They are generally formed by karst processes (*i.e.*, the dissolution of subsurface soluble rocks), creating underlying caves or voids that collapse when insufficiently supported, or by suffusion (when loose soil is washed into cavities beneath). Sinkholes may form suddenly or may be associated with gradual, dissolution-induced land subsidence, which occurs before, during, and after the surface collapse of the sinkhole itself. While sudden movement cannot be either detected or monitored by SAR interferometry, the magnitude and duration of subsidence (both precursory and residual) can be successfully investigated with InSAR approaches. A total of 16 contributions focuses on this topic within the literature database.

Baer et al. (2018) and Nof et al. (2019) exploited SAR interferometry to detect minute precursory subsidence before the catastrophic collapse of the sinkholes and to map zones susceptible to future sinkhole formation in the Dead Sea (Israel), a zone where evaporite dissolution is increased by seasonal flash floods (Avni et al., 2016; Shviro et al., 2017). Residual subsidence of Wink Sinks #1 and #2, two sinkholes in West Texas (USA), collapsed in 1980 and 2002, respectively, due to the dissolution of the subsurface evaporite deposits as a result of freshwater intrusion associated with hydrocarbon drilling and production, has been measured with L-Band (Shi et al., 2019) and X-band (Kim et al., 2019). Karst dissolution of subsurface carbonate rocks can be a contributing factor to land subsidence also in urbanized areas (Bai et al., 2016; Zhou et al., 2017b). The combination of conventional DInSAR and MT-InSAR techniques proposed by Raucoules et al. (2013a) turned out to be valuable for the analysis of localized salt dissolution-induced subsidence: while DInSAR can reveal a clear boundary for the affected area, MT-InSAR gives information regarding the beginning of the event.

In permafrost areas, seasonal freeze-thaw cycles result in upward and downward movements of the ground. Despite the limitations related to

the characteristics of the observed scenario (snow cover, fast phase coherence loss, atmospheric artifacts) InSAR demonstrated in 15 contributions to be a valuable tool to detect and measure permafrost-related deformation. Antonova et al. (2018) used DInSAR to estimate ground displacements related to thawing and freezing processes in permafrost environments in the Siberian Arctic, especially in thermokarst basins. Bartsch et al. (2019) identified seasonal ground displacements in northwest Siberia (Russia) tightly correlated with unusually warm periods, demonstrating that InSAR displacement can provide information on the magnitude of ground thaw and soil properties in extreme years. Iwahana et al. (2016) and Liu et al. (2014a) demonstrated the effectiveness of InSAR to quantify wildfire impacts, in terms of increase of ground subsidence, in regions underlain by ice-rich permafrost. Seasonal dynamics of a permafrost landscape in Svalbard (Norway) have been investigated by Rouyet et al. (2019) using TerraSAR-X InSAR.

The Qinghai-Tibet Plateau (Zhang et al., 2020), the Qinghai province (Dai et al., 2018) and Alsaka (Liu et al., 2015) are other well-known permafrost zones affected by surface deformation and where InSAR demonstrated to be an effective tool for mapping and studying active thermokarst processes.

Land reclamation is a common practice in many territories characterized by scarcity of usable land, as coastal regions become more attractive for industrial complexes and residences. Reclamation is usually performed over unconsolidated fine-grained sediments. Reclaimed land from the sea usually undergoes long periods of progressive settlement that may affect buildings, facilities and infrastructures. Satellite InSAR has been demonstrated to be a valuable tool to monitor the compaction of fine-grained deposits of reclaimed land in 13 contributions. Teatini et al. (2005), supported by DInSAR and MT-InSAR analysis of ERS acquisitions, recognized that compaction of fine-grained deposits in recently reclaimed lagoon sectors can have a significant role to play in the subsidence recorded in the area of Venice. Peatlands in tropical regions (Umarhadi et al., 2021) are particularly susceptible to irreversible subsidence due to changes in land use (*e.g.*, deforestation) and land management practices (*e.g.*, drainage alteration). Settlement due to reclamation is a serious problem in Hong Kong (Ding et al., 2004), as highlighted by ERS interferograms, which show movements affecting the airport and residential areas. Kim et al. (2005b) successfully estimated the subsidence rate in the reclaimed coastal areas in Korea with the JERS satellite and found L-band very effective to overcome difficulties related to severe temporal decorrelation and intense deformation gradients typical of reclaimed land scenarios. Satellite InSAR supported Gebremichael et al. (2018) to solve the spatial variability of land subsidence over the entire Nile Delta of Egypt, and to identify the factors controlling the deformation, including land reclamation, besides gas extraction, groundwater pumping and natural processes.

In modern society, handling waste is a challenging issue and, despite alternative approaches existing, landfill is still a common method for waste disposal. The artificial landfill has the potential problem of subsidence (Gido et al., 2020b), related to mechanical compression and biochemical processes. Barra et al. (2017) used Sentinel-1 data to spot active deformation areas related to the vertical motion of a waste dump in Tenerife Island. Baek et al. (2019), relying on a combined L- and X-band approach, observed ground subsidence of a solid waste landfill park in Seoul, Korea.

Finally, it is worth reporting that a positive correlation between surface subsidence and the occurrence of heavy rainfall is highlighted by some authors (Rateb and Hermas, 2020). Precipitation has been also recognized as a dominant factor influencing the seasonal component of subsidence (Li et al., 2021b; Zhou et al., 2017b). Reduced rainfall infiltration has been claimed as a concurrent cause of land subsidence (Catalao et al., 2016; Suganthi et al., 2017).

5.3. Data application and usage

The last two decades witnessed the launches, by different space agencies worldwide, of several satellite platforms hosting different SAR sensors and operating with different frequencies and wavelengths. A general increase in imaging capabilities, both in terms of spatial and temporal resolution, has been guaranteed by a new generation of satellites.

Satellite InSAR has a major role to play in studying subsidence events. The exploitation of extensive image datasets dating back to the early '90s (*e.g.*, ERS and JERS) and the systematic stream of information ensured by current conflict-free missions (*e.g.*, Sentinel-1) allowed to cover different aspects of subsidence analysis, from historical mapping to monitoring. The large availability of different microwave bands allowed flexible satellite InSAR data to be used at different scales of analysis (from a local to a national level) and in different settings, including urban, agricultural and vegetated scenarios.

The 1059 records within the literature database have been critically analysed to identify the type of application. Seven macro-classes of data usage have been identified to provide a comprehensive overview of satellite InSAR applications for subsidence analysis. The first four classes have been defined to cover different stages needed to study subsidence events and bearing in mind the different actions required for subsidence mitigation, as stated by the Panel on Land Subsidence of the US National Research Council (1991): *i*) mapping, *ii*) monitoring, *iii*) characterization and *iv*) monitoring. Three more categories have been added, covering aspects that cannot be included in the previous four classes: *v*) simulated subsidence, *vi*) review and *vii*) technical paper.

A summary of the type of data usage and application is presented in Fig. 10. A very minor portion of the contributions (68 of 1059, *i.e.*, 6.4%) belongs to two different categories when the content could not be univocally attributed to one class. This stands for those contributions focusing on different aspects of subsidence analysis, for instance, the creation of a synoptic view of ground deformation or the analysis of displacement time series.

5.3.1. Mapping

Mapping activities rely on the detection of magnitude and distribution of subsidence through retrieval of basic earth-science data at different scales to address localized problems and to identify wide-area events. Evaluation of possible interference with the urban fabric, facilities, and infrastructures can be performed.

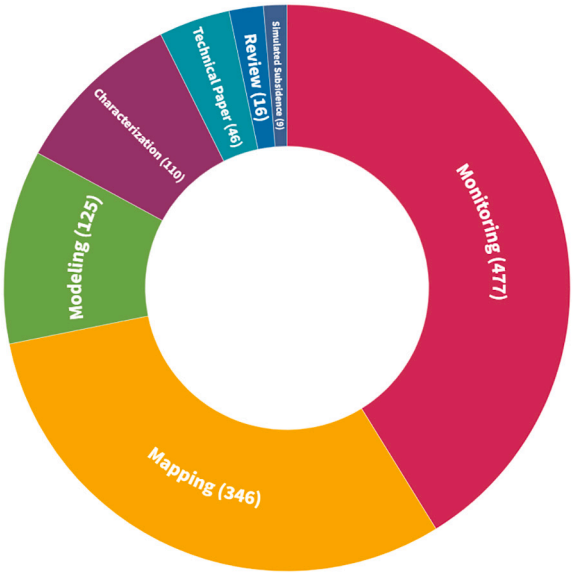

Fig. 10. Data usage and applications from literature analysis. The first four classes (Mapping, Monitoring, Characterization and Modeling) represent more than 90% of applications within the database, though Technical Paper and Review contributions are well represented

Retrieval of robust estimation of ground deformation occurring at the regional scale is the most consolidated application of satellite interferometry. Since the late 90's (Fielding et al., 1998), subsidence has been measured from space using single pairs (Buckley et al., 2003) and stacks of interferograms (Ng et al., 2010) with time separations ranging from a few days to several months (Baer et al., 2002) to cover phenomena with different kinematics. DInSAR successfully measured a wide range of deformation velocities ranging from m/year to mm/year (Strozzi et al., 2001). Chang et al. (2005) used the ERS-1/2 tandem mission to map areas where large ground displacement happens within 24 h.

By exploiting several interferometric pairs (Strozzi et al., 2003) and their temporal combination (Cigna et al., 2019), the occurrence of ground deformation has been observed over thousands of squared kilometres, leveraging on the wide-area mapping capability of spaceborne sensors. To discriminate between different deformation regimes in mining areas DInSAR and PSI can be used (Perski et al., 2009).

Wide-area survey provides the first overview of ground displacement hotspots, assessing the relationship with different geological processes and various geological environments (Floris et al., 2019; Meisina et al., 2008). A simple procedure to map subsidence at the regional scale using interferometric techniques is presented by Rosi et al. (2014), consisting of the combination of the vertical and horizontal components of the deformation measured by satellite. This approach has been largely used to calculate the displacement direction and characterize ground subsidence related to groundwater exploitation (Raspini et al., 2012) and geothermal prospect (Temtime et al., 2018) and modeling studies that consider tectonic and anthropogenic activity (Papoutsis et al., 2017). The use of cross-heading tracks allows for the identification of horizontal movements induced by sharp subsidence.

Knowledge gathered thanks to regional surveys and hotspot identification provides supporting information for the first delimitation of areas affected by ground deformations (Fernandez et al., 2009), to pinpoint areas with limited or null pre-existing information (Castellazzi et al., 2016a), to spot illegal activities (Hu et al., 2013) and to track the shift of the locus of maximum subsidence (Cabral-Cano et al., 2008), with particular attention to urbanized areas.

Given the intrinsic characteristic of processing approaches, satellite interferometry has been largely used to detect, map and quantify subsidence in urbanized areas (Crosetto et al., 2003; Raucoules et al., 2003a; Zhang et al., 2011) which represent the ideal scenario given the diffuse presence of stable radar reflectors. Many international projects have fostered the use of satellite interferometry to measure ground motion related to subsidence at a pan-European scale (Radutu et al., 2017; Raspini et al., 2016), including geohazards affecting cultural heritage (Cigna et al., 2016b) and vertical ground movements in the coastal areas (Graniczny et al., 2015). Many metropolitan areas have become the target for interferometric analysis, among which Mexico City (Cigna et al., 2011; Sowter et al., 2016), Athens (Parcharidis et al., 2006), Rome (Blasco et al., 2019) Guangzhou (Zhao et al., 2009b) and Beijing (Zhou et al., 2017a), where resolving effects of large underground engineering projects can be valuable (Fruneau and Sarti, 2000; Tesauro et al., 2000). Taking advantage of high-resolution X-band imagery Cigna et al. (2014) and Le et al. (2016) depicted the deformation of the historic centre of Rome and Hanoi, with details at the level of single building and monument. Analysis of linear infrastructures has been successfully carried out with the interferometric technique (Parcharidis et al., 2009; Raspini et al., 2013) mainly to identify differential displacements and ground fracture delineation, essential for urban development planning (Castellazzi et al., 2017).

Despite well-known limitations, SAR interferometry has been used to give a two-dimensional spatial coverage over non-urban, natural areas (Aly et al., 2012; Da Lio et al., 2018), mainly thanks to applications of different bands (Wegmuller et al., 2004; Wempen and McCarter, 2017; Zhou et al., 2018), adoption of current SAR satellites which perform better than their predecessors (Cascini et al., 2013; Ng et al., 2017) and, finally through the combination of different processing algorithms (Poitevin et al., 2019) and synergy of persistent and distributed scatterers (Zhang et al., 2019a; Zhang et al., 2015b).

5.3.2. Monitoring

Monitoring means the regular measure of the surface displacement field induced by the event and reconstruction of its evolution history. While data on spatial variations and patterns are commonly available, the temporal evolution of the investigated event is usually hampered by suitable information acquired in a systematic fashion.

Ma et al. (2019) adopted a synergistic approach based on multi-sensor SAR images to demonstrate the practicability of the operational monitoring of subsidence at different scales from regional surveying to the fine surveillance of specific areas. Many authors recognized that the exploitation of large archives to retrieve very long deformation time series can play a key role in understanding the dynamics of natural and human-induced subsidence (Del Ventisette et al., 2013; Ge et al., 2007; Teatini et al., 2012; Tosi et al., 2016). Zhang et al. (2016b) reported a complete tracking of ground subsidence for the Beijing-Tianjin-Hebei region over a long-time span from 1992 to 2014 using the existing C-band archives (ERS, Envisat and RADARSAT-2). Having suffered dramatic ground subsidence during the last two to three decades, the spatial-temporal characteristics of the development of ground subsidence in Beijing and Tianjin have been analysed by many researchers using multi-temporal InSAR technology (Du et al., 2018a; Guo et al., 2019), also using high-resolution X-band data to increase the detail of surface evolution of strategic infrastructures (Gao et al., 2019) and to extend the application of PSI in detecting subsidence in areas with frequent surface changes (Yu et al., 2013) with the deployment of artificial corner reflectors.

Supported by accessible satellite datasets and by the flourishing of software packages, subsidence monitoring is feasible worldwide (Cian et al., 2019) covering a wide range of scenarios: deltaic environment (Parcharidis et al., 2013), tunnel excavation advancement (Roccheggiani et al., 2019; Strozzi et al., 2017), land reclamation (Sun et al., 2018), peat settlement (Marshall et al., 2018), natural gas (Gee et al., 2016) and oil extraction (Moghaddam et al., 2013) and civil infrastructures analysis (Cigna et al., 2017; Corsetti et al., 2018; Luo et al., 2017).

Besides the reconstruction of historical evolution, the production of surface deformation maps for different periods is devoted to highlight any changes in trends, including oscillations, steps, or accelerations within displacement time series. Raucoules et al. (2013b) evidenced temporally variable ground deformation in the Manila urban area (Philippines) based on satellite SAR interferometry from 1993 to 2010. Ojha et al. (2018) presented a multitemporal InSAR measurement of land subsidence in Central Valley (California, USA), which shows seasonal oscillations and response to frequent and intensified droughts. Hsieh et al. (2011) reported that the subsidence rate in dry seasons is about 3 cm larger than in wet seasons for south-western Taiwan. Time-dependent deformation signals are reported, including seasonal uplift and lowering for areas interested by subsidence related to groundwater exploitation and recovery (Schmidt and Bürgmann, 2003), hydraulic head fluctuations (Dehghani et al., 2009), dynamic freeze-thaw processes of the active layer (Chen et al., 2018c). Signatures of CO_2 injection regime (Bohloli et al., 2018), tunnel drainage-induced pore pressure changes (Strozzi et al., 2011), upward movement after closure and flooding of deep mines (Vervoort and Declercq, 2018) and water table restoration (Blachowski et al., 2019) can also be tracked with InSAR data.

Carnec and Delacourt (2000) and Raucoules et al. (2003b) recognized the great potential of SAR interferometry to regularly monitor mining subsidence. Following these pioneering works, SAR interferometry opened up wide application prospects, including analysis of slow but continuous subsidence associated with abandoned coal mines (Jung et al., 2007), subsidence increases due to rapid coal fires (Jiang et al.,

2011) and residual mining deformations after the end of the mining exploitation (Blachowski et al., 2018; Gueguen et al., 2009; Modeste et al., 2021; Vervoort and Declercq, 2017).

Validation and intercomparison of InSAR products (velocity maps and displacement time series) deriving from different processing techniques are presented by Herrera et al. (2009b) for subsidence induced by the overexploitation of aquifers and by Raucoules et al. (2009) for mining areas, to assess similarities and discrepancies. Rigorous approaches and methods of trend analysis to exploit InSAR time series for subsidence monitoring at their full potential are presented by (Notti et al., 2015) and by Del Soldato et al. (2019).

5.3.3. Characterization

Characterization activities include the synergic analysis of deformation data, ground survey evidence, *in situ* measurements and hydrogeological information of the subsoil. While a general understanding of the subsidence processes is well consolidated, identification of triggering factors is commonly hampered by the inability to determine subsurface conditions and geological properties of the material affected by deformation.

Hoffmann et al. (2001) derive estimates of the elastic storage coefficient for the aquifer system in Las Vegas Valley by comparing hydraulic head fluctuations and seasonal subsidence and rebound yielded by ERS interferograms. Subsidence and uplift have been detected also by Robson et al. (2021) in the Arctic environment, where differences in terrain condition (in terms of topography, humidity, temperature, depth to the frost table) generate seasonal vertical movements (freeze and thaw cycle).

Herrera et al. (2010a) performed a comparison of TerraSAR-X InSAR results for the subsidence phenomenon in the city of Murcia (SE Spain) with conditioning and triggering factors: thickness of the compressible layers, presence of pumping wells, piezometric level variations. This synergic analysis permitted to demonstrate that ground surface displacement variations have occurred as a result of soil consolidation due to piezometric level depletion caused by excessive pumping of groundwater. Bru et al. (2013) presented a detailed structural damage analysis of several buildings in Murcia, founding a positive correlation between the presence of buildings with superficial foundations and a high deformation rates. Tomás et al. (2012) and Herrera et al. (2012) presented the potential of satellite InSAR as a complementary tool for the forensic analysis and characterization of settlement of building structures.

Several studies have used InSAR techniques to evaluate the ground deformation in Los Angeles and San Joaquin basins in California. ERS data were deployed by Watson et al. (2002) to infer the seasonal land deformations in the Los Angeles basin related to water table, whose widespread and repeated annual variations in the elevation (extraction and replenishment) may mask the existing tectonic signals. Khorrami et al. (2019) detailed the ground displacement patterns along a new metro tunnel in Los Angeles, looking for asymmetrical subsidence related to heterogeneities of the ground layers. Ground lowering occurring in the San Joaquin Valley, one of the most productive agricultural regions in the USA, has been analysed by multi-band InSAR data, showing strong variability in location, magnitude and rate of subsidence (Jeanne et al., 2019) depending on groundwater demand for irrigation purposes (Levy et al., 2020), groundwater level change (Liu et al., 2019) and occurrence of drought periods.

Spatial and temporal investigations of land subsidence patterns are particularly important in coastal areas, where a comprehensive and exhaustive understanding of the deformation mechanism is of paramount importance. Bianchini and Moretti (2015) and Cianflone et al. (2015) provided a quantitative evaluation of the subsidence process in the Sibari plain on the Ionian coast of Calabria (South Italy), along with temporal evolution trends of the phenomenon. Da Lio and Tosi (2018) and Amato et al. (2020) presented InSAR results for the Adriatic and Tyrrhenian coastal areas, respectively. Despite the variability in geomorphological, geological and environmental settings, all the authors stressed the importance of a multidisciplinary approach to understand land subsidence along densely populated coastal lowland areas, widely recognized as highly vulnerable to the impacts of global climate change, namely sea-level rise, erosion, inundation and saltwater intrusion.

Northumberland and Durham coalfields in the United Kingdom (Gee et al., 2017), Lisbon in Portugal (Heleno et al., 2011), Orihuela in Spain (Tomas et al., 2010b), the Po Plain in Italy (Boni et al., 2016), Teheran in Iran (Haghighi and Motagh, 2019) and Mexico City (Chaussard et al., 2021) are other areas where multi-platform InSAR measurements, analysed in conjunction with stratigraphy, tectonics, urbanization changes and groundwater extraction locations and volumes, allowed to identify triggering factors, to resolve spatial and temporal variations of land subsidence and to assess socioeconomic landscape consequences.

Mainly due to the aquifer over-exploitation and to the decrease in regional groundwater storage (Yu et al., 2021), the Beijing region in China has been suffering from land subsidence since 1935 and several studies have been conducted to provide comprehensive spatio-temporal analysis, to reveal the mechanism of land subsidence and to build a hydrogeological model. Chen et al. (2019) quantified the lag time between groundwater level drops in the main exploited aquifer layers and land subsidence observed with RADARSAT-2 images. Guo et al. (2021) quantified the relationship between the urban expansion of Beijing and land subsidence from 1990 to 2015 and, adopting a multidisciplinary approach, analysed the mechanism of subsidence variation in this time interval. Guo et al. (2020) combined InSAR and seismic prospecting to reveal the contribution of compressible layers to the occurrence of uneven land subsidence. Effects on water balance and land subsidence of the Water Diversion Project, designed to alleviate the water resource crisis in the Beijing area, have been evaluated by Du et al. (2021) and Zhu et al. (2020) using InSAR data spanning from 2007 to 2020.

5.3.4. Modeling and prediction

This activity relies on the integration of displacement data and geological and geotechnical modeling to support the definition of the deformation process and on the use of interferometric data as inputs for the assessment and refinement of future scenarios. Ingestion of interferometric data within subsidence risk evaluation is also included in this category. This type of information is of great value, especially in those urbanized areas endangered by ground movement and where the investigated phenomenon is going to threaten valuable elements at risk and mitigation measures are needed.

Coda et al. (2019) and Ezquerro et al. (2017) highlighted the importance of InSAR monitoring data for the implementation of an appropriate hydro-mechanical deformation model of land subsidence in urban areas. Tomas et al. (2010a) and Ezquerro et al. (2014) used multitemporal InSAR datasets to calibrate deformation parameters of a one-dimensional model and to validate predicted subsidence for the city of Murcia and Madrid in Spain, respectively. Tessitore et al. (2016) implemented a series of 1D FEM to reproduce the time-dependent and superficial distribution of displacements. Model computations have been validated with InSAR data. Two-dimensional finite element modeling analyses have been carried out along representative sections to determine land subsidence occurring due to mining operations (Unlu et al., 2013) and groundwater exploitation (Raspini et al., 2014). In both cases, land subsidence predicted from modeling studies has been successfully compared to InSAR measurements. Modeling and prediction of 3-D mining-induced displacements, constrained and calibrated by InSAR monitoring data, are presented by Woo et al. (2012) and Yang et al. (2017b).

Despite the simplicity of some theoretical deformation models adopted to simulate the peculiar features of subsidence (Canova et al., 2012), findings presented in the literature show the usefulness of the InSAR-derived displacement information to characterize mechanisms involved in subsidence phenomena (in terms of depths and locations of

the source area, *e.g.*, to define deformational behaviour of groundwater storage (Smith et al., 2017), to calibrate response model to the dynamic variations of groundwater (Chen et al., 2011) and to predict subsidence given different hydrological scenarios (Smith and Knight, 2019).

Many authors have exploited InSAR data to support the definition of parameters necessary to model and assess land subsidence risk. Hernandez-Espriu et al. (2014) proposed a modified version of the DRASTIC methodology, to develop reliable vulnerability assessments on the urban fabric in subsiding basins. Subsidence models and InSAR interferometry have been integrated to produce hazard maps (Choi et al., 2011; Diao et al., 2016; Zhang et al., 2016a) and to train machine learning algorithms for susceptibility assessment (Hakim et al., 2020). Ezquerro et al. (2020a) performed a vulnerability assessment of buildings to land subsidence and produced damage probability and potential economic loss maps by taking advantage of different SAR missions for the city of Pistoia (Italy). Nadiri et al. (2018) and (Nadiri et al., 2020) introduced a general framework to assess subsidence vulnerability based on different input data, including satellite InSAR.

The importance of a detailed understanding of past and current deformation rates for the prediction of future subsidence is stressed by several authors. Burbey and Zhang (2015), based on high spatial and temporal resolution subsidence observations from InSAR and hydraulic head data, developed a refined hydrogeological model for the Las Vegas basin to evaluate future predictions up to year 2030 and to assess potential mitigation measures. Catalao et al. (2020) and Gao et al. (2021) merged InSAR measurements with sea-level rise scenarios proposed by 2100 projections to identify projected inundated areas and to provide a map of flood vulnerability in Singapore and Penang Island (Malaysia), respectively. Yin et al. (2019) studied the long-term coastal flood risk of Shanghai considering 100- and 1000-year coastal flood return periods, local sea-level rise projections, and ground deformation rates for the 2030s and 2050s estimated by using the current InSAR datasets. Miller and Shirzaei (2021) adopted a similar approach to quantify the extent of flooding hazards in the coastal area of Texas (USA) under different scenarios.

Integration of satellite InSAR data with a deep learning-based method (Li et al., 2021a) and artificial neural network was demonstrated to be an accurate and reliable method for time series analysis and prediction of their near-future displacement (Rahmani and Ahmadi, 2018) and for evaluating the influences of different geology and hydrogeology factors on the subsidence (Dehghani et al., 2013). More recently, the application of the Gray-Markov model to land subsidence prediction has been proposed by Yuan et al. (2021) and Deng et al. (2017) for areas interested by mining activities and groundwater withdrawal, respectively.

5.3.5. Simulated subsidence

In this category are included those works that simulate land subsidence occurrence by assuming a set of geological and triggering conditions and that considered geometrical imaging characteristics of different radar sensors to mimic real InSAR data. Ng et al. (2009) presented a simulated assessment of the performance of satellite radar data acquired using different operating frequencies (C-, X- and L-band) from the ERS, ENVISAT, TerraSAR-X, COSMO-SkyMed, JERS-1 and ALOS-1 satellite missions. In particular, the paper reports the impact of noise effects of spatial and temporal decorrelation between the interferometric pair for monitoring mining-induced ground subsidence, turning out that longer radar wavelength, greater incident angle and finer ground imaging resolution can improve the quality of interferograms. Fan et al. (2014) tested the ability of mine subsidence monitoring trough DInSAR, by comparing simulated and measured values of deformation.

Li et al. (2017) used simulated land subsidence, mimicking InSAR data to reproduce a surface deformation pattern derived from InSAR analyses, to inversely infer inelastic specific storage, a parameter that plays a more important role in the development of the long-term delayed land subsidence. Wang et al. (2018), assuming specific acquisition parameters (satellite incidence angle and track direction), simulated the cumulative D-InSAR deformation along the LOS direction caused by working face mining and, following a comparison with real TerraSAR-X data, an assessment of errors was provided. Jiang et al. (2021) proposed a method to extract 3D deformation related to mining activity based on the simulated geological and mining conditions *(e.g.*, mining depth and velocity, seam thickness), assuming SAR imaging capabilities like those provided by Sentinel-1. Obtained results then are used to assist the phase unwrapping of real DInSAR processing applied to Sentinel-1 pair to resolve large-gradient deformation in a short period in a coal mine in the Anhui Province in China (Dai et al., 2021). The same area has been selected by Wang et al. (2021a) to model the spatio-temporal relationship between underground mining and ground surface response by using simulated DInSAR deformation data.

5.3.6. Review

A review is a type of contribution that analyses and discusses a specific topic, summarizing the state of the art at the time of publication, including the latest progress made in a given area of research. Bibliographic collection, survey and synopsis of previously published studies, dealing with both technical aspects and applications of satellite InSAR for subsidence analysis, have been labelled as review. Smith (2002) provided the first review of pioneering geomorphic and hydrologic applications of satellite InSAR, emphasizing its great ability to provide ground measurements, complementary to traditional field data, suitable for a wide range of applications in the earth sciences. Following a collective assessment of these applications, this author recognized land subsidence as the most consolidated among geohazard and encouraged the use of InSAR within the geophysical science community.

Following some initial hesitation, the hydrogeology community (Hoffmann, 2005) has embraced satellite sensors as tools in its works and InSAR has gained a high level of visibility, thanks to a series of investigations showing how spatially detailed time-lapse images of ground displacements provided by InSAR, used in concert with ground-truth information, have fostered hydrogeologic understanding (Galloway and Hoffmann, 2007). Despite some technical limitations related to satellite orbital configurations, the use of InSAR was considered promising, and great expectations were placed on future sensors (*e.g.*, TerraSAR-X and ALOS-PALSAR), which would have extended InSAR applicability. An extensive review of detection, assessment, monitoring and simulation models of land subsidence accompanying groundwater pumping is presented by Galloway and Burbey (2011). More recently, Guzy and Malinowska (2020) reviewed the various types of models used to simulate groundwater withdrawal-induced land subsidence and discussed recent advancements, including details on the current role of measurement data derived from InSAR observations.

Technological improvement, enhanced imaging capability and availability of different spaceborne platforms made InSAR widely used to study surface subsidence due to underground mining. Ishwar and Kumar (2017) provided a detailed review of the applications of spaceborne SAR interferometric techniques in the mapping, monitoring and prediction of surface subsidence due to underground mining. More recently, Hu et al. (2021) discuss the challenges in the use of SAR images to monitor fast and large gradient coal mining subsidence, summarizing the main approaches to overcome these problems, including the combination of InSAR with prediction models and *in-situ* measurements and use of offset-tracking approaches on amplitude information.

Ferretti et al. (2015) proposed the potential prospects of using SAR for monitoring land subsidence, identifying some promising areas for future research and highlighting the key points for the operational use of this technology. A relevant facet is the transition from historical satellite analyses to near-real-time monitoring schemes based on systematic SAR imagery processing.

5.3.7. Technical paper

This last category encompasses documents that describe: i)

significant developments and improvements of algorithms, ii) novel aspects or new results of processing approaches, iii) progress and advances of experimental and theoretical methods relevant to the scope. This category includes a wide range of documents that contributed to define the applicability of satellite InSAR for subsidence analysis and, through continuous technical improvements, had the merit to pave the way for the growing use of EO information. Ferretti et al. (2000) introduced the PS technique (Permanent Scatterers, *i.e.*, radar targets that are coherent over several years), a game-changer in the interferometry approaches, having the capability to separate and identify the different contributions within the interferometric phase of each PS. Crosetto et al. (2005) suggested the adoption of two levels of analysis for deformation measurement based on the DInSAR technique: the first one includes a low-cost screening over wide areas carried out using a limited set of SAR images to spot deformation phenomena; the second one relies on a finer analysis at local scale based on larger image stacks. This approach guarantees a proper allocation of data processing resources, saving time in case of operational use of DInSAR data. Navarro-Sanchez et al. (2014), Navarro-Sanchez and Lopez-Sanchez (2012) and Navarro-Sanchez and Lopez-Sanchez (2014) presented and evaluated the polarimetric diversity to optimize the results of persistent scatterers interferometry. Subsidence maps are computed for dual-pol, and full-pol RADARSAT-2 and TerraSAR-X acquisitions. Approaches succeeded in increasing the density of selected stable pixels, with respect to single-pol data.

Further improvements include mitigation of errors resulting from phase delay of the radar signal propagating through the atmosphere adopting stochastic filtering (Crosetto et al., 2002), stratified atmosphere model (Tang et al., 2016; Tang et al., 2018), ECMWF products (Haji-Aghajany and Amerian, 2020) or MERIS data (Aguemoune et al., 2019).

Algorithm refinement has been proposed to minimize the effects of residual topography (Gaber et al., 2017), large perpendicular baselines and strong temporal decorrelation (Foroughnia et al., 2019) and to assess the interferometric coherence to baselines, doppler difference, land surface evolution and polarization (Engelbrecht et al., 2014). Hybrid methods, fusing different methodological approaches have been proposed to better estimate land subsidence over noisy pixels (Chi et al., 2021; Neely et al., 2020; Taravatrooy et al., 2018) and for rural areas (Sadeghi et al., 2012). Gheorghe and Armas (2015) presented a comparison between the most popular MT-InSAR methods that are used for subsidence analysis, *i.e.*, the PS and SBAS techniques, the first one more suitable for studying infrastructure behaviour, the latter for long-term geological patterns.

Strozzi et al. (2013) deployed a network of dozens of trihedral corner reflectors to improve the coverage of satellite SAR-derived estimates in salt marshes and lagoon environments, where lack of long-term stable targets led interferometry to fail. Peduto et al. (2015) provide guidelines and protocols for the use of DInSAR data in the study of subsidence phenomena. These authors introduced a general protocol, tested on sample areas of Italy and tailored at different scales, for the analysis of subsidence and related consequences to exposed facilities. The need for a standardized methodology for the assessment of land subsidence is highlighted by Comerci and Vittori (2019).

Web-based platforms and collaborative projects, such as the GEP (Galve et al., 2017) and open-source InSAR time series analysis package (Morishita et al., 2020) are revolutionizing the way to analyse remote sensing data, fostering the exploitation of abundant SAR dataset globally available with the launch of Sentinel-1 mission.

In the last years, convolutional neural networks emerged as a promising tool in subsidence analysis, supporting phase unwrapping and extraction of interferometric fringes (Wang et al., 2021b) and the development of an effective system for the detection of subsidence troughs in SAR interferograms (Rotter and Muron, 2021).

5.4. Data integration

Collection of multiple environmental data, as well as the intervention of different scientific specialties, is often required to validate satellite SAR data and to support the interpretation of ground subsidence mechanism and origins. The 1059 contributions collected have been scanned to check if and how satellite SAR information has been used in synergy with other data (whatever their source may be). Finally, the existence of a field check of the analysed subsidence has been determined, relying on information provided by the authors.

Among the 1059 contributions, 744 (70.2%) include an integration (single or multiple) with other data, in line with the percentage (68%) reported by Solari et al. (2020) for landslide analysis and by Mondini et al. (2021) for failure detection, testifying that, whatever the geohazard, validation/integration of InSAR data with other sources is an important task for the authors. In general, the purpose of this integration can be twofold:

i) a validation activity, *i.e.*, to assess the consistency of InSAR results with measurements data retrieved by other instruments. This activity consists of the spatial and temporal comparison of InSAR results with independent ground movement data mostly collected from conventional, ground-based sensors or other InSAR results to assess any similarities and discrepancies.

ii) a comparison of InSAR results with other thematic information, following the "radar-interpretation" approach conceived by Farina et al. (2008) in the field of landslide investigation and extended by the scientist community also to subsidence analyses. This comparison relies on the combination of InSAR with thematic data (*e.g.*, hydrogeological, geomorphologic, geological and land use maps), optical images (both aerial and satellite data) to assign a geomorphological meaning to LOS displacements measurements and to support the analysis of the phenomenon, in terms of typology, causes and temporal evolution.

Summaries of the sources of data and information used for satellite InSAR validation and comparison are presented in Fig. 11 e Fig. 12 respectively.

5.4.1. Data validation

Not surprisingly, geodetic precise leveling, which is the most accurate method to detect elevation changes, being utilized with

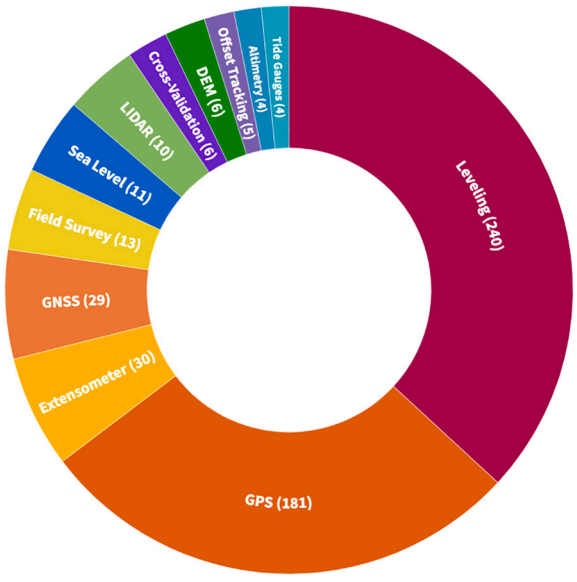

Fig. 11. Instruments, information and methods used for satellite InSAR validation as extracted from the literature analysis. Assessment of consistency between InSAR data and other sources of information is considered a fundamental activity by many authors to increase reliability of satellite methods.

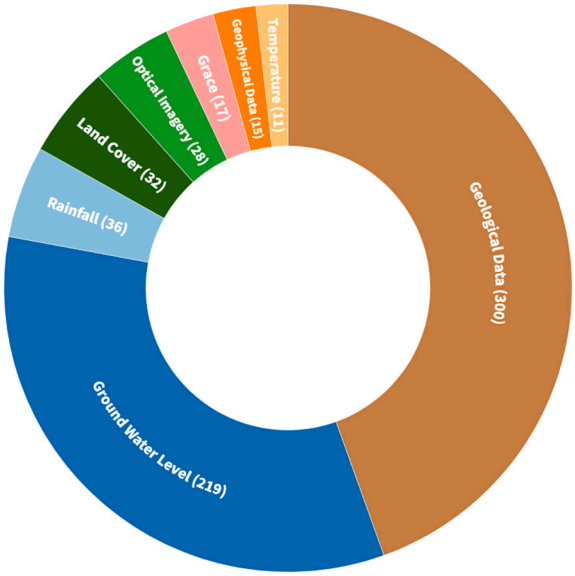

Fig. 12. Thematic information, used in thigh synergy with satellite InSAR, extracted from the literature analysis. Comparison of InSAR data with ground truth information is a consolidated strategy adopted by many authors to support interpretation of the analysed phenomenon.

standardized procedures for several decades, represents the most used (240 times, corresponding to 23% of the whole database) measurement tool for InSAR validation. Both leveling and PSI deliver the pointwise and pixel-wise vertical component of displacements, and the former may be 10 times more accurate than the latter (mm *vs.* cm, depending on processing characteristics), while the density of PSI observations may be thousands of times higher than that of leveling observations. Zhou et al. (2003), Hung et al. (2011) and Sarychikhina et al. (2011) proposed fusion methods to merge PSI and leveling results, based on geostatistical approaches to assess errors contained in the InSAR measurements and to retrieve a merged field, which better represents the overall subsidence pattern, improving the understanding of the temporal and spatial distributions of subsidence. Karila et al. (2013) presented results of a comparison between urban subsidence rates retrieved from SAR interferometry and precise leveling of building foundations. Examples of validation of InSAR data through leveling observations are presented by many authors (*e.g.*, Anderssohn et al., 2008; Chen et al., 2013; Lubis et al., 2011; Luo et al., 2014a; Zhang et al., 2015a), pointing out that, despite obvious differences between two techniques, PSI results generally agreed rather well with the leveling data.

Information collected by GPS networks, both continuous (Bock et al., 2012) and periodically surveyed (Bejar-Pizarro et al., 2016) are other trusted sources (counted 181 times) of validation and comparison (Zhang et al., 2009) since they provide users with high accuracy 3D positioning at the sub-centimetre level. To assess consistency between different source data (Akbari and Motagh, 2012; Ustun et al., 2015), GPS and InSAR motions must be referred to the same frame, usually projecting the three-dimensional GPS vectors collected in the local reference frame (N, E, U) into the InSAR satellite's LOS (Hu et al., 2019b) or comparing the vertical component only (Miller et al., 2017).

GNSS permanent networks, which consist of a series of stations that belongs to national continuously operating reference stations are also used (29 times) to validate the SAR velocities (Yalvac, 2020) and to obtain absolute measurements (Del Soldato et al., 2018). Farolfi et al. (2019) proposed a methodology to calibrate and fix relative InSAR displacements and velocities into conventional geodetic reference systems. GNSS acquisitions can be used to retrieve higher detail of horizontal displacement (Hu et al., 2019a), complementing InSAR data that are more sensitive to the vertical component and overcoming the lack of absolute reference both in time and space of satellite data.

Extensometers measurements, providing convenient ground control along columns of soil, have been also used (30 times) to constrain the interferometry results (Buckley et al., 2003; Calderhead et al., 2010; Tessitore et al., 2016) being aware that, depending on the depths of the extensometer bases relative to the compacting layer, the extensometers may measure only a partial amount of the total subsidence.

Some authors investigated the relationship between spatial patterns of ground deformation and topographic changes by using DEM, built with stereo images using space-borne optical photogrammetry (Pu et al., 2021) or the space-based radar such as the Coastal-DEM (Duffy et al., 2020). This latter has the great advantage, with respect to other prevalent DEMs, to have a reduced vertical bias in low-lying, coastal densely populated areas, where accurate elevation data is vital for accurate inundation risk assessment. High-resolution elevation measurements produced with airborne LiDAR sensors have been integrated with InSAR subsidence trends where microtopography and detailed reconstruction of landforms are highly valuable, such as permafrost- (Liu et al., 2015; Strozzi et al., 2018) and sinkhole-related subsidence scenarios (Baer et al., 2018; Nof et al., 2019) and where accurate topographic mapping is vital, such as in urban fabric (He et al., 2021), coastal areas (Anzidei et al., 2021; Miller and Shirzaei, 2021) and for strategic infrastructure analysis (Ma et al., 2019).

In the latter scenario, vertical land motion measured by InSAR is often used in synergy with tide gauges, a conventional point-wise method to measure sea level relative to the land (Carbognin et al., 2004; Di Paola et al., 2018; Raucoules et al., 2013b) and with satellite radar altimetry (Catalao et al., 2020; Ma et al., 2017) to monitor coastal sea-level changes, the latter being highly valuable, especially along coastal areas where tide gauge data are not available. The combination of space-borne and geodetic methods to monitor relative sea-level changes (Tang et al., 2021) and vertical land motion has been highlighted as essential for coastal management by many authors (Elias et al., 2020; Poitevin et al., 2019), sometimes including GPS stations (Vadivel et al., 2019).

The use of satellite InSAR, in synergy with data collected by different techniques for analysis of land subsidence, has been discussed by many authors, which proposed multiple combinations, including leveling and GPS (Chatterjee et al., 2015; Ezquerro et al., 2020b; Fiaschi et al., 2018; Motagh et al., 2007; Zhao et al., 2018), leveling and GNSS (Morishita et al., 2020) and GNSS and GPS (Zhang et al., 2019b). One-dimensional measures of compaction and expansion of a specific depth interval are often used with information provided by superficial sensors, such as leveling (Zhu et al., 2015) and GPS (Kim et al., 2015; Qu et al., 2015). The complementarity of three remote sensing techniques (GPS, LiDAR and InSAR) has been discussed by Khan et al. (2014). The advantages of multi-sensor monitoring results for subsidence interpretation are highlighted by Hsu et al. (2015).

Cross-validation between two multi-temporal SAR data stacks that cover the same area is presented by Kim et al. (2008), while Peng et al. (2019) used four independent datasets sharing a similar time coverage to cross-validate both deformation rates and time series. Validated approaches to merge InSAR technology and Pixel-Offset approaches have been proposed, being the latter able to retrieve 3-D mining-related displacements (Fan et al., 2021), displacements in those mining areas characterized by large magnitudes (Chen et al., 2015b) and/or steep gradients of surface deformation (Ou et al., 2018; Xu et al., 2020; Yang et al., 2017a).

Other common validation practices include field surveys (Jung et al., 2007), aimed to collect geomorphological evidence on the ground or damage catalogues to buildings and infrastructures (Tomás et al., 2012). One of the most challenging aspects when performing campaigns is that subsidence phenomena can be subtle and hardly detectable. Most likely land subsidence phenomena extend gently over large areas (tens to hundreds of km^2), present low to moderate deformation rates and can place for several decades, sometimes without being noticed at the

beginning (Carbognin, 1985). Deleterious effects of subsidence range from minor (Zhao et al., 2018) and moderate (Ma et al., 2016) changes in the landscape to major damage to structures (Bru et al., 2017; Zhang et al., 2015a) or to the environment itself (Zhao et al., 2009a), including aquifer quality degradation (van der Horst et al., 2018) and increased intensity and duration of flooding (Figueroa-Miranda et al., 2020) and storm surges. Localized differential settlement causes serious damage to buildings (Bru et al., 2017; Li et al., 2019; Nappo et al., 2021), while severe translational and rotational movements make them uninhabitable and force their demolishment (Comerci et al., 2015). Long-lasting ground deformations can trigger damage (Gao et al., 2016) as well as loss of structural integrity (Erten and Rossi, 2019) of linear and point infrastructures in the form of pipeline and road network deformations, well-casing failures and protrusion (Raspini et al., 2014). Subsidence can cause damage to key transport infrastructures, requiring reparation works and constant attention (Gao et al., 2019).

The most pernicious consequence of land subsidence is the development of a series of ground fractures and surface ruptures, activated by horizontal strain generated by the bending of overburden associated with areas of differential (vertical) displacement. A ground fracture is an earth fissure that usually begins as hairline cracks and then develops into long, linear or arcuate or sigmoidal, almost vertical cracks in the ground (Budhu, 2011). Earth fissures may be several kilometres long (Long et al., 2021) and are commonly located near shallow bedrock or at the margins of the subsiding areas (Othman, 2018). While groundwater pumping has been recognized as the most diffuse mechanism (Holzer, 1984), fissures have been detected in areas with sinkholes (Kim et al., 2019), mining activities (Zhou et al., 2013), geothermal exploitation (Sarychikhina et al., 2010) and gas extraction ((van Thienen-Visser and Breunese, 2015)).

Lithologic variations (*e.g.*, degree of consolidation) and position of geologic structures such as buried faults (Murgia et al., 2019; Yang et al., 2019) control not only the development of fissures but also their location. Arid/hyper-arid conditions play an important role in fissures development (Ghazifard et al., 2017; Othman and Abotalib, 2019).

The city of Xi'an (Shi et al., 2020b; Zhao et al., 2009a) and Datong (Xiuming et al., 2008; Yang et al., 2014) in China, as well major cities in Mexico (Brunori et al., 2015; Cigna and Tapete, 2021a) and Iran (Ghazifard et al., 2016) are well-known areas undergoing significant land subsidence along with ground fissures development and where it turned out necessary to obtain the rate, extent, and temporal evolution of subsidence gradients, movements of fissures and the associated geohazards. The presence of fissures limits the continuity of groundwater flow and aggravates localized subsidence. Therefore, land subsidence and ground fissures mutually promote each other (Qu et al., 2014). In southern Arizona, a place where problems related to land subsidence and earth fissuring date back to the early 1950s, more than 251 km of earth fissures have been mapped (Conway, 2016), and warning signs are posted along roads.

5.4.2. Data comparison

Counted 300 and 219 times respectively, geological data and information on groundwater levels are the primary information used in synergy with satellite InSAR data for subsidence analysis. Both piezometric level evolution (Dang et al., 2014), pumping wells location (Tomas et al., 2011) and water extraction rates (Cigna and Tapete, 2021b) are included in the second group of information. Also geological data encompass a wide spectrum of information, from geomorphological mapping (Da Lio et al., 2018; Floris et al., 2019), details on the geological (Castellazzi et al., 2016a; Goorabi et al., 2020), tectonic (Woppelmann et al., 2013; Zhao et al., 2009a) and lithostratigraphic setting (Conesa-Garcia et al., 2016; Stramondo et al., 2008) to geotechnical investigations (Herrera et al., 2009b; Khorrami et al., 2019).

Hydraulic head variations provided by observation wells are often used to correlate the evolution of land subsidence and spatial-temporal changes in groundwater level (Bui et al., 2021), allowing the detection of spatially variable elastic and plastic deformation behaviour of subsoil (Tessitore et al., 2016), understanding seasonal surface deformation (Chang et al., 2004; Watson et al., 2002) and assessment of lag time (Chen et al., 2019; Gao et al., 2018). Recently, Smith and Li (2021) presented and discussed a method based on sparsely sampled measurements of InSAR deformation and groundwater levels to estimate hydrologic parameters, including elastic and inelastic deformation signals. Over wide areas, groundwater change series and trends are derived also from GRACE data (Gido et al., 2020a; Guo et al., 2016), that, despite the coarse spatial resolution (approximately hundreds of km^2), can retrieve large TWS changes from Earth's global gravity field every month (Strassberg et al., 2009). TWS is a cumulate measure that includes several components (biomass, soil moisture, surface water, snow and ice, groundwater). Therefore, to infer one component from total TWS (*e.g.*, groundwater storage), other components need to be measured or modelled. Groundwater storage changes have been estimated by subtracting soil moisture and surface water data (Castellazzi et al., 2016b; Liu et al., 2019) monitored on the field or estimated by simulation models. While in specific climate scenarios the snow and ice cover can be considered negligible (Agarwal et al., 2020), in others needs to be estimated (Yu et al., 2021), especially in cold areas when it contribute largely to the total TWS. Integration of GRACE data, groundwater levels, precipitation anomalies and InSAR data can provide guidance for groundwater management, highlighting delayed compaction despite the recovery of aquifer-systems (Ojha et al., 2020).

Groundwater level variation data are often used in conjunction with geological information (Goorabi et al., 2020) especially in a metropolitan area (Terranova et al., 2015), to assess governing parameters (Castellazzi et al., 2016a), to explain spatial and temporal variations of measured subsidence (Bozzano et al., 2015), to distinguish between triggering and conditioning factors (Tomas et al., 2011) and to implement coupled hydro-geomechanical model (Ezquerro et al., 2017). Luo et al. (2014b) combined L- and X-Band Multi-Temporal InSAR data with geological data, providing evidence that the degree of land subsidence in Tianjin (China) depends on the lithological patterns and the depth of the wells used for water exploitation. Some authors (Khakim et al., 2014) reported that where subsidence patterns do not correlate with groundwater withdrawal and well location, additional geological variables play important role in the subsidence process. Dehghani et al. (2013), comparing InSAR displacement with geological and piezometric data, found that geologic deposits are the most important factor controlling the subsidence rate in the southwestern Tehran Basin, regardless of the water level decline. Positive correlation between subsidence and Holocene deposit thickness (Du et al., 2020; Raspini et al., 2014), filled river valleys (Floris et al., 2019) and Quaternary sediments (Chen et al., 2012) is often found. Bonì et al. (2015) monitored the evolution of the severe cumulated displacements that occurred between 1992 and 2012 in the Alto Guadalentín Basin (Spain), founding a direct correlation with the thickness of the compressible alluvial deposits (Bejar-Pizarro et al., 2016) which, in turn, reveals that a delayed consolidation process occurring in a thick, soft soil layer with low permeability is responsible for the measured displacement. In the case of building loads, the comparison between InSAR data, stratigraphic sequence and geotechnical reconstruction allowed the evaluation of the timing of the primary and secondary consolidation processes (Ciampalini et al., 2019).

Geophysical investigations represent valuable support for the interpretation of InSAR data, as they depict the same geological elements from a complementary perspective: while geophysics analyses anomalies in mass distribution, InSAR measures corresponding ground deformation, with a mutual benefit (Closson et al., 2005). Gravimetric surveys have been used to determine the distribution of sediments susceptible to consolidation (Pacheco-Martinez et al., 2015) and to detect subsurface cavities (Closson, 2005) or shallow mass deficits (Paine et al., 2010), particularly useful to assess and monitor areas prone to collapse. Seismic surveys, unveiling subsurface architecture, supported the

evaluation of ground surface movements induced by gas storage activities (Codegone et al., 2016), geothermal exploitation (Temtime et al., 2018), and long-term exploitation of groundwater (Guo et al., 2020). GPR is another valid support to understand the physical state of the subsoil at different depth levels (Hubatka et al., 2021) and characterizing depressions mantled by artificial fills and buried structures (Gutierrez et al., 2011). Electrical resistivity data, collected by field surveys (Ghazifard et al., 2017) or with airborne platforms (Smith and Knight, 2019) has been successfully used to map stratigraphy of the subsurface and to distinguish different sediment layers. Mutual benefits of interferometry matched with electrical measurement profiles are shown by Raucoules et al. (2013a). Integration of different geophysical methods, hydrogeological data and satellite InSAR can resolve complex land processes and mechanisms (Long et al., 2021).

InSAR displacement maps have been compared and examined alongside meteorological records for analysis of land subsidence related to groundwater dynamics (Lei et al., 2014) and in permafrost environments (Robson et al., 2021). In the first scenario, precipitation has been recognized as one of the conditioning components of land subsidence, both as a predisposing parameter in semi-arid regions with limited water resources (El Kamali et al., 2021; Pulido-Bosch et al., 2012) and as a controlling factor, since nonlinear subsidence is often correlated with the seasonal rainfall (Shi et al., 2021). Wet season highly correlates with piezometric fluctuations in the aquifer (Li et al., 2021b; Notti et al., 2016) and may induce elastic expansion (rebound) (Khakim et al., 2014), as a response to seasonal-natural recharge of the aquifer itself. In permafrost environments, the displacement rate varies spatially and temporally depending on environmental factors (Chen et al., 2018c). However, the timing of seasonal surface displacements is closely related to ground temperature variation at the surface (Li et al., 2016) and at depth (Rouyet et al., 2019) and secondly to precipitation (Zhao et al., 2016), with the latter determining a direct heat exchange within the active layer, whose response to climate change can be observed with CALM grid (Bartsch et al., 2019). Temperature anomaly maps can be derived from Thermal Infrared data acquired from the Landsat-8 (band 10) (Karanam et al., 2021).

Relation between subsidence rates and land use has been also widely investigated (Du et al., 2018b; Zhou et al., 2017a; Zhou et al., 2016), as the latter can amplify existing deformation processes or initiate new phenomena (Minderhoud et al., 2018). Land use classes are also used for preliminary spatial analysis to evaluate PS density (Bakon et al., 2016) and radar visibility before interferometric processing (Cianflone et al., 2018).

Finally, it is worth remarking that optical imagery acquired from different satellite platforms was collected and effectively used to assess environmental parameters (Radman et al., 2021) and to detect the spatial and temporal features of land subsidence in conjunction with InSAR data (Zhu et al., 2015), including Landsat TM (Chen et al., 2015a), Landsat ETM+ (Poreh et al., 2021), Landsat 8 processed on GEE (Shi et al., 2020a), Sentinel-2 (Cigna and Tapete, 2021a). MERIS data were applied to remove the atmospheric noise in the interferogram (Aguemoune et al., 2019; Suganthi et al., 2017; Tang et al., 2018), while surface reflectance provided by MODIS turned out valuable for retrieval of soil condition (Mirzadeh et al., 2021; Wei and Chao, 2018).

6. Discussion and future perspective

In the last three decades satellite InSAR has largely demonstrated to be highly valuable for subsidence assessment, being adopted for different aims, at different scales of analysis and in a variety of settings. The literature examination conducted in this work provided an overview of all the satellite interferometry techniques and possible applications for the analysis of subsidence phenomena. More than 1000 papers were collected and thoroughly reviewed to comprehend the scientific progresses achieved since the launch of the first spaceborne SAR missions back in the 90s.

All the categories and the information collected and stored in the bibliographic database surrounding the use of satellite InSAR for subsidence analysis are here critically analyses and discussed. This section is divided into three major sub-sections: *i*) in the first one authors focus on the technical and technological aspects dealing with the acquisition and the processing of SAR data; *ii*) next authors outline the "radar-interpretation" matter *i.e.*, methods and approach to obtain an accurate characterization of the phenomenon, for both its cognitive frame and its temporal evolution; *iii*) finally, the perspectives for the advancement of the technical framework and the consolidation of the current capabilities for the analysis of subsidence are defined.

Within these sections, on the bases of the analysis of the existing literature and their own expertise, authors attempt to identify general and specific recommendations for a sound subsidence analysis with satellite interferometry.

6.1. Technical framework

The main technological evolution in the InSAR community has been surely represented by the development of the so-called MT-InSAR approaches, such as the pioneering approaches of PSInSAR and SBAS techniques. In this sense, the bibliography clearly reflects this evolution: all the works carried out in the late 90's exclusively exploited simple DInSAR approaches, relying on single or multiple pairs of SAR images. The revolutionary concept of the permanent scatterers was introduced by Ferretti et al. (2000), allowing the retrieval of millimetric terrain motion by removing any atmospheric contribution and provided the basis of the MT-InSAR approach development. To underline the importance of this innovation, the aforementioned work is the most cited in our database, counting more than 1500 citations, three-times the second most cited article.

According to the collection here performed, PSInSAR and SBAS approaches are the most adopted by far, thus confirming their suitability for both large areas or single building analyses; other important developed algorithms were adopted, such as StaMPS, IPTA and CPT. Following StaMPS, several other open-source software packages have been recently developed and are today available for InSAR processing, among which GMTSAR (Sandwell et al., 2011), ISCE (Rosen et al., 2012), SNAP (Blasco et al., 2019; Foumelis et al., 2018), which allow constructing interferometric mapping products and GIAnT (Agram et al., 2013), MintPy (Yunjun et al., 2019) and Π-RATE (Biggs et al., 2007) for estimation of time series of displacement. However, their use is slightly more limited since they remain technically complex and can be challenging to use for nonexperts or not completely easy to be digested by geoscientists.

Flourishing of processing chains, witnessing the great vitality of the interferometric community, has been fostered by the huge availability of several satellite platforms hosting SAR sensors operating within different acquisitions bands and characterized by variable ground resolution. Following the launch of ERS-1 platform in 1992, the temporal and spatial imaging capabilities of available SAR sensors have increased dramatically. Pixel resolution of SAR acquisitions dictates the size of the smallest ground elements that can be distinguished and ranges from 3.0 m × 3.0 m to 15.0 m × 5 m. These values are suitable to detect subsidence phenomena, that, generally, have a much larger spatial extension than the pixel sizes, with the only exception of small sinkholes that can have dimension of few to several meters (Nof et al., 2019).

To date, the microwave domain used to analyse subsidence ranges from 3.1 cm (X-band) to 5.6 cm (C-band), to ≈ 23 cm (L-band), including the new generation of radar satellites which has revolutionised our ability to measure Earth's surface deformation. The increased quantity and quality of satellite acquisitions paved the way to a paradigm 'shift, transforming InSAR from a research topic to an operative monitoring tool (Biggs and Wright, 2020).

The availability of high-resolution X-band data (*i.e.*, COSMO-SkyMed constellation, TerraSAR-X and TanDEM-X) (Fig. 1) from the second

decade of 2000 offers new opportunities for InSAR applications to ground deformation analysis, with respect to previous studies that used medium resolution C-band data from ERS-1/2, ENVISAT and RADARSAT-1. X-band sensors provide finer spatial resolutions, usually one order of magnitude better than C-band (and L-band) data, leading to an increase in the number of potential PS and to more precise detection of subtle (few mm/yr) ground lowering, thanks to the shorter wavelength. Moreover, given the higher resolution and the shorter wavelength of the X- band, it is possible to use shorter datasets with respect to C-band within the same time interval (Bovenga et al., 2012). X-band micro-satellites such as ICEYE (Ignatenko et al., 2020) have the potential to offer very high-resolution data, fundamental for InSAR monitoring in urban scenarios.

The regular orbital repat cycle in the order of several days ensured by the launch of C-band constellations (Sentinel-1 and Radar Constellation Mission), allows building interferometric stacks six-to-eight times faster than first-generation C-band satellites, or alternatively, obtaining a higher number of SAR images within the same time span. With respect to other SAR platforms, C-band data exhibit some favourable characteristics: regional-scale mapping capability (large image swath width), systematic SAR observations, and, in the case of Sentinel-1, free accessibility to SAR products and rapid delivery. In August 2022 ESA declared Sentinel-1B unrecoverable and announced the end, with only Sentinel-1A remaining in orbit and continuing to deliver radar images with a revisiting time of 12 days. The launch, scheduled for the second quarter of 2023, of the Sentinel-1C is expected to solve the problem, restoring the frequency of coverage.

Interferometry with L-band (among which the ALOS family, the recently launched SAOCOM and the scheduled ROSE-L) turned out extremely valuable over vegetated areas, where radar echoes are completely decorrelated, preventing coherence from being preserved even in low normal baseline interferograms. L-band signal, with a wavelength larger than the X- and C-bands, penetrates deeper into the vegetation cover, and it is less sensitive to the temporal decorrelation due to vegetation changes (Strozzi et al., 2005). Finally, the higher wavelength of the L-band counterbalances the potential limitations of the lower revisiting time over the same target area in presence of a high-magnitude displacement rate (Strozzi et al., 2004).

Another fundamental turning point for subsidence analysis through satellite InSAR is given by the launch of Sentinel-1 mission in 2014. A significant boost has been given by the free accessibility and the global coverage of Sentinel-1 data, opening new scenarios for public administrations and institutions, as well as for private companies, counting also on the constant revisit of the orbit with an unprecedent time span. Given the short latency time (about 5–6 h) and the rapid delivery, Sentinel-1 makes feasible near real-time response and operational monitoring.

Some of the existing SAR platforms, potentially suitable for subsidence analysis, have not been used yet, including the KARI X-band KOMPSAT-5 (Lee, 2010), the CONAE L-band SAOCOM-1 (Euillades et al., 2015) and the Spanish X-band satellite PAZ (Bach et al., 2018). The current lack of published studies may be due to several factors: some of these satellites are quite recent (*e.g.*, SAOCOM-1A and PAZ have been launched in October and February 2018), whereas for others it may be difficult or expensive to retrieve the images.

Test of new sensors should be fostered, considering that preliminary results seem to be promising for both PAZ (Abdikan et al., 2020) and SAOCOM-1 (Roa et al., 2021). As already pointed out by Mondini et al. (2021) for landslide investigations, exploitation of new satellites should be encouraged. A more systematic use of the SAR imagery would allow to better define benefits and drawbacks of existing methods and to explore new possible solutions. In particular, elaboration of images acquired by different platforms in different physiographic settings would support their applicability evaluation. This will help investigating if, when, and how satellite InSAR can be used in subsidence analysis, identifying the most appropriate solutions according to different geomorphological conditions and data availability.

While our literature review shows evidence that characteristics of existing satellite SAR sensors (in terms of wavelength and ground resolution) are, in theory, appropriate for subsidence detection and mapping in a wide range of settings, there is no clear indication on the suitability of their temporal repetitiveness, a key technical aspect when dealing with the operational use of satellite SAR data as a monitoring tool. The long revisit time of current satellite missions (in the order of several days in the best case) limits their use as a mean for effective monitoring even when subsidence occurrence can be obvious, as it is in the case of sinkholes or mine collapses, permitting only a regular update of deformative filed induced by gradual settling. Additionally, the purpose of identification of precursors to severe subsidence cannot be chased with the temporal sampling offered by current satellite platforms, as these could not yield information acquired in sufficiently systematic way. In other words, monitoring cannot be carried out when movements are too instantaneous with respect to the acquisition frequency of the sensor. In this sense, the increased frequency of acquisition and the operational readiness currently ensured by the Sentinel-1 constellation may be suitable for pinpointing only gradual changes in subsidence dynamic over relatively short time lengths (from 3 to 5 acquisitions according to Raspini et al. (2019)), offering early indications of non-linear ground motions.

In addition, data availability may be still a problem when setting up monitoring applications, that largely benefit from consistent archives of openly available radar data. With this aim, interferometric mapping services at national level has been activated in the past, for instance the so-called Map Italy project activated in 2009 by ASI using Stripmap images acquired by the COSMO-SkyMed Mission. However, the dual nature of the constellation (civilian and defence with possible task conflicts), as well as the data policy, limited the creation of long data stacks regularly populated with SAR images. Recognizing the strategic importance of systematic and regular SAR observations, the CSK SG has been designed with an automatic background mission, whose priority is to strengthen the Map Italy project, building up consistent data sets for the interferometric monitoring.

Following the inspection of literature database, authors recommend, when possible, to adopt multi-sensors analysis with different space segments used in synergy, to create a sort of virtual constellation, where different satellite data sources are used in conjunction to create a more effective Earth observation system. Being aware that measurements collected by different sensors cannot combined on a per pixel basis, because they have different spectral and spatial characteristics, derived products from each data source can help to mitigate intrinsic limitations of any one particular sensor. Rather than relying on a single sensor, adoption of a virtual constellation model (Ciampalini et al., 2019; Ezquerro et al., 2020a; Ma et al., 2019; Solari et al., 2017) provides complementary information that would not be possible with either sensor alone, improving spatial coverage, solving issues relate to scene unavailability or obscurity for single sensors.

6.2. *Operational framework*

Analysis of the literature database of 1059 articles revealed that geoscientist have performed subsidence investigations in 1063 non-unique study areas located in 76 different countries and in six continents. The study areas range in size from few hundred square metres (Raucoules et al., 2013a) to about 1 million square km (Semple et al., 2017). Analysis of Fig. 5 reveals an uneven distribution of the study areas, with the great majority in subsidence analysis in China and Europe. Not surprisingly, some of them have been target of multiple investigations, especially major cities such as Beijing, Hanoi, Ho Chi Minh, Jakarta, Shanghai or Mexico City or basins with a long history of subsidence (Antelope Valley, Murcia basin, San Joaquin valley), as investigators tend to repeat analysis of subsidence where the scenario is familiar and where setting is favourable.

Considering the issues related to the geographical bias and to the

non-uniqueness of study areas, the total areas covered by subsidence analysis is significantly less than global surface potentially threatened by subsidence, which is estimated to be about 12 million km^2 (8% of Earth's land area) by Herrera-García et al. (2021). This is in line with findings of Reichenbach et al. (2018), who pointed out how the total area covered by landslide susceptibility models is significantly less than the area covered by landslide database (Guzzetti et al., 2012). While the geographic coverage of subsidence analysis has increased in the recent periods (the great majority of studies in Africa and South America is *post*-2017), for large parts of the world (especially for Oceania, Africa and South America) the spatial dimension of subsidence remains unknown, and the number of applications is still very limited.

From a temporal point of view, a fundamental turning point for subsidence analysis through satellite InSAR is represented by the launch of Sentinel-1 mission in 2014. Inspection of literature database reveals a progressive growth in the number of contributions, with a yearly scientific production of about one hundred papers per year, since the 2015, almost 5 times the yearly production from 1997 to 2015. In authors opinion, beside the mere increase of number of contributions, the added value of Sentinel-1 relies in its global coverage which made possible investigations in less-studied areas: one-third (9 out 26 in total) and the great majority (5 out of 7 in total) of literature contributions in Africa and South America, respectively, has been published after 2018 using Sentinel-1, introducing thus a real world-wide sensibility towards subsidence issues, including more and more the developing countries (Fig. 13).

In general, the highest number of papers has been always given by C-band imagery, with ERS and ENVISAT taking over up to 2016, when Sentinel-1 started to be effective and consistent also in the number of scenes. The abundancy of C-band applications may be given on one hand by the higher versatility of the medium resolution, being well-suited for large areas monitoring and being characterized by worldwide coverage and regular acquisition plans; on the other hand, the open policy of data distribution by the ESA and the long-lasting continuity given by RADARSAT 1/2, operating uninterruptedly since 1995, are two major factors as well. X-Band imagery has been also widely used, especially for extremely detailed applications, oriented towards the assessment of building stability and vulnerability (*e.g.*, Le et al., 2016; Nappo et al., 2021). L-Band imagery, conversely, is adopted in 15% of the scientific contribution (including those cases where they are used in combination with other band images). In the latest year, the great availability of SAR images led to a growing number of research exploiting long stacks of images coming from different missions, making possible to analyse up to 30 years of displacements.

The launch of Sentinel-1 has had a massive effect also in the geographical distribution of the scientific works. Indeed, the first satellite missions, such as JERS and ALOS, operated by JAXA, were mostly dedicated to case studies of their own "homeland" continents (Fig. 14). A case in point is represented by the L-band missions operated by JAXA, whose acquisitions have been exploited almost exclusively for subsidence analysis in Asia, with a more limited use in other continents. Among the 233 L-band interferometric datasets of our database, 170 (*i.e.*, 73%) have been processed for case studies located in Asia, 36 (16%) in North America and 27 (11%) in the remain continents. This was mostly due to several aspect: *i*) some mission requirements have been defined in order to allow for a continuous interferometric monitoring of the national territory (the already mentioned Map Italy project implemented with CSK and consolidated with SG), establishing strategic archives suitable for interferometric applications; *ii*) policy of national space agencies on data access and sharing usually supports institutional users (scientific community, Academia, Government) easing exploitation of their own satellite imagery and allowing the utilization of the service for acquisitions and products ordering; *iii*) both geoscientist and end users community focus on familiar scenarios, which make data collection and field validation easier.

Conversely, the policy of access and usage of ESA C-band missions, such as ERS, ENVISAT and Sentinel-1 allowed both enlarging and differentiating the study areas and increasing the number of investigations. For each continent, the value of the ratio between the ESA C-band interferometric datasets with respect to the total amount of applications is always quite high, ranging from 55% of Asia to 77% of Europe. Even more significant is this percentage calculated considering only Sentinel-1 interferometric dataset for less-studied continents (Africa and South America, with 26% and 62%, respectively) witnessing that for these areas ESA datasets are the primary source of information.

This flooding of information is going to even increase in the next future, with the recently released missions (*e.g.*, SAOCOM-1, KOMPSAT-5, *etc.*) and the upcoming launches of further constellations, such as PLATiNO or NISAR. The synergy between all the satellite data will create a consistent EO system, which will provide a massive source of information for research scopes, but also for the implementation of operational services, treasuring on existing experiences already started as described by Confuorto et al. (2021) for some Italian Regions.

Literature database reveals that most studies have focused on static mapping, focusing on the spatial analysis of ground movement, and, possibly retrospectively, back-analysing past evolution of already established motion. Despite the maturity of interferometric chains and recent advances in satellite sensors, investigators concentrated on static analysis of archive images and dynamic monitoring of ground displacement remains uncommon in literature. Some exceptions exist (Bianchini et al., 2019; Del Soldato et al., 2019), that exploit InSAR results obtained with the systematic imagery processing and analysis of deformation time series for subsidence analysis, in the same fashion as proposed for landslide investigation (Raspini et al., 2019) or for sinkholes monitoring with ground-based instruments (Intrieri et al., 2015). The narrow interest on operation programmes for subsidence continuous monitoring may depend on several issues. Besides technical issues related to satellite temporal repetitiveness and data availability already discusses in 6.1, other two aspects are considered relevant by authors.

First, despite well-known consequences on the affected areas and related problems including environmental, economic and social aspects, land subsidence threat may be somehow overlooked or, at least, deemed less urgent than that posed by landslides or other geohazards. Systematic subsidence tracking is not considered a priority. Second, authors are aware that implementation of operational monitoring services based on satellite SAR images is not linear, as several difficult aspects must be covered: definition of needs and requirements, availability of large computing capacity, expertise in interpretation and dissemination capacity to release understandable messages for the users.

Considering that design and implementation of operational services over wide areas are technically, computationally and economically feasible with the existing tools and capabilities (Raspini et al., 2018), authors believe that potential and opportunities offered by satellite technologies currently available should be exploited. What is missing, for a systematic exploitation of SAR imagery for subsidence monitoring, is a consolidate interest within the wide community of end users and decision makers, whose requests and demand may drive development of new services and solutions.

The worldwide coverage and the very broad sense of the subsidence phenomena, along with the progressive refinement of monitoring and analysis methodologies, have made possible the identification of many driving forces (Table 1), although the interpretation of subsidence mechanisms is not always an easy and homogeneous task; moreover, several areas are affected by multiple causes (26%), confirming that subsidence is usually not a phenomenon caused individually by a single factor.

The implementation of InSAR, especially due to its capability to exploit long-lasting image archives, has represented a significant addition for the recognition of the triggering factors, thanks to its ease of comparison with other sources of information, both monitoring and strictly hydro-geomorphological data.

Among the main driving forces identified in this review, a major role

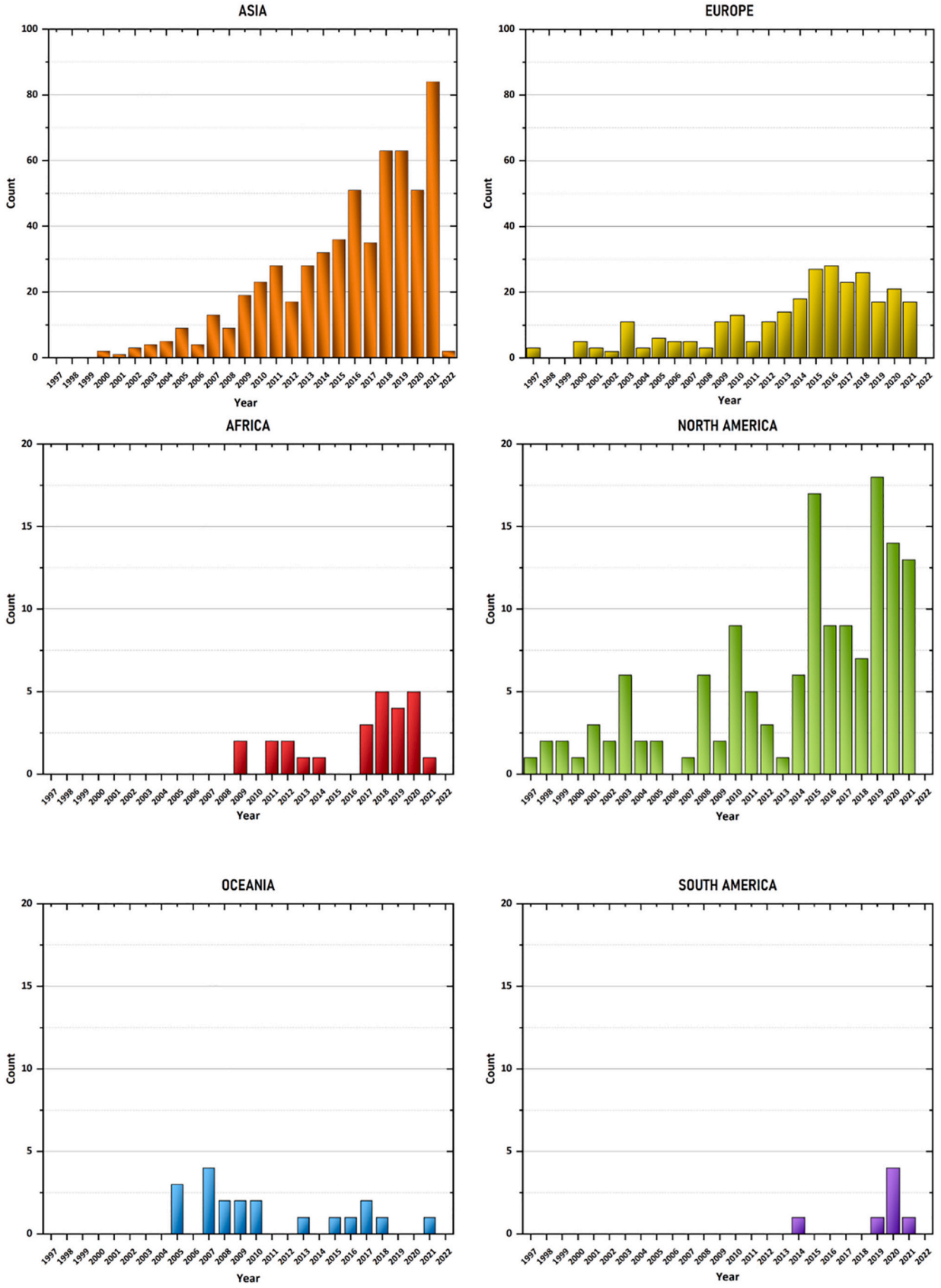

Fig. 13. Temporal distribution of the articles in the literature database for each continent the (vertical bars show number of published articles per year). Note the difference in the y-axes between Asia and Europe and the other continents.

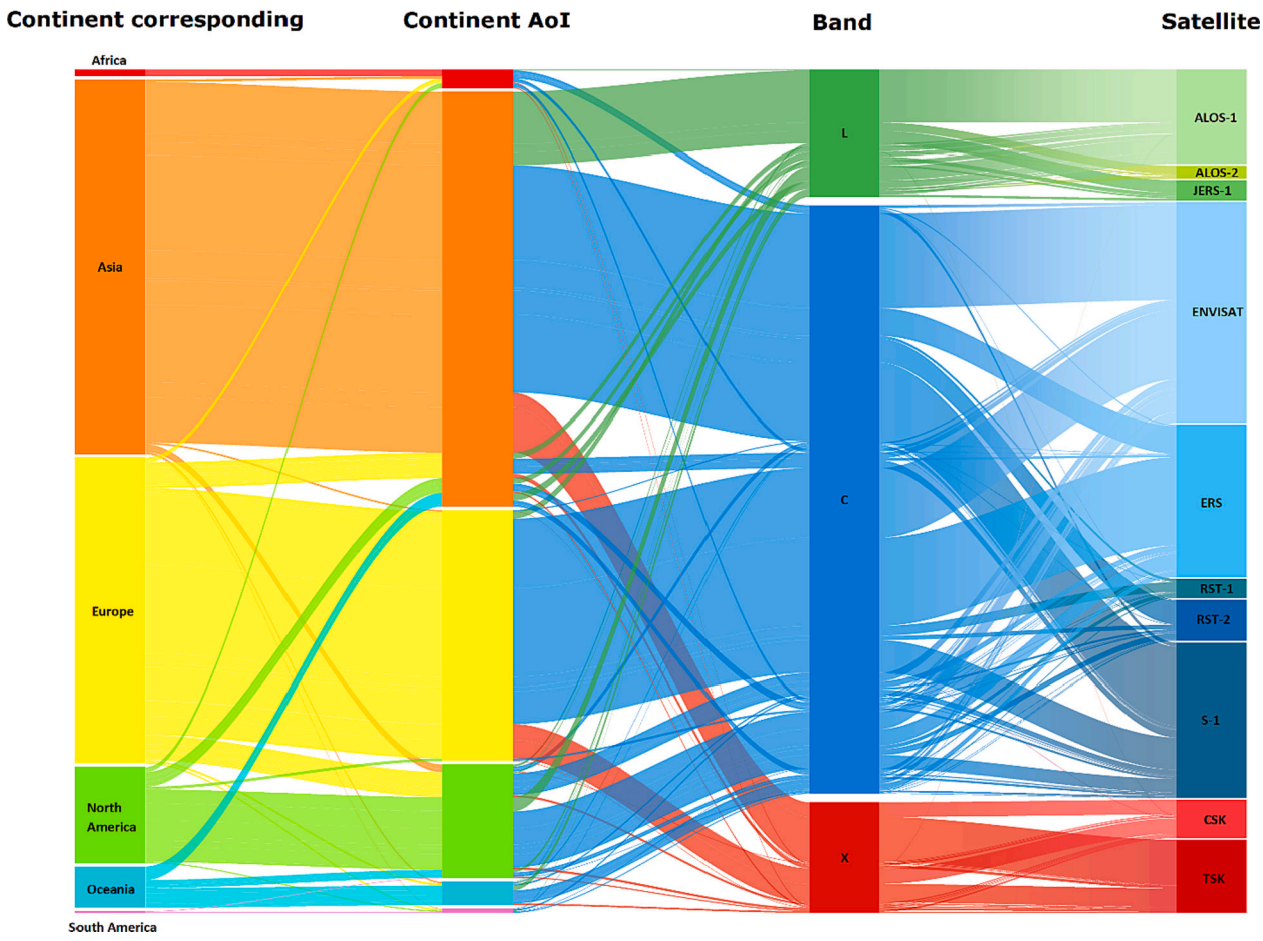

Fig. 14. Alluvial diagram illustrating relationship between affiliation of corresponding authors, geographic localization of study areas and employed satellites and bands.

is represented by the anthropogenic actions, especially by the groundwater overexploitation, counting more than a half of the contributions, and involving megacities like Mexico City, Los Angeles, Beijing, and Calcutta. Other major anthropogenic factors are mining activities and urban loading due to the sprawl in big urban areas. Mining-related subsidence has been studied since the pioneering InSAR applications, such as the case of Gardanne coal mine in France (Carnec and Delacourt, 2000) or the Gaeum coal mining area in Korea, (Jung et al., 2007). On the other hand, urban growth has been more recently identified as a major cause of subsidence, as testified by the recent works of Chen et al. (2018d), where the subsidence associated with the construction of new building in Canadian coastal cities was investigated by means of RADARSAT-2 and polarimetric information, or Erten and Rossi (2019), which exploited a 3-years Sentinel-1 stack to study the new infrastructures of Rize, Turkey. In this sense, SAR data may provide a significant support to the assessment of the hazards and to guide the policies for correct and sustainable urban planning.

As highlighted in section 5.3, the availability of large SAR datasets and the recent stream of information given by Sentinel-1 has allowed to cover each aspect of the subsidence analysis (Table 2). The literature analysis on this topic has highlighted seven different macro-classes of data usage for subsidence study. The first four classes, namely mapping, monitoring, characterization and modeling, corresponds to the main pillars, required for subsidence mitigation, indicated by the Panel on Land Subsidence of the US National Research Council (1991). Since the late 90's, with the usage of single pairs of SAR images, the main activities were oriented towards the static mapping of the subsiding area over wide areas, in order to test the capacity of the newly launched SAR missions. More sophisticated mapping procedures were developed through clustering activities over large areas processing (*e.g.*, Fernandez et al., 2009; Meisina et al., 2008) or through combination of the vertical and horizontal components of the deformation (Rosi et al., 2014). With the technological innovations achieved in the latest years (MT-InSAR techniques, multi-band acquisitions, *etc.*) and the possibility to obtain long time series, the tracking of subsidence deformation has become a solid reality and a standard practice, at a very variegated scale of analysis, *e.g.*, from the single buildings or infrastructure (*e.g.*, tunnels, such as in Scoular et al. (2020), which analysed the deformations related to the tunnelling in London or single skyscrapers in Hong Kong presented by Ma et al. (2019)) to whole regions (*e.g.*, Hanoi, Vietnam, in Dang et al. (2014)). The possibility of analysing 30 years of data enable the reconstruction of the historical evolution as well as to highlight the trend changes, either due to seasonal variation or to anthropogenic actions. In this sense, monitoring activities are still nowadays fundamental, in particular if conducted in quasi-real-time.

Summarizing, this literature review indicates the growing capabilities of satellite InSAR, being adopted for different aims, for different subsidence types, at different scales, and in different physiographical settings. Most of the applications indicate that the use of single-sensor SAR images to analyse land subsidence has some limitations, because they suffer from either low resolution or small coverage. The synergic use of different SAR sensors is adopted by investigators to perform multi-scale analysis from regional screening to the local scale monitoring. While C-band coverage width is designed to meet requirements for regional surveying, high-resolution X-band is tailored to perform finer analysis of critical areas and infrastructures, by identifying 3–6 times

Table 1
Summary of the reference papers for each class of type and trigger of the literature database. For the complete refence list, we refer to the four sub-sections of Chapter 5.

Multi-band analysis			25 five years-long monitoring (Cigna et al., 2016a); C-, X- and L-bands combination (Du et al., 2019); exploitation of five satellite missions (Scoular et al., 2020)
Type and triggers	**Natural**	Sinking	Ganges-Brahmaputra Delta in Bangladesh (Higgins et al., 2014)
		Compaction	Nile Delta in Egypt (Becker and Sultan, 2009); Semarang in Indonesia (Yastika et al., 2019); Uppsala in Sweden (Fryksten and Nilfouroushan, 2019)
		Tectonics	Morelia in Mexico (Cabral-Cano et al., 2010); Nile Delta in Egypt (Woppelmann et al., 2013); Po plain in Italy (Stramondo et al., 2007)
	Anthropogenic	Overpumping	Mexico City (Lopez-Quiroz et al., 2009; Osmanoglu et al., 2011) and Morelia in Mexico (Cigna et al., 2012); Los Angeles basin (Zhang et al., 2012), Las Vegas (Amelung et al., 1999) in the USA; the Segura River valley (Herrera et al., 2009a; Tomás et al., 2005) in Spain; Xi'an (Qu et al., 2014), Tianjin (Liu et al., 2010) and Beijing (Chen et al., 2016; Ng et al., 2012b) in China; Calcutta in India (Chatterjee et al., 2006); the Pistoia basin in Italy (Del Soldato et al., 2018); Thessaloniki in Greece (Nikos et al., 2016).
		Loading	Rome (Stramondo et al., 2008), Venice (Bock et al., 2012) and Guasticce (Ciampalini et al., 2019) in Italy; Mokpo in Korea (Kim et al., 2010); Beijing in China (Yang et al., 2018).
		Mining	La Unión in Spain (Herrera et al., 2007); French-German border (Samsonov et al., 2013); the Silesian Basin in Poland (Przylucka et al., 2015); Anhui Province (Li et al., 2015) and Datong (Yang et al., 2017c) in China
		Urban sprawl	Hanoi in Vietnam (Dang et al., 2014); Jakarta in Indonesia (Abidin et al., 2011; Ng et al., 2012a); Pearl River Delta (Chen et al., 2012; Wang et al., 2012), Shanghai (Dong et al., 2014) and Beijing (Chen et al., 2017; Gao et al., 2016) in China; London in UK (Milillo et al., 2018); Busan in Korea (Kim et al., 2007)
		Reclamation	Venice in Italy (Teatini et al., 2005); Hong Kong (Ding et al., 2004); Bengkalis Island in Indonesia (Umarhadi et al., 2021); Incheon and Busan in Korea (Kim et al., 2007)
		HC extraction	Bergermeer in the Netherlands (Fokker et al., 2016); Houston–Galveston in the USA (Miller and Shirzaei, 2019; Qu et al., 2015), Ravenna coastline (Fiaschi et al., 2017) and the Po Plain (Codegone et al., 2016) in Italy; Yellow River delta in China (Liu et al., 2016)
	Minor causes		Permafrost dynamics (Antonova et al., 2018; Bartsch et al., 2019; Iwahana et al., 2016; Rouyet et al., 2019); sinkholes (Baer et al., 2018; Kim et al., 2019; Nof et al., 2019); salt (Raucoules et al., 2013a) and carbonate dissolution (Zhou et al., 2017b); geothermal fields (Bekesi et al., 2019; Rosi et al., 2016; Sarychikhina et al., 2011); landfill (Gido et al., 2020b) and waste dump (Barra et al., 2017) compaction

more targets than the medium-resolution C-band satellites, albeit at expense of spatial coverage.

However, although data on subsidence extent and causes are often available or they can be inferred, information on the impacts is scarce, economic loss unaccounted and details on mitigation measures from null to very limited. Despite almost 30 years of consolidated applications, some operational challenges need to be faced. From the literature review clearly emerge that information on ground lowering are rarely used either for risk management and mitigation processes or territorial zonation and planning. Authors suggest fostering the operational readiness of InSAR data to meet the needs of public administrations and to guarantee the necessary homogenous standards of geographical data. Our suggestion is to include InSAR data into hazard maps to obtain a complete and flexible representation of the complexity of the physical landscape evolution (including geology, land use, climate, landforms, active processes). Method for prediction of subsidence susceptibility at global scale (spatial resolution of 1 km^2) proposed by Herrera-García et al. (2021) is a virtuous example to follow, with, wherever possible, ingestion of more detailed variables (both environmental and anthropogenic) governing land subsidence. Even if hazard maps do not directly generate any alert or early warning to decision maker, they should serve as an indicator for potential subsidence occurrence, finally leading any action and decision on the territory, from land planning to civil engineering applications.

The versatility of InSAR data and the possibility to combine them with other sources, either hydro-geomorphological and deformation data, enable accurate characterization and modeling activities, to best understand and re-construct the subsiding mechanisms and the triggering factors. In particular, groundwater induced subsidence cases have been extensively characterized and modelled by means of engineering and/or physical parameters and models, underlining the importance of multidisciplinary approaches to fully characterize the deformation. The recent literature trends are oriented towards the prediction and prevention of subsidence displacements, exploiting the abovementioned characteristics of InSAR data and new methodologies such as deep learning or machine learning. This may open new scenarios, providing a fundamental aid for hazard or vulnerability mapping activities.

There are still two main limitations in practical use of InSAR. The first one is that it is difficult to resolve phase ambiguity in case of non-linear deformation and it is almost impossible to measure sudden movements, such as those relate to sinkholes occurrence or mining collapse. Although there are examples in literature where non-linear models can partly solve this issues, phase unwrapping errors related to very high deformation rates are reported also in case of pumping-induced subsidence (Del Soldato et al., 2019). These limitations are particularly relevant when the spatial density of InSAR information is too low with respect to deformation magnitude and when movements are too instantaneous with respect to the temporal sampling of satellite. The launch of more satellites with increased revisiting time, along with the development of more sophisticated processing chains is expected to overcome this limitation. The second one is that detection and mapping of different deformation regime is not trivial. Some target scenarios, such as mining-related subsidence, can be challenging for satellite InSAR, as they may exhibit complex displacement pattern, coupling minor deformation and remarkable displacement rates. In these scenarios, the combination of different SAR processing approaches should be explored: while slow subsidence can be analysed using both DInSAR and PSI approach, rapid movement can be identified only with individual interferograms. For large magnitude dynamics subsidence, information on surface displacement can be obtained also using pixel-offset tracking approaches.

As previously stated, the integration between different data sources with InSAR (Table 3) has supported the identification of different types of subsidence analyses and interpretations. In the early works external data were mostly adopted to validate, *i.e.*, assess the consistency of InSAR measurements, since their potentiality was still to be fully ascertained. One of the mostly adopted "control" data sources is surely represented by geodetic leveling data, present in more than 20% of the works collected, followed by GNSS/GPS and extensometers. The first two data are perfectly combined with InSAR since they can provide vertical deformation measurements, thus representing a perfect

Table 2
Summary of the reference papers for each class of applications literature database.

Applications	Mapping	DInSAR: Single pairs (Buckley et al., 2003; Fielding et al., 1998); interferograms stacking (Ng et al., 2010); ERS1/2 tandem (Chang et al., 2005); discrimination of deformation regimes (Perski et al., 2009) and velocities (Strozzi et al., 2001) MT-InSAR: regional screening (Castellazzi et al., 2016a; Meisina et al., 2008; Rosi et al., 2014); urban fabric (Blasco et al., 2019; Cigna et al., 2011; Zhang et al., 2011; Zhou et al., 2017b); infrastructures (Parcharidis et al., 2009; Raspini et al., 2013) and single building (Cigna et al., 2014; Le et al., 2016); natural areas (Aly et al., 2012; Da Lio et al., 2018; Zhang et al., 2015b)
	Monitoring	Multi-scales monitoring (Ma et al., 2019); large archives stitching (Ge et al., 2007; Tosi et al., 2016; Zhang et al., 2016b); wide areas (Cian et al., 2019); trend changes identification (Del Soldato et al., 2019; Notti et al., 2015); seasonal variations (Hsieh et al., 2011; Ojha et al., 2018; Schmidt and Bürgmann, 2003); time-dependent signals (Bohloli et al., 2018; Chen et al., 2018c; Strozzi et al., 2011; Vervoort and Declercq, 2018)
	Characterization	Comparison with conditioning factors at wide (Chaussard et al., 2021; Gee et al., 2017; Heleno et al., 2011; Hoffmann et al., 2001; Robson et al., 2021) and local scale (Bru et al., 2013; Herrera et al., 2012; Tomás et al., 2012); multidisciplinary approach (Amato et al., 2020; Cianflone et al., 2015; Da Lio and Tosi, 2018)
	Modeling	Model implementation (Coda et al., 2019; Ezquerro et al., 2017), calibration (Ezquerro et al., 2014; Tomas et al., 2010a) and validation (Raspini et al., 2014; Unlu et al., 2013). Assessment of subsidence susceptibility (Hakim et al., 2020), hazard (Choi et al., 2011), vulnerability (Nadiri et al., 2020; Nadiri et al., 2018) and economic loss (Ezquerro et al., 2020a). Prediction (Rahmani and Ahmadi, 2018; Yuan et al., 2021) and scenarios assessment (Catalao et al., 2020; Gao et al., 2021; Miller and Shirzaei, 2021)
	Simulated	InSAR mimicking (Li et al., 2017; Wang et al., 2018) and performance evaluation (Ng et al., 2009)
	Review	Hydrologic applications (Galloway and Burbey, 2011; Hoffmann, 2005; Smith, 2002) and models (Guzy and Malinowska, 2020); mining (Hu et al., 2021; Ishwar and Kumar, 2017)
	Technical paper	PSInSAR for subsidence (Ferretti et al., 2015); polarimetrc analysis (Navarro-Sanchez et al., 2014); corner reflectors (Strozzi et al., 2013); free platforms (Galve et al., 2017).

Table 3
Summary of the reference papers for each class of integrations literature database.

Integrations	Validation	Leveling (Hung et al., 2011; Karila et al., 2013; Sarychikhina et al., 2011; Zhou et al., 2003); continuous GPS (Bock et al., 2012), periodically surveyed GPS (Bejar-Pizarro et al., 2016) and adoption of common data frame (Hu et al., 2019a; Miller et al., 2017); GNSS (Del Soldato et al., 2018; Farolfi et al., 2019; Yalvac, 2020); extensometer (Buckley et al., 2003; Calderhead et al., 2010); tide gauge (Carbognin et al., 2004; Di Paola et al., 2018) and altimetry (Catalao et al., 2020; Ma et al., 2017); pixel-offset (Chen et al., 2015a; Fan et al., 2021; Yang et al., 2017a). Field validation (Jung et al., 2007; Tomás et al., 2012)
	Comparison	Piezometric level (Bui et al., 2021; Dang et al., 2014; Gao et al., 2018), pumping wells location (Tomas et al., 2011), water extraction rates (Cigna and Tapete, 2021b); geomorphological mapping (Da Lio et al., 2018; Floris et al., 2019), geological (Castellazzi et al., 2016a; Goorabi et al., 2020; Terranova et al., 2015), tectonic (Woppelmann et al., 2013; Zhao et al., 2009a) and lithostratigraphic setting (Conesa-Garcia et al., 2016; Stramondo et al., 2008); geotechnical investigations (Herrera et al., 2009b; Khorrami et al., 2019); deposit thickness (Bejar-Pizarro et al., 2016; Du et al., 2020; Raspini et al., 2014); GRACE (Gido et al., 2020a; Guo et al., 2016); geophysical investigations (Closson et al., 2005; Ghazifard et al., 2017; Pacheco-Martinez et al., 2015; Paine et al., 2010; Smith and Knight, 2019); meteo records (Lei et al., 2014; Robson et al., 2021; Rouyet et al., 2019); land use (Du et al., 2018b; Zhou et al., 2017a; Zhou et al., 2016); multi-spectral satellite (Chen et al., 2015a; Cigna and Tapete, 2021a; Mirzadeh et al., 2021; Poreh et al., 2021)

matching and, at the same time, a complementary information, since InSAR basic information is provided along the LOS. On the other hand, extensometer data are used to collect specific data on the subsoil layer experiencing deformation. One of the first and most effective examples of multi-source data integration was provided by Raucoules et al. (2009), who validated PSI displacement data and time series with leveling information, within the framework of the PSIC4 project. Other data, such as groundwater and/or geological data, whereas available, instead, are among the major sources of information used for the characterization of the subsidence, since they represent precious information about the geological setting and help in determining the causes. Also, other remote sensing data play a significant role when integrated with InSAR: among the most adopted, optical imagery, DEM derived from UAV Lidar systems or GRACE data provide additional material for determining environmental parameters (*e.g.*, soil moisture, land cover, urban sprawl, topography, water storage, *etc.*) which perfectly fit subsidence analyses. In this current era, the availability of multiple remote sensing sources of information is a crucial aspect which will foster more precise and faster analysis.

Literature analysis revealed that validation and integration of InSAR data are considered fundamental activities, especially when investigators need to support interpretation of InSAR data, allowing assesses of governing parameters and distinction between triggering and conditioning factors (Fig. 15). Data validation with external sources is important to assess reliability of InSAR data, although some little precautions need to be adopted when assess their consistency with measurements data collected by other instruments: *i*) the spatial dimension of measured displacement can be different (pointwise for geodetic instruments and pixel-wise for satellite InSAR, with a spatial averaging of the backscatter cell contributors); *ii*) temporal sampling can be highly variable, from continuous in case of permanent stations to systematic and dense or sparse and uneven for spaceborne platforms; *iii*) measuring capabilities (accuracy and precision) and detectable components can be very different; iv) a common reference frame must be adopted, both spatially and temporally.

Finally, adoption of common procedures for data validation and comparison would increase credibility and diffusion of InSAR products, whose exploitation is still sometimes hampered, by their perception among users' community, as new techniques needed to be consolidated. The first example of a blind validation exercise between different InSAR suppliers is provided by (Adam et al., 2009) during the Terrafirma project. More recently, another virtuous example is represented by the recent EGMS validation protocol, which include an overview on the most common InSAR validation approaches.

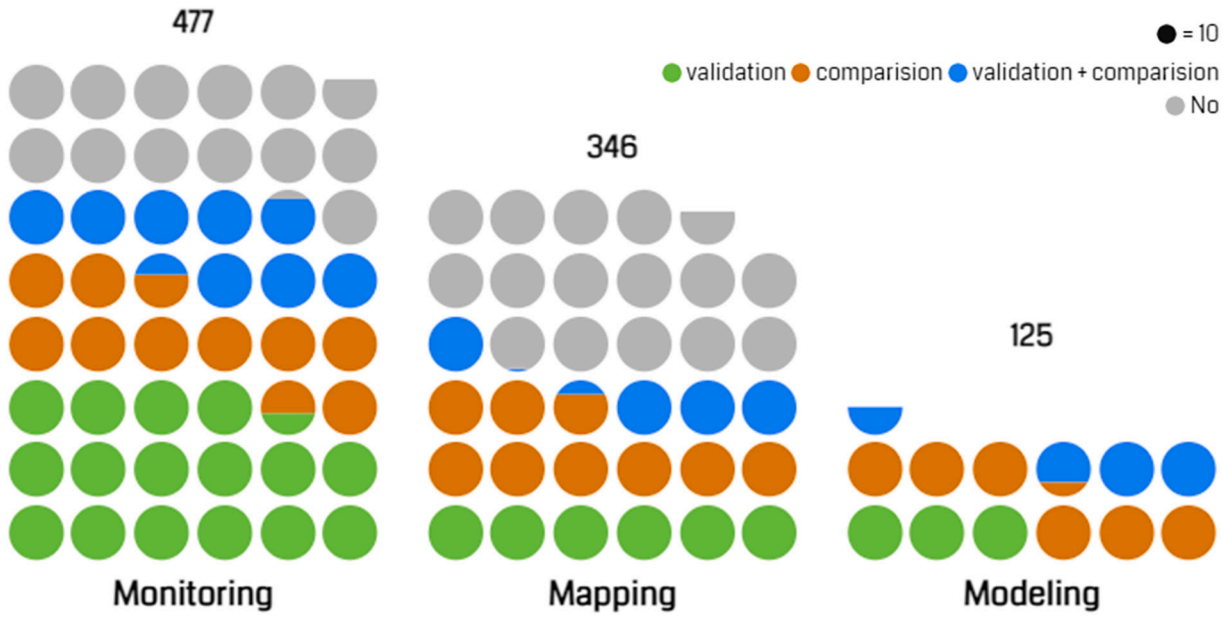

Fig. 15. Validation and comparison activities performed within the three major classes of application (monitoring, mapping and modeling) of the literature database.

6.3. *Future perspective and challenges*

Despite recent advances in satellite system imaging capabilities, there is still room for further technical improvements. The revisiting time remains a main hurdle for an extensive adoption of satellite InSAR as a tool for systematic monitoring of subsiding areas. In the future, InSAR data acquired in a sufficiently systematic fashion (daily, or sub-daily) could be provided by geosynchronous satellites (Hobbs et al., 2019 G-CLASS). The increased frequency of acquisitions of geosynchronous satellites will represent a major advance in the science of solid earth. The possibility of hourly/daily update would be a value added, making it possible to early identify the onset of acceleration, at least for some typologies of rapid vertical phenomena (*e.g.*, sinkholes). The upcoming release of reliable data coming from recent constellations (*e.g.*, SAOCOM) and scheduled launch of new mission, such as the ASI PLATiNO minisatellite platform or the ESA ROSE-L (Pierdicca et al., 2019) will provide additional information that cannot be gathered by other means, contributing to solve significant spatial and temporal variability of subsidence. With the launch planned for January 2023, the NISAR mission will be the first dual frequency fully polarimetric SAR satellite, operating in both L and S (3,2 GHz ~9,3 cm wavelength) microwave bands (Rosen et al., 2017). Integration of data from multiple bands will provide deeper insight into the dynamics of subsidence, especially in rural/agricultural settings.

In addition to synergic use of spaceborne sensors with different imaging capabilities, another important step would be a more systemic integration between satellite remote sensing and airborne measurements, which is still lacking. Aircrafts can be equipped with different payloads and sensors to collect key measurements of the land surface. While efforts to integrate satellite InSAR measurements and airborne payloads have been made (including LiDAR, (Strozzi et al., 2018) and geophysical instrumentation (Smith and Knight, 2019)), few attempts have been made to compare multi-platforms InSAR data. Preliminary results of cross-comparison of InSAR airborne and satellite data over permafrost areas (Xu et al., 2021) and for rapid drought-induced land subsidence (Miller et al., 2020) seem promising, showing that, despite different spatial resolution, imaging geometry, error source and calibration processing, the two measurements are self-consistent.

Authors believe that use of airborne SAR data as an addition to satellite measurements would enables effective applications in mapping and monitoring ground lowering due to subsidence, treasuring also on the existing experience with other geohazards (Delbridge et al., 2016; Schaefer et al., 2017). Having a flexible spatial baseline and revisiting time, acquisitions plan of airborne SAR can be designed and scheduled according to the observed scenario. Having finer resolution with respect to satellite InSAR, airborne SAR can be more sensitive to fine-scale variations in surface subsidence, improving the spatial coverage and scale of remote sensing. Spatially, the fine resolution of airborne SAR would allow to capture those small-scale subsidence feature (*e.g.*, local permafrost degradation, mine collapse, sinkholes, interference with linear structures) that are missed by satellite observations. From a temporal point of view, flexibility of configuration will allow to successfully depict those rapid movements that cannot be solved with current long and pre-programmed revisiting time of satellites.

From an operational point of view, authors recommend that geoscientists will focus their attention to sites that were not previously investigated, to increase the number and extent of areas covered by subsidence analysis, concentrating their efforts in those scenarios where knowledge of subsidence rate, magnitude and extent is of paramount importance for practical applications (*e.g.*, urban development, land planning, resources exploitation). Increasing records of subsidence extent is beyond the mere academic interest. Model evaluation for potential subsidence indicates that 54% of the global exposed population lives in low-income countries (Herrera-García et al., 2021), which are expected to have minor capability to adopt prevention policies and implement measures to mitigate subsidence impact. Definition of geographic priorities for subsidence analysis should be dictated by physiographic and social aspect, starting from situation deemed to be most urgent: megacities in developing country where population is expected to increase in the future, flood-risk zones, low-lying areas prone to coastal inundation. Last but not least climatic projections should be considered as, during the next decades, increasing in the intensity and duration of drought (Trenberth, 2011) may exacerbate subsidence in water-stressed basins, absolute sea-level rise may increase vulnerability of coastal zones (Nicholls and Cazenave, 2010)and temperature rise may trigger subsidence in high-latitude northern countries (Herrera-García et al., 2021). Drier and warmer climate will increase the risk of urban fabric built over clay formations, that are vulnerable to lose moisture.

Fundamental, in this sense, is the EGMS (Costantini et al., 2022; Crosetto et al., 2020), whose first release has been made in June 2022. With its pan-European coverage, EGMS represents the largest wide-area MT-InSAR deformation monitoring system ever developed. Based on

Sentinel-1 SAR data processed at full resolution, EGMS is fundamental for subsidence analyses, being conceived as a direct response to the request of users for consistent, regular, standardized, seamless information regarding natural and anthropogenic ground motion phenomena over Europe and across national borders. The availability of new and fresh information, along with the massive quantities of archive data, provides new inspirations and insights for subsidence studies. This aspect assumes a growing importance especially for those European countries like Netherlands and Italy with high percentage of population exposed to subsidence or living in areas that are below the mean sea level. Update information on spatial and temporal pattern of subsidence turned out valuable in the current climate change context, which may initiate and or aggravate well-known hazardous land subsidence areas, such as coastal and river delta areas, where projected sea-level rise, groundwater depletion and severe droughts may contribute to increase subsidence impact.

Subsidence information and sea level rise due to climate change should be taken into account also during design and implementation of future coastal defences and structural interventions, as suggested by Foti et al. (2020) for the Venice lagoon. This specific area (Carbognin et al., 2004; Teatini et al., 2005) is an example of non-stationarity natural processes, with a gradual lowering associated with natural causes (*i.e.*, differential sediment consolidation due to its own weight and tectonic movements) and acceleration by human intervention (*i.e.*, fluid removal from the subsurface and drainage of coastal territories rich in organic matter with oxidation of outcropping peat soils) and where sea level rise and increase in frequency and magnitude of extreme events are contributing to recurrent coastal flooding, which is likely to be one of the biggest socioeconomic impacts of sea-level rise in the 21st century (Shirzaei and Bürgmann, 2018).

So far, major efforts have been put into data processing methods and capacity and the flooding of satellite SAR data is a concrete reality nowadays. However, operational challenges remain to be faced and there are still two main limitations in practical use. The first one is that the unprecedented quantities of monitoring data cannot be longer investigated manually. Different post-processing approaches should be adopted to automatic detect and classify large volumes of interferometric data, including clustering analysis, hot-spot mapping and machine learning methods. The latter approach has also the advantage of assessing relationship between land subsidence and various influencing factors (Shi et al., 2020a), with automatic recognition of the source of the motion. The second one is the lack of appropriate sets of tools for simplifying the satellite InSAR data and of shared methods of analysis to generate maps to support hazard, exposure and risk-assessment against subsidence. Virtuous examples exist (Barra et al., 2017) and institutional interest is high (Comerci and Vittori, 2019), but efforts must be made. Authors believe that two common goals should be pursued by the by communities of end users and researchers: *i*) creation of tools to transform InSAR data and geological knowledge into understandable and usable information and *ii*) definition of standardized methodologies, interpretation criteria and guidelines for data analysis, ensuring transferability, avoiding misinterpretation, and facilitating homogenous products.

Therefore, in the current era, in which climate change and increasing anthropogenic activities pose unprecedented threats to the population and infrastructures, satellite InSAR data still provide vital information to be used for improving the risk awareness and the policies to reduce the hazards. In this context, to increase usefulness of the related products, authors stress the importance to provide decision makers as territorial managers and Civil Protection authorities with information on societal impacts, economic loss and, eventually, mitigation strategies and measures.

CRediT authorship contribution statement

Federico Raspini: Conceptualization, Methodology, Investigation, Formal analysis, Writing – original draft, Data curation, Visualization. **Francesco Caleca:** Data curation, Visualization. **Matteo Del Soldato:** Investigation, Writing – original draft, Data curation, Visualization. **Davide Festa:** Data curation. **Pierluigi Confuorto:** Writing – original draft, Data curation. **Silvia Bianchini:** Conceptualization, Writing – original draft, Data curation.

Declaration of Competing Interest

The authors declare that they have no known competing financial interests or personal relationships that could have appeared to influence the work reported in this paper.

Data availability

Data will be made available on request.

Appendix A. Supplementary data

Supplementary data to this article can be found online at https://doi.org/10.1016/j.earscirev.2022.104239.

References

Abdikan, S., Arıkan, M., Sanli, F.B., Cakir, Z., 2014. Monitoring of coal mining subsidence in peri-urban area of Zonguldak city (NW Turkey) with persistent scatterer interferometry using ALOS-PALSAR. Environ. Earth Sci. 71 (9), 4081–4089.
Abdikan, S., Bayik, C., Ustuner, M., Balik Şanli, F., 2020. Repeat-pass interferometric and backscatter analysis of X-band PAZ satellite-First results.
Abidin, H.Z., Andreas, H., Gumilar, I., Fukuda, Y., Pohan, Y.E., Deguchi, T., 2011. Land subsidence of Jakarta (Indonesia) and its relation with urban development. Nat. Hazards 59 (3), 1753–1771.
Adam, N., Parizzi, A., Eineder, M., Crosetto, M.J., 2009. Practical persistent scatterer processing validation in the course of the Terrafirma project. J Appl. Geophys. 69 (1), 59–65.
Agarwal, V., Kumar, A., Gomes, R.L., Marsh, S., 2020. Monitoring of ground movement and groundwater changes in London using InSAR and GRACE. Appl. Sci. Basel 10 (23), 21.
Agram, P., Jolivet, R., Riel, B., Lin, Y., Simons, M., Hetland, E., Doin, M.P., Lasserre, C., 2013. New radar interferometric time series analysis toolbox released. Eos, Trans. Am. Geophys. Union 94 (7), 69–70.
Aguemoune, S., Ayadi, A., Belhadj-Aissa, A., Bezzeghoud, M., 2019. A novel interpolation method for InSAR atmospheric wet delay correction. J. Appl. Geophys. 163, 96–107.
Akbari, V., Motagh, M., 2012. Improved Ground Subsidence monitoring using small baseline SAR interferograms and a Weighted Least Squares Inversion Algorithm. IEEE Geosci. Remote Sens. Lett. 9 (3), 437–441.
Aly, M.H., Klein, A.G., Zebker, H.A., Giardino, J.R., 2012. Land subsidence in the Nile Delta of Egypt observed by persistent scatterer interferometry. Remote Sens. Lett. 3 (7), 621–630.
Amato, V., Aucelli, P.P.C., Corrado, G., Di Paola, G., Matano, F., Pappone, G., Schiattarella, M., 2020. Comparing geological and Persistent Scatterer Interferometry data of the Sele River coastal plain, southern Italy: implications for recent subsidence trends. Geomorphology 351, 19.
Amelung, F., Galloway, D.L., Bell, J.W., Zebker, H.A., Laczniak, R.J., 1999. Sensing the ups and downs of Las Vegas: InSAR reveals structural control of land subsidence and aquifer-system deformation. Geology 27 (6), 483–486.
Ammirati, L., Mondillo, N., Rodas, R.A., Sellers, C., Di Martire, D., 2020. Monitoring land surface deformation associated with gold artisanal mining in the Zaruma City (Ecuador). Remote Sens. 12 (13), 17.
Anderssohn, J., Wetzel, H.U., Walter, T.R., Motagh, M., Djamour, Y., Kaufmann, H., 2008. Land subsidence pattern controlled by old alpine basement faults in the Kashmar Valley, Northeast Iran: results from InSAR and levelling. Geophys. J. Int. 174 (1), 287–294.
Antonova, S., Sudhaus, H., Strozzi, T., Zwieback, S., Kaab, A., Heim, B., Langer, M., Bornemann, N., Boike, J., 2018. Thaw subsidence of a Yedoma landscape in Northern Siberia, measured in Situ and estimated from TerraSAR-X Interferometry. Remote Sens. 10 (4), 27.
Anzidei, M., Scicchitano, G., Scardino, G., Bignami, C., Tolomei, C., Vecchio, A., Serpelloni, E., De Santis, V., Monaco, C., Milella, M., Piscitelli, A., Mastronuzzi, G., 2021. Relative sea-level rise scenario for 2100 along the Coast of South Eastern Sicily (Italy) by InSAR data, satellite images and high-resolution topography. Remote Sens. 13 (6), 25.
Ao, M.S., Wang, C.C., Xie, R.A., Zhang, X.Q., Hu, J., Du, Y.A., Li, Z.W., Zhu, J.J., Dai, W. J., Kuang, C.L., 2015. Monitoring the land subsidence with persistent scatterer interferometry in Nansha District, Guangdong,China. Nat. Haz. 75 (3), 2947–2964.
Aobpaet, A., Cuenca, M.C., Hooper, A., Trisirisatayawong, I., 2013. InSAR time-series analysis of land subsidence in Bangkok,Thailand. Int. J. Remote Sens. 34 (8), 2969–2982.

Arnaud, A., Adam, N., Hanssen, R., Inglada, J., Duro, J., Closa, J., Eineder, M., 2003. ASAR ERS interferometric phase continuity. In: IGARSS 2003. 2003 IEEE International Geoscience and Remote Sensing Symposium. Proceedings (IEEE Cat. No. 03CH37477). IEEE, pp. 1133–1135.
Aslan, G., Cakır, Z., Ergintav, S., Lasserre, C., Renard, F., 2018. Analysis of secular ground motions in Istanbul from a long-term InSAR time-series (1992–2017). Remote Sens. 10 (3), 408.
Aucelli, P.P.C., Di Paola, G., Incontri, P., Rizzo, A., Vilardo, G., Benassai, G., Buonocore, B., Pappone, G., 2017. Coastal inundation risk assessment due to subsidence and sea level rise in a Mediterranean alluvial plain (Volturno coastal plain–southern Italy). Estuar. Coast. Shelf Sci. 198, 597–609.
Avila-Olivera, J.A., Farina, P., Garduno-Monroy, V.H., 2007. Integration of InSAR and GIS in the study of surface faults caused by subsidence-creep-fault processes in Celaya, Guanajuato, Mexico. In: 4th International Conference on Geographical Information Systems in Geology in Earth Sciences. AIP Conference Proceedings. Amer Inst Physics, Queretaro, MEXICO, 200-+.
Avni, Y., Lensky, N., Dente, E., Shviro, M., Arav, R., Gavrieli, I., Yechieli, Y., Abelson, M., Lutzky, H., Filin, S., Haviv, I., Baer, G., 2016. Self-accelerated development of salt karst during flash floods along the Dead Sea Coast, Israel. J. Geophys. Res. Earth Surf. 121 (1), 17–38.
Bach, K., Kahabka, H., Fernando, C., Perez, J.C., 2018. The TerraSAR-X/PAZ Constellation: Post-Launch Update. In: EUSAR 2018; 12th European Conference on Synthetic Aperture Radar. VDE, pp. 1–3.
Baek, W.K., Jung, H.S., Jo, M.J., Lee, W.J., Zhang, L., 2019. Ground subsidence observation of solid waste landfill park using multi-temporal radar interferometry. Int. J. Urban Sci. 23 (3), 406–421.
Baer, G., Magen, Y., Nof, R.N., Raz, E., Lyakhovsky, V., Shalev, E., 2018. InSAR Measurements and Viscoelastic Modeling of Sinkhole Precursory Subsidence: Implications for Sinkhole Formation, early Warning, and Sediment Properties. J. Geophys.Res.Earth Surf. 123 (4), 678–693.
Baer, G., Schattner, U., Wachs, D., Sandwell, D., Wdowinski, S., Frydman, S., 2002. The lowest place on Earth is subsiding - an InSAR (interferometric synthetic aperture radar) perspective. Geol. Soc. Am. Bull. 114 (1), 12–23.
Bai, L., Jiang, L.M., Wang, H.S., Sun, Q.S., 2016. Spatiotemporal characterization of land subsidence and uplift (2009–2010) over Wuhan in Central China revealed by TerraSAR-X InSAR analysis. Remote Sens. 8 (4), 14.
Bakon, M., Marchamalo, M., Qin, Y., Garcia-Sanchez, A.J., Alvarez, S., Perissin, D., Papco, J., Martinez, R., 2016. Madrid as seen from Sentinel-1: preliminary results, 2016 CENTERIS/ProjMAN/HCist. Procedia Computer Science. Elsevier Science Bv, Porto, PORTUGAL.
Bamler, R., Hartl, P., 1998. Synthetic aperture radar interferometry. Inverse problems 14 (4), R1.
Barra, A., Solari, L., Béjar-Pizarro, M., Monserrat, O., Bianchini, S., Herrera, G., Crosetto, M., Sarro, R., González-Alonso, E., Mateos, R.M., 2017. A methodology to detect and update active deformation areas based on sentinel-1 SAR images. Remote Sens. 9 (10), 1002.
Bartsch, A., Leibman, M., Strozzi, T., Khomutov, A., Widhalm, B., Babkina, E., Mullanurov, D., Ermokhina, K., Kroisleitner, C., Bergstedt, H., 2019. Seasonal progression of ground displacement identified with satellite radar interferometry and the impact of unusually warm conditions on permafrost at the Yamal Peninsula in 2016. Remote Sens. 11 (16), 25.
Bayuaji, L., Sumantyo, J.T.S., Kuze, H., 2010. ALOS PALSAR D-InSAR for land subsidence mapping in Jakarta,Indonesia. Can. J. Remote Sens. 36 (1), 1–8.
Becker, R.H., Sultan, M., 2009. Land subsidence in the Nile Delta: inferences from radar interferometry. The Holocene 19 (6), 949–954.
Bejar-Pizarro, M., Guardiola-Albert, C., Garcia-Cardenas, R.P., Herrera, G., Barra, A., Molina, A.L., Tessitore, S., Staller, A., Ortega-Becerril, J.A., Garcia-Garcia, R.P., 2016. Interpolation of GPS and geological data using InSAR deformation maps: method and application to land subsidence in the Alto Guadalentin Aquifer (SE Spain). Remote Sens. 8 (11), 17.
Bekesi, E., Fokker, P.A., Martins, J.E., Limberger, J., Bonte, D., Van Wees, J.D., 2019. Production-induced subsidence at the los humeros geothermal field inferred from PS-InSAR. Geofluids 2019, 12.
Berardino, P., Fornaro, G., Lanari, R., Sansosti, E., 2002. A new algorithm for surface deformation monitoring based on small baseline differential SAR interferograms. Geosci. Remote Sens. IEEE Trans. 40 (11), 2375–2383.
Bianchini, S., Moretti, S., 2015. Analysis of recent ground subsidence in the Sibari plain (Italy) by means of satellite SAR interferometry-based methods. Int. J. Remote Sens. 36 (18), 4550–4569.
Bianchini, S., Solari, L., Del Soldato, M., Raspini, F., Montalti, R., Ciampalini, A., Casagli, N., 2019. Ground subsidence susceptibility (GSS) mapping in Grosseto Plain (Tuscany, Italy) based on satellite InSAR. Remote Sens. 11 (17), 27.
Biggs, J., Wright, T., Lu, Z., Parsons, B., 2007. Multi-interferogram method for measuring interseismic deformation: Denali Fault, Alaska. Geophys. J. Int. 170 (3), 1165–1179.
Biggs, J., Wright, T.J., 2020. How satellite InSAR has grown from opportunistic science to routine monitoring over the last decade. Nat. Commun. 11 (1), 1–4.
Bitelli, G., Bonsignore, F., Del Conte, S., Novali, F., Pellegrino, I., Vittuari, L., 2015. Integrated use of Advanced InSAR and GPS data for subsidence monitoring. In: Engineering Geology for Society and Territory-Volume 5. Springer, pp. 147–150.
Blachowski, J., Jirankova, E., Lazecky, M., Kadlecik, P., Milczarek, W., 2018. Application of satellite radar interferometry (PSInSAR) in analysis of secondary surface deformations in mining areas.Case studies from Czech Republic and Poland. Acta Geodynamica Et Geomaterialia 15 (2), 173–185.
Blachowski, J., Kopec, A., Milczarek, W., Owczarz, K., 2019. Evolution of secondary deformations captured by satellite radar interferometry: case study of an abandoned coal basin in SW Poland. Sustainability 11 (3), 21.
Blasco, J.M.D., Foumelis, M., Stewart, C., Hooper, A., 2019. Measuring urban subsidence in the Rome Metropolitan Area (Italy) with Sentinel-1 SNAP-StaMPS persistent scatterer interferometry. Remote Sens. 11 (2), 17.
Bock, Y., Wdowinski, S., Ferretti, A., Novali, F., Fumagalli, A., 2012. Recent subsidence of the Venice Lagoon from continuous GPS and interferometric synthetic aperture radar. Geochemistry Geophysics Geosystems 13, 13.
Bohloli, B., Bjornara, T.I., Park, J., Rucci, A., 2018. Can we use surface uplift data for reservoir performance monitoring? A case study from in Salah, Algeria. Int. J. Greenhouse Gas Control 76, 200–207.
Bonì, R., Herrera, G., Meisina, C., Notti, D., Béjar-Pizarro, M., Zucca, F., González, P.J., Palano, M., Tomás, R., Fernández, J., 2015. Twenty-year advanced DInSAR analysis of severe land subsidence: the Alto Guadalentín Basin (Spain) case study. Eng. Geol. 198, 40–52.
Bonì, R., Meisina, C., Cigna, F., Herrera, G., Notti, D., Bricker, S., McCormack, H., Tomás, R., Béjar-Pizarro, M., Mulas, J., 2017. Exploitation of satellite A-DInSAR time series for detection, characterization and modelling of land subsidence. Geosciences 7 (2), 25.
Boni, R., Pilla, G., Meisina, C., 2016. Methodology for detection and interpretation of ground motion areas with the A-DInSAR time series analysis. Remote Sens. 8 (8), 24.
Bovenga, F., Wasowski, J., Nitti, D., Nutricato, R., Chiaradia, M., 2012. Using COSMO/SkyMed X-band and ENVISAT C-band SAR interferometry for landslides analysis. Remote Sens. Environ. 119, 272–285.
Bozzano, F., Esposito, C., Franchi, S., Mazzanti, P., Perissin, D., Rocca, A., Romano, E., 2015. Understanding the subsidence process of a quaternary plain by combining geological and hydrogeological modelling with satellite InSAR data: the Acque Albule Plain case study. Remote Sens. Environ. 168, 219–238.
Briole, P., Massonnet, D., Delacourt, C., 1997. Post-eruptive deformation associated with the 1986–87 and 1989 lava flows of Etna detected by radar interferometry. Geophys. Res. Lett. 24 (1), 37–40.
Bru, G., Gonzalez, P.J., Mateos, R.M., Roldan, F.J., Herrera, G., Bejar-Pizarro, M., Fernandez, J., 2017. A-DInSAR monitoring of landslide and subsidence activity: a case of urban damage in Arcos de la Frontera,Spain. Remote Sens. 9 (8), 17.
Bru, G., Herrera, G., Tomas, R., Duro, J., De la Vega, R., Mulas, J., 2013. Control of deformation of buildings affected by subsidence using persistent scatterer interferometry. Struct. Infrastruct. Eng. 9 (2), 188–200.
Brunori, C.A., Bignami, C., Albano, M., Zucca, F., Samsonov, S., Groppelli, G., Norini, G., Saroli, M., Stramondo, S., 2015. Land subsidence, ground fissures and buried faults: InSAR monitoring of Ciudad Guzman (Jalisco, Mexico). Remote Sens. 7 (7), 8610–8630.
Buckley, S.M., Rosen, P.A., Hensley, S., Tapley, B.D., 2003. Land subsidence in Houston, Texas, measured by radar interferometry and constrained by extensometers. J. Geophys. Res.Solid Earth 108 (B11), 18.
Budhu, M., 2011. Earth fissure formation from the mechanics of groundwater pumping. Int. J. Geomech. 11 (1), 1–11.
Bui, L.K., Le, P.V.V., Dao, P.D., Nguyen, N.Q., Pham, H.V., Tran, H.H., Xie, L., 2021. Recent land deformation detected by Sentinel-1A InSAR data (2016–2020) over Hanoi, Vietnam, and the relationship with groundwater level change. Gisci. Remote Sens. 58 (2), 161–179.
Burbey, T.J., Zhang, M., 2015. Inverse modeling using PS-InSAR for improved calibration of hydraulic parameters and prediction of future subsidence for Las Vegas Valley, USA. In: Prevention and Mitigation of Natural and Anthropogenic Hazards due to Land Subsidence. Proceedings of the International Association of Hydrological Sciences (IAHS). Copernicus Gesellschaft Mbh, Nagoya, JAPAN, pp. 411–416.
Cabral-Cano, E., Arciniega-Ceballos, A., Diaz-Molina, O., Cigna, F., Avila-Olivera, A., Osmanoglu, B., Dixon, T., Demets, C., Garduno-Monroy, V.H., Vergara-Huerta, F., Hernandez-Quintero, J.E., 2010. there a tectonic component to the subsidence process in Morelia, Mexico?. In: 8th International Symposium on Land Subsidence. IAHS Publication. Int Assoc Hydrological Sciences, Natl Autonomous Univ Mexico, Santiago de Queretaro, MEXICO, 164-+.
Cabral-Cano, E., Dixon, T.H., Miralles-Wilhelm, F., Diaz-Molina, O., Sanchez-Zamora, O., Carande, R.E., 2008. Space geodetic imaging of rapid ground subsidence in Mexico City. Geol. Soc. Am. Bull. 120 (11–12), 1556–1566.
Calderhead, A.I., Martel, R., Alasset, P.J., Rivera, A., Garfias, J., 2010. Land subsidence induced by groundwater pumping, monitored by D-InSAR and field data in the Toluca Valley,Mexico. Can. J. Remote Sens. 36 (1), 9–23.
Calderhead, A.I., Therrien, R., Rivera, A., Martel, R., Garfias, J., 2011. Simulating pumping-induced regional land subsidence with the use of InSAR and field data in the Toluca Valley,Mexico. Adv. Water Resourc. 34 (1), 83–97.
Calo, F., Notti, D., Galve, J.P., Abdikan, S., Gorum, T., Pepe, A., Sanli, F.B., 2017. DInSAR-based detection of land subsidence and correlation with groundwater depletion in Konya Plain,Turkey. Remote Sens. 9 (1), 25.
Canova, F., Tolomei, C., Salvi, S., Toscani, G., Seno, S., 2012. Land subsidence along the Ionian coast of SE Sicily (Italy), detection and analysis via Small Baseline Subset (SBAS) multitemporal differential SAR interferometry. Earth Surf. Process. Landf. 37 (3), 273–286.
Carbognin, L., 1985. Land subsidence: a worldwide environmental hazard. Nat. Resourc. 21 (3).
Carbognin, L., Teatini, P., Tosi, L., 2004. Eustacy and land subsidence in the Venice Lagoon at the beginning ofthe new millennium. J. Mar. Syst. 51 (1–4), 345–353.
Carnec, C., Delacourt, C., 2000. Three years of mining subsidence monitored by SAR interferometry, near Gardanne,France. J. Appl. Geophys. 43 (1), 43–54.
Cascini, L., Ferlisi, S., Fornaro, G., Lanari, R., Peduto, D., Zeni, G., 2006. Subsidence monitoring in Sarno urban area via multi-temporal DInSAR technique. Int. J. Remote Sens. 27 (8), 1709–1716.

Cascini, L., Peduto, D., Reale, D., Arena, L., Ferlisi, S., Verde, S., Fornaro, G., 2013. Detection and monitoring of facilities exposed to subsidence phenomena via past and current generation SAR sensors. J. Geophys. Eng. 10 (6), 14.
Castaneda, C., Gutierrez, F., Manunta, M., Galve, J.P., 2009. DInSAR measurements of ground deformation by sinkholes, mining subsidence, and landslides, Ebro River, Spain. Earth Surf. Process. Landforms 34 (11), 1562–1574.
Castellazzi, P., Arroyo-Dominguez, N., Martel, R., Calderhead, A.I., Normand, J.C.L., Garfias, J., Rivera, A., 2016a. Land subsidence in major cities of Central Mexico: interpreting InSAR-derived land subsidence mapping with hydrogeological data. Int. J. Appl. Earth Obs. Geoinf. 47, 102–111.
Castellazzi, P., Garfias, J., Martel, R., Brouard, C., Rivera, A., 2017. InSAR to support sustainable urbanization over compacting aquifers: the case of Toluca Valley, Mexico. Int. J. Appl. Earth Obs. Geoinf. 63, 33–44.
Castellazzi, P., Martel, R., Rivera, A., Huang, J.L., Pavlic, G., Calderhead, A.I., Chaussard, E., Garfias, J., Salas, J., 2016b. Groundwater depletion in Central Mexico: use of GRACE and InSAR to support water resources management. Water Resour. Res. 52 (8), 5985–6003.
Catalao, J., Nico, G., Lollino, P., Conde, V., Lorusso, G., Silva, C., 2016. Integration of InSAR analysis and numerical modeling for the assessment of ground subsidence in the City of Lisbon, Portugal. Ieee J. Select. Top. Appl. Earth Observ.Remote Sens. 9 (4), 1663–1673.
Catalao, J., Raju, D., Nico, G., 2020. Insar maps of land subsidence and sea level scenarios to quantify the flood inundation risk in coastal cities: the case of Singapore. Remote Sens. 12 (2), 17.
Chang, C.P., Chang, T.Y., Wang, C.T., Kuo, C.H., Chen, K.S., 2004. Land-surface deformation corresponding to seasonal ground-water fluctuation, determining by SAR interferometry in the SW Taiwan. Math. Comput. Simul. 67 (4–5), 351–359.
Chang, H.C., Ge, L.L., Rizos, C., Ieee, 2005. ERS tandem DInSAR: The change of ground surface in 24 hours. In: 25th IEEE International Geoscience and Remote Sensing Symposium (IGARSS 2005). IEEE International Symposium on Geoscience and Remote Sensing IGARSS. Ieee, Seoul, SOUTH KOREA, pp. 5265–5267.
Chatterjee, R.S., Fruneau, B., Rudant, J.P., Roy, P.S., Frison, P.L., Lakhera, R.C., Dadhwal, V.K., Saha, R., 2006. Subsidence of Kolkata (Calcutta) City, India during the 1990s as observed from space by differential synthetic aperture radar interferometry (D-InSAR) technique. Remote Sens. Environ. 102 (1–2), 176–185.
Chatterjee, R.S., Thapa, S., Singh, K.B., Varunakumar, G., Raju, E.V.R., 2015. Detecting, mapping and monitoring of land subsidence in Jharia Coalfield, Jharkhand, India by spaceborne differential interferometric SAR, GPS and precision levelling techniques. J. Earth Syst. Sci. 124 (6), 1359–1376.
Chaussard, E., Havazli, E., Fattahi, H., Cabral-Cano, E., Solano-Rojas, D., 2021. Over a century of sinking in Mexico City: no hope for significant elevation and storage capacity recovery. J. Geophys. Res.Solid Earth 126 (4), 18.
Chaussard, E., Wdowinski, S., Cabral-Cano, E., Amelung, F., 2014. Land subsidence in Central Mexico detected by ALOS InSAR time-series. Remote Sens. Environ. 140, 94–106.
Chen, B.B., Gong, H.L., Lei, K.C., Li, J.W., Zhou, C.F., Gao, M.L., Guan, H.L., Lv, W., 2019. Land subsidence lagging quantification in the main exploration aquifer layers in Beijing plain, China. Int. J. Appl. Earth Obs. Geoinf. 75, 54–67.
Chen, B.B., Gong, H.L., Li, X.J., Lei, K.C., Ke, Y.H., Duan, G.Y., Zhou, C.F., 2015a. Spatial correlation between land subsidence and urbanization in Beijing,China. Nat. Haz. 75 (3), 2637–2652.
Chen, B.B., Gong, H.L., Li, X.J., Lei, K.C., Zhang, Y.Q., Li, J.W., Gu, Z.Q., Dang, Y.A., 2011. Spatial-temporal characteristics of land subsidence corresponding to dynamic groundwater funnel in Beijing Municipality,China. Chinese Geograph. Sci. 21 (6), 753–764.
Chen, B.Q., Deng, K.Z., Fan, H.D., Yu, Y., 2015b. Combining SAR interferometric phase and intensity information for monitoring of large gradient deformation in coal mining area. Eur. J.Remote Sens. 48, 701–717.
Chen, F., Lin, H., Zhang, Y., Lu, Z., 2012. Ground subsidence geo-hazards induced by rapid urbanization: implications from InSAR observation and geological analysis. Nat. Hazards Earth Syst. Sci. 12 (4), 935–942.
Chen, G., Zhang, Y., Zeng, R.Q., Yang, Z.K., Chen, X., Zhao, F.M., Meng, X.M., 2018a. Detection of land subsidence associated with land creation and rapid urbanization in the Chinese Loess Plateau using Time Series InSAR: a Case Study of Lanzhou New District. Remote Sens. 10 (2), 23.
Chen, J., Gunther, F., Grosse, G., Liu, L., Lin, H., 2018b. Sentinel-1 InSAR measurements of elevation changes over Yedoma Uplands on Sobo-Sise Island,Lena Delta. Remote Sens. 10 (7), 16.
Chen, J., Liu, L., Zhang, T.J., Cao, B., Lin, H., 2018c. Using persistent scatterer interferometry to map and quantify permafrost Thaw subsidence: a case study of Eboling Mountain on the Qinghai-Tibet Plateau. J.Geophys.Res.Earth Surf. 123 (10), 2663–2676.
Chen, J., Wu, J.C., Zhang, L.N., Zou, J.P., Liu, G.X., Zhang, R., Yu, B., 2013. Deformation trend extraction based on multi-temporal InSAR in Shanghai. Remote Sens. 5 (4), 1774–1786.
Chen, M., Tomas, R., Li, Z.H., Motagh, M., Li, T., Hu, L.Y., Gong, H.L., Li, X.J., Yu, J., Gong, X.L., 2016. Imaging land subsidence induced by groundwater extraction in Beijing (China) using Satellite Radar Interferometry. Remote Sens. 8 (6), 21.
Chen, W.F., Gong, H.L., Chen, B.B., Liu, K.S., Gao, M., Zhou, C.F., 2017. Spatiotemporal evolution of land subsidence around a subway using InSAR time-series and the entropy method. Gisc. Remote Sens. 54 (1), 78–94.
Chen, Z.H., Wang, J.F., Huang, X.D., 2018d. Land Subsidence monitoring in Greater Vancouver through Synergy of InSAR and polarimetric analysis. Can. J. Remote. Sens. 44 (3), 202–214.
Chi, B.W., Fan, H.D., Gao, Y.T., Zhao, L.F., Zhuang, H.F., 2021. A distributed scatterers InSAR method based on adaptive window with statistically homogeneous pixel selection for mining subsidence monitoring. Geocarto International 24.
Choi, J.K., Won, J.S., Lee, S., Kim, S.W., Kim, K.D., Jung, H.S., 2011. Integration of a subsidence model and SAR interferometry for a coal mine subsidence hazard map in Taebaek,Korea. Int. J. Remote Sens. 32 (23), 8161–8181.
Ciampalini, A., Solari, L., Giannecchini, R., Galanti, Y., Moretti, S., 2019. Evaluation of subsidence induced by long-lasting buildings load using InSAR technique and geotechnical data: the case study of a Freight Terminal (Tuscany, Italy). Int. J. Appl. Earth Obs. Geoinf. 82, 14.
Cian, F., Blasco, J.M.D., Carrera, L., 2019. Sentinel-1 for monitoring land subsidence of coastal cities in Africa using PSInSAR: a methodology based on the integration of SNAP and StaMPS. Geosciences 9 (3), 32.
Cianflone, G., Tolomei, C., Brunori, C.A., Dominici, R., 2015. InSAR time series analysis of natural and anthropogenic coastal plain subsidence: the case of Sibari (Southern Italy). Remote Sens. 7 (12), 16004–16023.
Cianflone, G., Tolomei, C., Brunori, C.A., Monna, S., Dominici, R., 2018. Landslides and subsidence assessment in the Crati Valley (Southern Italy) using InSAR data. Geosciences 8 (2), 22.
Cigna, F., 2018. Observing geohazards from space. Geosciences 8 (2), 6.
Cigna, F., Banks, V.J., Donald, A.W., Donohue, S., Graham, C., Hughes, D., McKinley, J. M., Parker, K., 2017. Mapping ground instability in areas of geotechnical infrastructure using satellite InSAR and small UAV surveying: a case study in Northern Ireland. Geosciences 7 (3), 25.
Cigna, F., Cabral-Cano, E., Osmanoglu, B., Dixon, T.H., Wdowinski, S., Ieee, 2011. Detecting subsidence-induced faulting in Mexican urban areas by means of persistent scatterer interferometry and subsidence horizontal gradient mapping. In: IEEE International Geoscience and Remote Sensing Symposium (IGARSS). IEEE International Symposium on Geoscience and Remote Sensing IGARSS. Ieee, Vancouver, CANADA, pp. 2125–2128.
Cigna, F., Confuorto, P., Novellino, A., Tapete, D., Di Martire, D., Ramondini, M., Calcaterra, D., Plank, S., Ietto, F., Brigante, A., Sowter, A., 2016. 25 years of satellite InSAR monitoring of ground instability and coastal geohazards in the archaeological site of Capo Colonna, Italy, Conference on SAR Image Analysis, Modeling, and Techniques XVI. Proceedings of SPIE. Spie-Int Soc Optical Engineering, Edinburgh, SCOTLAND..
Cigna, F., Lasaponara, R., Masini, N., Milillo, P., Tapete, D., 2014. Persistent scatterer interferometry processing of COSMO-SkyMed StripMap HIMAGE time series to depict deformation of the historic centre of Rome,Italy. Remote Sens. 6 (12), 12593–12618.
Cigna, F., Osmanoglu, B., Cabral-Cano, E., Dixon, T.H., Avila-Olivera, J.A., Garduno-Monroy, V.H., DeMets, C., Wdowinski, S., 2012. Monitoring land subsidence and its induced geological hazard with synthetic aperture radar interferometry: a case study in Morelia, Mexico. Remote Sens. Environ. 117, 146–161.
Cigna, F., Tapete, D., 2020. Sentinel-1 InSAR assessment of present-day lans subsidence due to exploitation of groundwater resources in Central Mexico. In: IEEE International Geoscience and Remote Sensing Symposium (IGARSS). Ieee, Electr Network, pp. 4215–4218.
Cigna, F., Tapete, D., 2021a. Present-day land subsidence rates, surface faulting hazard and risk in Mexico City with 2014–2020 Sentinel-1 IW InSAR. Remote Sens. Environ. 253, 19.
Cigna, F., Tapete, D., 2021b. Satellite InSAR survey of structurally-controlled land subsidence due to groundwater exploitation in the Aguascalientes Valley,Mexico. Remote Sens. Environ. 254, 23.
Cigna, F., Tapete, D., Garduno-Monroy, V.H., Muniz-Jauregui, J.A., Garcia-Hernandez, O.H., Jieenez-Haro, A., 2019. Wide-Area InSAR survey of surface deformation in urban areas and geothermal fields in the Eastern Trans-Mexican Volcanic Belt,Mexico. Remote Sens. 11 (20), 33.
Cigna, F., Tapete, D., Lee, K., 2016. Geohazards affecting UNESCO WHL sites in the UK observed from geological data and satellite InSAR. In: 4th International Conference on Remote Sensing and Geoinformation of the Environment (RSCy). Proceedings of SPIE. Spie-Int Soc Optical Engineering, Paphos, CYPRUS.
Clarivate, A., 2019. Web of science. Clarivate Analytics.
Closson, D., 2005. Structural control of sinkholes and subsidence hazards along the Jordanian Dead Sea coast. Environ. Geol. 47 (2), 290–301.
Closson, D., Abou Karaki, N., Klinger, Y., Hussein, M.J., 2005. Subsidence and sinkhole hazard assessment in the southern Dead Sea area,Jordan. Pure Appl. Geophys. 162 (2), 221–248.
Coda, S., Tessitore, S., Di Martire, D., Calcaterra, D., De Vita, P., Allocca, V., 2019. Coupled ground uplift and groundwater rebound in the metropolitan city of Naples (southern Italy). J. Hydrol. 569, 470–482.
Codegone, G., Rocca, V., Verga, F., Coti, C., 2016. Subsidence modeling validation through back analysis for an italian gas storage field. Geotech. Geol. Eng. 34 (6), 1749–1763.
Comerci, V., Vittori, E., 2019. The need for a standardized methodology for quantitative assessment of natural and anthropogenic land subsidence: the Agosta (Italy) gas field case. Remote Sens. 11 (10), 19.
Comerci, V., Vittori, E., Cipolloni, C., Di Manna, P., Guerrieri, L., Nisio, S., Succhiarelli, C., Ciuffreda, M., Bertoletti, E., 2015. Geohazards monitoring in Roma from InSAR and in situ data: outcomes of the PanGeo Project. Pure Appl. Geophys. 172 (11), 2997–3028.
Conesa-Garcia, C., Tomas, R., Herrera, G., Lopez-Bermudez, F., Cano, M., Navarro-Hervas, F., Perez-Cutillas, P., 2016. Deformational behaviours of alluvial units detect by advanced radar interferometry in the Vega Media of the Segura river, Southeast Spain. Geografiska Annaler Series a-Physical Geography 98 (1), 15–38.

Confuorto, P., Del Soldato, M., Solari, L., Festa, D., Bianchini, S., Raspini, F., Casagli, N., 2021. Sentinel-1-based monitoring services at regional scale in Italy: state of the art and main findings. Int. J. Appl. Earth Observ. Geoinform. 102, 102448.
Conway, B.D., 2016. Land subsidence and earth fissures in south-central and southern Arizona, USA. Hydrogeol. J. 24 (3), 649–655.
Corsetti, M., Fossati, F., Manunta, M., Marsella, M., 2018. Advanced SBAS-DInSAR technique for controlling large civil infrastructures: an application to the Genzano di Lucania Dam. Sensors 18 (7), 30.
Costantini, M., Falco, S., Malvarosa, F., Minati, F., 2008. A new method for identification and analysis of persistent scatterers in series of SAR images. In: Geoscience and Remote Sensing Symposium, 2008. IGARSS 2008. IEEE International. IEEE. II-449-II-452.
Costantini, M., Minati, F., Trillo, F., Ferretti, A., Passera, E., Rucci, A., Dehls, J., Larsen, Y., Marinkovic, P., Eineder, M., 2022. EGMS: Europe-wide ground motion monitoring based on full resolution InSAR processing of all Sentinel-1 acquisitions. In: IGARSS 2022-2022 IEEE International Geoscience and Remote Sensing Symposium. IEEE, pp. 5093–5096.
Crosetto, M., Castillo, M., Arbiol, R., 2003. Urban subsidence monitoring using radar interferometry: algorithms and validation. Photogramm. Eng. Remote. Sens. 69 (7), 775–783.
Crosetto, M., Crippa, B., Biescas, E., 2005. Early detection and in-depth analysis of deformation phenomena by radar interferometry. Eng. Geol. 79 (1–2), 81–91.
Crosetto, M., Devanthery, N., Cuevas-Gonzalez, M., Monserrat, O., Crippa, B., 2015. Exploitation of the full potential of PSI data for subsidence monitoring. In: Prevention and Mitigation of Natural and Anthropogenic Hazards due to Land Subsidence. Proceedings of the International Association of Hydrological Sciences (IAHS). Copernicus Gesellschaft Mbh, Nagoya, JAPAN, pp. 311–314.
Crosetto, M., Monserrat, O., Cuevas-González, M., Devanthéry, N., Crippa, B., 2016. Persistent scatterer interferometry: a review. ISPRS J. Photogramm. Remote Sens. 115, 78–89.
Crosetto, M., Solari, L., Mróz, M., Balasis-Levinsen, J., Casagli, N., Frei, M., Oyen, A., Moldestad, D.A., Bateson, L., Guerrieri, L., 2020a. The evolution of wide-area dinsar: from regional and national services to the European ground motion service. Remote Sens. 12 (12), 2043.
Crosetto, M., Tscherning, C.C., Crippa, B., Castillo, M., 2002. Subsidence monitoring using SAR interferometry: reduction of the atmospheric effects using stochastic filtering. Geophys. Res. Lett. 29 (9), 4.
Czikhardt, R., Papco, J., Bakon, M., Liscak, P., Ondrejka, P., Zlocha, M., 2017. Ground stability monitoring of undermined and landslide prone areas by meansof Sentinel-1 Multi-Temporal InSAR,case study from Slovakia, 7 (3), 17.
Da Lio, C., Teatini, P., Strozzi, T., Tosi, L., 2018. Understanding land subsidence in salt marshes of the Venice Lagoon from SAR Interferometry and ground-based investigations. Remote Sens. Environ. 205, 56–70.
Da Lio, C., Tosi, L., 2018. Land subsidence in the Friuli Venezia Giulia coastal plain, Italy: 1992–2010 results from SAR-based interferometry. Sci. Total Environ. 633, 752–764.
Dai, K.R., Liu, G.X., Li, Z.H., Ma, D.Y., Wang, X.W., Zhang, B., Tang, J., Li, G.Y., 2018. Monitoring highway stability in permafrost regions with X-band temporary scatterers stacking InSAR. Sensors 18 (6), 17.
Dai, Y.W., Ng, A.H.M., Wang, H., Li, L.Y., Ge, L.L., Tao, T.Y., 2021. Modeling-assisted InSAR phase-unwrapping method for mapping mine subsidence. IEEE Geosci. Remote Sens. Lett. 18 (6), 1059–1063.
Dang, V.K., Doubre, C., Weber, C., Gourmelen, N., Masson, F., 2014. Recent land subsidence caused by the rapid urban development in the Hanoi region (Vietnam) using ALOS InSAR data. Nat. Hazards Earth Syst. Sci. 14 (3), 657–674.
Dehghani, M., Zoej, M.J.V., Entezam, I., Mansourian, A., Saatchi, S., 2009. InSAR monitoring of progressive land subsidence in Neyshabour, Northeast Iran. Geophys. J. Int. 178 (1), 47–56.
Dehghani, M., Zoej, M.J.V., Hooper, A., Hanssen, R.F., Entezam, I., Saatchi, S., 2013. Hybrid conventional and Persistent Scatterer SAR interferometry for land subsidence monitoring in the Tehran Basin,Iran. Isprs J. Photogramm. Remote Sens. 79, 157–170.
Del Soldato, M., Confuorto, P., Bianchini, S., Sbarra, P., Casagli, N., 2021. Review of works combining GNSS and InSAR in Europe. Remote Sens. 13 (9), 1684.
Del Soldato, M., Farolfi, G., Rosi, A., Raspini, F., Casagli, N., 2018. Subsidence evolution of the Firenze–Prato–Pistoia Plain (Central Italy) combining PSI and GNSS Data. Remote Sens. 10 (7), 1146.
Del Soldato, M., Solari, L., Raspini, F., Bianchini, S., Ciampalini, A., Montalti, R., Ferretti, A., Pellegrineschi, V., Casagli, N., 2019. Monitoring ground instabilities using SAR satellite data: a practical approach. ISPRS Int. J. Geo Inf. 8 (7), 307.
Del Ventisette, C., Ciampalini, A., Manunta, M., Calo, F., Paglia, L., Ardizzone, F., Mondini, A.C., Reichenbach, P., Mateos, R.M., Bianchini, S., Garcia, I., Fusi, B., Deak, Z.V., Radi, K., Graniczny, M., Kowalski, Z., Piatkowska, A., Przylucka, M., Retzo, H., Strozzi, T., Colombo, D., Mora, O., Sanchez, F., Herrera, G., Moretti, S., Casagli, N., Guzzetti, F., 2013. Exploitation of large archives of ERS and ENVISAT C-Band SAR data to characterize ground deformations. Remote Sens. 5 (8), 3896–3917.
Delbridge, B.G., Bürgmann, R., Fielding, E., Hensley, S., Schulz, W.H., 2016. Three-dimensional surface deformation derived from airborne interferometric UAVSAR: Application to the Slumgullion Landslide. J. Geophys. Res. Solid Earth 121 (5), 3951–3977.
Deng, Z., Ke, Y.H., Gong, H.L., Li, X.J., Li, Z.H., 2017. Land subsidence prediction in Beijing based on PS-InSAR technique and improved Grey-Markov model. Gisci. Remote Sens. 54 (6), 797–818.
Di Paola, G., Alberico, I., Aucelli, P.P.C., Matano, F., Rizzo, A., Vilardo, G., 2018. Coastal subsidence detected by Synthetic Aperture Radar interferometry and its effects coupled with future sea-level rise: the case of the Sele Plain (Southern Italy). J. Flood Risk Manag. 11 (2), 191–206.
Di Paola, G., Rizzo, A., Benassai, G., Corrado, G., Matano, F., Aucelli, P.P.C., 2021. Sea-level rise impact and future scenarios of inundation risk along the coastal plains in Campania (Italy). Environ. Earth Sci. 80 (17), 22.
Diao, X.P., Wu, K., Zhou, D.W., Li, L., 2016. Integrating the probability integral method for subsidence prediction and differential synthetic aperture radar interferometry for monitoring mining subsidence in Fengfeng,China. J. Appl. Remote Sens. 10, 15.
Ding, X.L., Liu, G.X., Li, Z.W., Li, Z.L., Chen, Y.Q., 2004. Ground subsidence monitoring in Hong Kong with satellite SAR interferometry. Photogramm. Eng. Remote. Sens. 70 (10), 1151–1156.
Dixon, T.H., Amelung, F., Ferretti, A., Novali, F., Rocca, F., Dokka, R., Sella, G., Kim, S.-W., Wdowinski, S., Whitman, D., 2006. Subsidence and flooding in New Orleans. Nature 441 (7093), 587–588.
Dong, S.C., Samsonov, S., Yin, H.W., Yao, S.P., Xu, C., 2015. Spatio-temporal analysis of ground subsidence due to underground coal mining in Huainan coalfield,China. Environ. Earth Sci. 73 (9), 5523–5534.
Dong, S.C., Samsonov, S., Yin, H.W., Ye, S.J., Cao, Y.R., 2014. Time-series analysis of subsidence associated with rapid urbanization in Shanghai, China measured with SBAS InSAR method. Environ. Earth Sci. 72 (3), 677–691.
Du, Y.N., Feng, G.C., Liu, L., Fu, H.Q., Peng, X., Wen, D.B., 2020. Understanding Land Subsidence along the Coastal areas of Guangdong, China, by analyzing multi-track MTInSAR data. Remote Sens. 12 (2), 20.
Du, Z.Y., Ge, L.L., Li, X.J., Ng, A.H.M., 2016. Subsidence monitoring over the Southern Coalfield, Australia using both L-Band and C-Band SAR Time Series Analysis. Remote Sens. 8 (7), 16.
Du, Z.Y., Ge, L.L., Ng, A.H.M., Li, X.J., Li, L.Y., 2018a. Mapping land subsidence over the eastern Beijing city using satellite radar interferometry. Int. J. Digital Earth 11 (5), 504–519.
Du, Z.Y., Ge, L.L., Ng, A.H.M., Lian, X.G., Zhu, Q.G.Z., Horgan, F.G., Zhang, Q., 2021. Analysis of the impact of the South-to-North water diversion project on water balance and land subsidence in Beijing, China between 2007 and 2020. J. Hydrol. 603, 13.
Du, Z.Y., Ge, L.L., Ng, A.H.M., Zhu, Q.G.Z., Yang, X.H., Li, L.Y., 2018b. Correlating the subsidence pattern and land use in Bandung, Indonesia with both Sentinel-1/2 and ALOS-2 satellite images. Int. J. Appl. Earth Obs. Geoinf. 67, 54–68.
Du, Z.Y., Ge, L.L., Ng, A.H.M., Zhu, Q.G.Z., Zhang, Q., Kuang, J.M., Dong, Y.F., 2019. Long-term subsidence in Mexico City from 2004 to 2018 revealed by five synthetic aperture radar sensors. Land Degrad. Dev. 30 (15), 1785–1801.
Duffy, C.E., Braun, A., Hochschild, V., 2020. Surface subsidence in urbanized coastal areas: PSI methods based on Sentinel-1 for Ho Chi Minh City. Remote Sens. 12 (24), 20.
El Kamali, M., Papoutsis, I., Loupasakis, C., Abuelgasim, A., Omari, K., Kontoes, C., 2021. Monitoring of land surface subsidence using persistent scatterer interferometry techniques and ground truth data in arid and semi-arid regions, the case of Remah, UAE. Sci. Total Environ. 776, 11.
Elias, P., Benekos, G., Perrou, T., Parcharidis, I., 2020. Spatio-temporal assessment of land deformation as a factor contributing to relative sea level rise in coastal urban and natural protected areas using multi-source earth observation data. Remote Sens. 12 (14), 2296.
Engelbrecht, J., Musekiwa, C., Kemp, J., Inggs, M.R., 2014. Parameters affecting interferometric coherence-the case of a dynamic agricultural region. IEEE Trans. Geosci. Remote Sens. 52 (3), 1572–1582.
Erten, E., Rossi, C., 2019. The worsening impacts of land reclamation assessed with Sentinel-1: the Rize (Turkey) test case. Int. J. Appl. Earth Obs. Geoinf. 74, 57–64.
Euillades, P.A., Euillades, L.D., Azcueta, M., Sosa, G., 2015. SAOCOM 1A interferometric error model and analysis, Proceedings of Fringe.
Ezquerro, P., Del Soldato, M., Solari, L., Tomás, R., Raspini, F., Ceccatelli, M., Fernández-Merodo, J.A., Casagli, N., Herrera, G., 2020a. Vulnerability assessment of buildings due to land subsidence using InSAR data in the ancient historical city of Pistoia (Italy). Sensors 20 (10), 2749.
Ezquerro, P., Guardiola-Albert, C., Herrera, G., Fernandez-Merodo, J.A., Bejar-Pizarro, M., Boni, R., 2017. Groundwater and subsidence modeling combining geological and multi-satellite SAR data over the Alto Guadalentin Aquifer (SE Spain). Geofluids 17.
Ezquerro, P., Herrera, G., Marchamalo, M., Tomas, R., Bejar-Pizarro, M., Martinez, R., 2014. A quasi-elastic aquifer deformational behavior: Madrid aquifer case study. J. Hydrol. 519, 1192–1204.
Ezquerro, P., Tomas, R., Bajar-Pizarro, M., Fernandez-Merodo, J.A., Guardiola-Albert, C., Staller, A., Sanchez-Sobrino, J.A., Herrera, G., 2020b. Improving multi-technique monitoring using Sentinel-1 and Cosmo-SkyMed data and upgrading groundwater model capabilities. Sci. Total Environ. 703, 18.
Fan, H.D., Cheng, D., Deng, K.Z., Chen, B.Q., Zhu, C.G., 2015. Subsidence monitoring using D-InSAR and probability integral prediction modelling in deep mining areas. Surv. Rev. 47 (345), 438–445.
Fan, H.D., Gu, W., Qin, Y., Xue, J.Q., Chen, B.Q., 2014. A model for extracting large deformation mining subsidence using D-InSAR technique and probability integral method. Trans. Nonferrous Metals Soc. China 24 (4), 1242–1247.
Fan, H.D., Li, T.T., Gao, Y.T., Deng, K.Z., Wu, H.A., 2021. Characteristics inversion of underground goaf based on InSAR techniques and PIM. Int. J. Appl. Earth Obs. Geoinf. 103, 9.
Farina, P., Avila-Olivera, J.A., Garduno-Monroy, V.H., Catani, F., 2008. DInSAR analysis of differential ground subsidence affecting urban areas along the Mexican Volcanic Belt (MVB). Rivista Italiana Di Telerilevamento 40 (2), 103–113.

Farolfi, G., Del Soldato, M., Bianchini, S., Casagli, N., 2019. A procedure to use GNSS data to calibrate satellite PSI data for the study of subsidence:an example from the north-western Adriatic coast (Italy). Eur. J. Remote Sens. 52, 54–63.
Fernandez, P., Irigaray, C., Jimenez, J., El Hamdouni, R., Crosetto, M., Monserrat, O., Chacon, J., 2009. First delimitation of areas affected by ground deformations in the Guadalfeo River Valley and Granada metropolitan area (Spain) using the DInSAR technique. Eng. Geol. 105 (1–2), 84–101.
Ferretti, A., Colombo, D., Fumagalli, A., Novali, F., Rucci, A., 2015. InSAR data for monitoring land subsidence: time to think big. In: Prevention and Mitigation of Natural and Anthropogenic Hazards due to Land Subsidence. Proceedings of the International Association of Hydrological Sciences (IAHS). Copernicus Gesellschaft Mbh, Nagoya, JAPAN, pp. 331–334.
Ferretti, A., Fumagalli, A., Novali, F., Prati, C., Rocca, F., Rucci, A., 2011. A new algorithm for processing interferometric data-stacks: SqueeSAR. IEEE Trans. Geosci. Remote Sens. 49 (9), 3460–3470.
Ferretti, A., Prati, C., Rocca, F., 2000. Nonlinear subsidence rate estimation using permanent scatterers in differential SAR interferometry. IEEE Trans. Geosci. Remote Sens. 38 (5), 2202–2212.
Ferretti, A., Prati, C., Rocca, F., 2001. Permanent scatterers in SAR interferometry. IEEE Trans. Geosci. Remote Sens. 39 (1), 8–20.
Fiaschi, S., Fabris, M., Floris, M., 2018. Estimation of land subsidence in deltaic areas through differential SAR interferometry: the Po River Delta case study (Northeast Italy). Int. J. Remote Sens. 39 (23), 8724–8725.
Fiaschi, S., Tessitore, S., Bonì, R., Di Martire, D., Achilli, V., Borgstrom, S., Ibrahim, A., Floris, M., Meisina, C., Ramondini, M., 2017. From ERS-1/2 to Sentinel-1: two decades of subsidence monitored through A-DInSAR techniques in the Ravenna area (Italy). GISci. Remote Sens. 54 (3), 305–328.
Fielding, E.J., Blom, R.G., Goldstein, R.M., 1998. Rapid subsidence over oil fields measured by SAR interferometry. Geophys. Res. Lett. 25 (17), 3215–3218.
Figueroa-Miranda, S., Hernandez-Madrigal, V.M., Tuxpan-Vargas, J., Villasenor-Reyes, C.I., 2020. Evolution assessment of structurally-controlled differential subsidence using SBAS and PS interferometry in an emblematic case in Central Mexico. Eng. Geol. 279, 16.
Floris, M., Fontana, A., Tessari, G., Mule, M., 2019. Subsidence zonation through satellite interferometry in coastal plain environments of NE Italy: a possible tool for geological and geomorphological mapping in urban areas. Remote Sens. 11 (2), 22.
Fokker, P.A., Wassing, B.B.T., van Leijen, F.J., Hanssen, R.F., Nieuwland, D.A., 2016. Application of an ensemble smoother with multiple data assimilation to the Bergermeer gas field, using PS-InSAR. Geomech. Energy Environ. 5, 16–28.
Foroughnia, F., Nemati, S., Maghsoudi, Y., Perissin, D., 2019. An iterative PS-InSAR method for the analysis of large spatio-temporal baseline data stacks for land subsidence estimation. Int. J. Appl. Earth Obs. Geoinf. 74, 248–258.
Foti, E., Musumeci, R.E., Stagnitti, M., 2020. Coastal defence techniques and climate change: a review. Rendiconti Lincei. Scienze Fisiche e Naturali 31 (1), 123–138.
Foumelis, M., Blasco, J.M.D., Desnos, Y.-L., Engdahl, M., Fernández, D., Veci, L., Lu, J., Wong, C., 2018. ESA SNAP-StaMPS integrated processing for Sentinel-1 persistent scatterer interferometry. In: IGARSS 2018-2018 IEEE International Geoscience and Remote Sensing Symposium. IEEE, pp. 1364–1367.
Fruneau, B., Sarti, F., 2000. Detection of ground subsidence in the city of Paris using radar interferometry: isolation of deformation from atmospheric artifacts using correlation. Geophys. Res. Lett. 27 (24), 3981–3984.
Fryksten, J., Nilfouroushan, F., 2019. Analysis of clay-induced land subsidence in Uppsala City using Sentinel-1 SAR data and precise leveling. Remote Sens. 11 (23), 17.
Gaber, A., Darwish, N., Koch, M., 2017. Minimizing the residual topography effect on interferograms to improve DInSAR results: estimating land subsidence in Port-said City,Egypt. Remote Sens. 9 (7), 22.
Galloway, D.L., Burbey, T.J., 2011. Regional land subsidence accompanying groundwater extraction. Hydrogeol. J. 19 (8), 1459–1486.
Galloway, D.L., Hoffmann, J., 2007. The application of satellite differential SAR interferometry-derived ground displacements in hydrogeology. Hydrogeol. J. 15 (1), 133–154.
Galloway, D.L., Hudnut, K.W., Ingebritsen, S., Phillips, S.P., Peltzer, G., Rogez, F., Rosen, P., 1998. Detection of aquifer system compaction and land subsidence using interferometric synthetic aperture radar, Antelope Valley, Mojave Desert,California. Water Resour. Res. 34 (10), 2573–2585.
Galve, J.P., Perez-Pena, J.V., Azanon, J.M., Closson, D., Calo, F., Reyes-Carmona, C., Jabaloy, A., Ruano, P., Mateos, R.M., Notti, D., Herrera, G., Bejar-Pizarro, M., Monserrat, O., Bally, P., 2017. Evaluation of the SBAS InSAR Service of the European Space Agency's Geohazard Exploitation Platform (GEP). Remote Sens. 9 (12), 21.
Gao, G.S., San, L.H., Zhu, Y.D., 2021. Flood inundation analysis in Penang Island (Malaysia) based on InSAR maps of land subsidence and local sea level scenarios. Water 13 (11), 15.
Gao, M.L., Gong, H.L., Chen, B.B., Li, X.J., Zhou, C.F., Shi, M., Si, Y., Chen, Z., Duan, G.Y., 2018. Regional land subsidence analysis in Eastern Beijing Plain by InSAR time series and wavelet transforms. Remote Sens. 10 (3), 17.
Gao, M.L., Gong, H.L., Chen, B.B., Zhou, C.F., Chen, W.F., Liang, Y., Shi, M., Si, Y., 2016. InSAR time-series investigation of long-term ground displacement at Beijing Capital International Airport, China. Tectonophysics 691, 271–281.
Gao, M.L., Gong, H.L., Li, X.J., Chen, B.B., Zhou, C.F., Shi, M., Guo, L., Chen, Z., Ni, Z.Y., Duan, G.Y., 2019. Land subsidence and ground fissures in Beijing Capital International Airport (BCIA): evidence from Quasi-PS InSAR Analysis. Remote Sens. 11 (12), 17.
Ge, D.Q., Wang, Y., Zhang, L., Zhang, X.D., Yan, D.P., Li, M., 2011. Integrating corner reflector and PSInSAR technique to monitor regional land subsidence. In: IEEE International Geoscience and Remote Sensing Symposium (IGARSS). IEEE International Symposium on Geoscience and Remote Sensing IGARSS. Ieee, Vancouver, CANADA, pp. 1619–1622.
Ge, L.L., Chang, H.C., Rizos, C., 2007. Mine subsidence monitoring using multi-source satellite SAR images. Photogramm. Eng. Remote. Sens. 73 (3), 259–266.
Ge, L.L., Ng, A.H.M., Li, X.J., Abidin, H.Z., Gumilar, I., 2014. Land subsidence characteristics of Bandung Basin as revealed by ENVISAT ASAR and ALOS PALSAR interferometry. Remote Sens. Environ. 154, 46–60.
Gebremichael, E., Sultan, M., Becker, R., El Bastawesy, M., Cherif, O., Emil, M., 2018. Assessing land deformation and sea encroachment in the Nile Delta: a radar interferometric and inundation modeling approach. J. Geophys.Res. Solid Earth 123 (4), 3208–3224.
Gee, D., Bateson, L., Sowter, A., Grebby, S., Novellino, A., Cigna, F., Marsh, S., Banton, C., Wyatt, L., 2017. Ground motion in areas of abandoned mining: application of the intermittent SBAS (ISBAS) to the Northumberland and Durham Coalfield,UK. Geosciences 7 (3), 26.
Gee, D., Sowter, A., Novellino, A., Marsh, S., Gluyas, J., 2016. Monitoring land motion due to natural gas extraction: validation of the Intermittent SBAS (ISBAS) DInSAR algorithm over gas fields of North Holland, the Netherlands. Mar. Pet. Geol. 77, 1338–1354.
Ghazifard, A., Akbari, E., Shirani, K., Safaei, H., 2017. Evaluating land subsidence by field survey and D-InSAR technique in Damaneh City,Iran. J. Arid Land 9 (5), 778–789.
Ghazifard, A., Moslehi, A., Safaei, H., Roostaei, M., 2016. Effects of groundwater withdrawal on land subsidence in Kashan Plain,Iran. Bull. Eng. Geol. Environ. 75 (3), 1157–1168.
Gheorghe, M., Armas, I., 2015. Comparison of multi-temporal differential interferometry techniques applied to the measurement of bucharest city subsidence. In: 25th International Conference on Environment at Crossroads - SMART Approaches for a Sustainable Future. Procedia Environmental Sciences. Elsevier Science Bv, Bucharest, ROMANIA, pp. 221–229, 268-+.
Gido, N.A.A., Amin, H., Bagherbandi, M., Nilfouroushan, F., 2020a. Satellite monitoring of mass changes and ground subsidence in Sudan's oil fields using GRACE and Sentinel-1 data. Remote Sens. 12 (11), 20.
Gido, N.A.A., Bagherbandi, M., Nilfouroushan, F., 2020b. Localized subsidence zones in Gavle City detected by Sentinel-1 PSI and leveling data. Remote Sens. 12 (16), 20.
Goorabi, A., Karimi, M., Yamani, M., Perissin, D., 2020. Land subsidence in Isfahan metropolitan and its relationship with geological and geomorphological settings revealed by Sentinel-1A InSAR observations. J. Arid Environ. 181, 17.
Graniczny, M., Cyziene, J., van Leijen, F., Minkevicius, W., Mikulenas, V., Satkunas, J., Przylucka, M., Kowalski, Z., Uscinowicz, S., Jeglinski, W., 2015. Vertical ground movements in the Polish and Lithuanian Baltic coastal area as measured by satellite interferometry. Baltica 28.
Grzovic, M., Ghulam, A., 2015. Evaluation of land subsidence from underground coal mining using TimeSAR (SBAS and PSI) in Springfield, Illinois, USA. Nat. Hazards 79 (3), 1739–1751.
Gueguen, Y., Deffontaines, B., Fruneau, B., Al Heib, M., de Michele, M., Raucoules, D., Guise, Y., Planchenault, J., 2009. Monitoring residual mining subsidence of Nord/Pas-de-Calais coal basin from differential and Persistent Scatterer Interferometry (Northern France). J. Appl. Geophys. 69 (1), 24–34.
Gumilar, I., Abidin, H.Z., Andreas, H., Sidiq, T.P., Gamal, M., Fukuda, Y., 2011. Land subsidence, groundwater extraction, and flooding in Bandung basin (Indonesia. In: IAG 25th General Assembly of the International-Union-of-Geodesy-and-Geophysics (IUGG). International Association of Geodesy Symposia. Springer-Verlag Berlin, Melbourne, AUSTRALIA, pp. 167–173.
Guo, J.M., Zhou, L., Yao, C.L., Hu, J.Y., 2016. Surface subsidence analysis by multi-temporal InSAR and GRACE: a case study in Beijing. Sensors 16 (9), 18.
Guo, L., Gong, H.L., Ke, Y.H., Zhu, L., Li, X.J., Lyu, M.Y., Zhang, K., 2021. Mechanism of land subsidence mutation in Beijing Plain under the background of urban expansion. Remote Sens. 13 (16), 21.
Guo, L., Gong, H.L., Li, J.W., Zhu, L., Xue, A.M., Liao, L., Sun, Y., Li, Y.S., Zhang, Z.X., Hu, L.Y., Gao, M.L., Zhou, C.F., Cheng, R., Zhou, J.H., 2020. Understanding uneven land subsidence in Beijing, China, using a novel combination of geophysical prospecting and InSAR. Geophys. Res. Lett. 47 (16), 11.
Guo, L., Gong, H.L., Zhu, F., Zhu, L., Zhang, Z.X., Zhou, C.F., Gao, M.L., Sun, Y.K., 2019. Analysis of the spatiotemporal variation in land subsidence on the Beijing Plain, China. Remote Sens. 11 (10), 20.
Gutierrez, F., Galve, J.P., Lucha, P., Castaneda, C., Bonachea, J., Guerrero, J., 2011. Integrating geomorphological mapping, trenching, InSAR and GPR for the identification and characterization of sinkholes: a review and application in the mantled evaporite karst of the Ebro Valley (NE Spain). Geomorphology 134 (1–2), 144–156.
Guzy, A., Malinowska, A.A., 2020. State of the art and recent advancements in the modelling of land subsidence induced by groundwater withdrawal. Water 12 (7), 41.
Guzzetti, F., Mondini, A.C., Cardinali, M., Fiorucci, F., Santangelo, M., Chang, K.-T., 2012. Landslide inventory maps: new tools for an old problem. Earth Sci. Rev. 112 (1), 42–66.
Haghighi, M.H., Motagh, M., 2019. Ground surface response to continuous compaction of aquifer system in Tehran, Iran: results from a long-term multi-sensor InSAR analysis. Remote Sens. Environ. 221, 534–550.
Haji-Aghajany, S., Amerian, Y., 2020. Atmospheric phase screen estimation for land subsidence evaluation by InSAR time series analysis in Kurdistan,Iran. J. Atmos. Solar-Terrestr. Physics 205, 8.
Hakim, W.L., Achmad, A.R., Lee, C.W., 2020. Land Subsidence susceptibility mapping in Jakarta using functional and meta-ensemble machine learning algorithm based on time-series InSAR data. Remote Sens. 12 (21), 25.

Haynes, M., Capes, R., Lawrence, G., Smith, A., Shilston, D., Nicholls, G., Esa, 1997. Major urban subsidence mapped by differential SAR interferometry. In: 3rd ERS Symposium on Space at the Service of Our Environment. Esa Special Publications. European Space Agency, Florence, Italy, pp. 573–577.
He, Y.F., Xu, G.C., Kaufmann, H., Wang, J.T., Ma, H., Liu, T., 2021. Integration of InSAR and LiDAR technologies for a detailed urban subsidence and hazard assessment in Shenzhen,China. Remote Sens. 13 (12), 17.
Heleno, S.I.N., Oliveira, L.G.S., Henriques, M.J., Falcao, A.P., Lima, J.N.P., Cooksley, G., Ferretti, A., Fonseca, A.M., Lobo-Ferreira, J.P., Fonseca, J., 2011. Persistent scatterers interferometry detects and measures ground subsidence in Lisbon. Remote Sens. Environ. 115 (8), 2152–2167.
Hernandez-Espriu, A., Reyna-Gutierrez, J.A., Sanchez-Leon, E., Cabral-Cano, E., Carrera-Hernandez, J., Martinez-Santos, P., Macias-Medrano, S., Falorni, G., Colombo, D., 2014. The DRASTIC-Sg model: an extension to the DRASTIC approach for mapping groundwater vulnerability in aquifers subject to differential land subsidence, with application to Mexico City. Hydrogeol. J. 22 (6), 1469–1485.
Herrera-García, G., Ezquerro, P., Tomás, R., Béjar-Pizarro, M., López-Vinielles, J., Rossi, M., Mateos, R.M., Carreón-Freyre, D., Lambert, J., Teatini, P., 2021. Mapping the global threat of land subsidence. Science 371 (6524), 34–36.
Herrera, G., Fernandez, J.A., Tomas, R., Cooksley, G., Mulas, J., 2009a. Advanced interpretation of subsidence in Murcia (SE Spain) using A-DInSAR data - modelling and validation. Nat. Hazards Earth Syst. Sci. 9 (3), 647–661.
Herrera, G., Fernandez, M.I.A., Tomas, R., Gonzalez-Nicieza, C., Lopez-Sanchez, J.M., Vigil, A.E.A., 2012. Forensic analysis of buildings affected by mining subsidence based on Differential Interferometry (Part III). Eng. Fail. Anal. 24, 67–76.
Herrera, G., Tomás, R., López-Sánchez, J.M., Delgado, J., Mallorqui, J., Duque, S., Mulas, J., 2007. Advanced DInSAR analysis on mining areas: La Union case study (Murcia, SE Spain). Eng. Geol. 90 (3), 148–159.
Herrera, G., Tomas, R., Lopez-Sanchez, J.M., Delgado, J., Vicente, F., Mulas, J., Cooksley, G., Sanchez, M., Duro, J., Arnaud, A., Blanco, P., Duque, S., Mallorqui, J. J., De la Vega-Panizo, R., Monserrat, O., 2009b. Validation and comparison of Advanced Differential Interferometry Techniques: Murcia metropolitan area case study. ISPRS J. Photogramm. Remote Sens. 64 (5), 501–512.
Herrera, G., Tomas, R., Monells, D., Centolanza, G., Mallorqui, J.J., Vicente, F., Navarro, V.D., Lopez-Sanchez, J.M., Sanabria, M., Cano, M., Mulas, J., 2010a. Analysis of subsidence using TerraSAR-X data Murcia case study. Eng. Geol. 116 (3–4), 284–295.
Herrera, G., Tomas, R., Vicente, F., Lopez-Sanchez, J.M., Mallorqui, J.J., Mulas, J., 2010b. Mapping ground movements in open pit mining areas using differential SAR interferometry. Int. J. Rock Mech. Min. Sci. 47 (7), 1114–1125.
Higgins, S.A., Overeem, I., Steckler, M.S., Syvitski, J.P.M., Seeber, L., Akhter, S.H., 2014. InSAR measurements of compaction and subsidence in the Ganges-Brahmaputra Delta,Bangladesh. J. Geophys. Res. Earth Surf. 119 (8), 1768–1781.
Hobbs, S.E., Guarnieri, A.M., Broquetas, A., Calvet, J.-C., Casagli, N., Chini, M., Ferretti, R., Nagler, T., Pierdicca, N., Prudhomme, C., 2019. G-CLASS: geosynchronous radar for water cycle scienceâ€"orbit selection and system design. . Eng. 2019 (21), 7534–7537.
Hoffmann, J., 2005. The future of satellite remote sensing in hydrogeology. Hydrogeol. J. 13 (1), 247–250.
Hoffmann, J., Galloway, D.L., Zebker, H.A., 2003. Inverse modeling of interbed storage parameters using land subsidence observations, Antelope Valley,California. Water Resour. Res. 39 (2), 13.
Hoffmann, J., Zebker, H.A., 2003. Prospecting for horizontal surface displacements in Antelope Valley, California, using satellite radar interferometry. J. Geophys. Res. Earth Surf. 108 (F1), 12.
Hoffmann, J., Zebker, H.A., Galloway, D.L., Amelung, F., 2001. Seasonal subsidence and rebound in Las Vegas Valley, Nevada, observed by synthetic aperture radar interferometry. Water Resour. Res. 37 (6), 1551–1566.
Hole, J.K., Bromley, C.J., Stevens, N.F., Wadge, G., 2007. Subsidence in the geothermal fields of the Taupo Volcanic Zone, New Zealand from 1996 to 2005 measured by InSAR. J. Volcanol. Geotherm. Res. 166 (3–4), 125–146.
Holzer, T.L., 1984. Ground failure induced by ground-water withdrawal from unconsolidated sediment. Rev. Eng. Geol. 6, 67–105.
Hooper, A., 2008. A multi-temporal InSAR method incorporating both persistent scatterer and small baseline approaches. Geophys. Res. Lett. 35 (16).
Hooper, A., Bekaert, D., Spaans, K., Arıkan, M., 2012. Recent advances in SAR interferometry time series analysis for measuring crustal deformation. Tectonophysics 514, 1–13.
Hooper, A., Zebker, H., Segall, P., Kampes, B., 2004. A new method for measuring deformation on volcanoes and other natural terrains using InSAR persistent scatterers. Geophys. Res. Lett. 31 (23).
Hsieh, C.S., Shih, T.Y., Hu, J.C., Tung, H., Huang, M.H., Angelier, J., 2011. Using differential SAR interferometry to map land subsidence: a case study in the Pingtung Plain of SW Taiwan. Nat. Hazards 58 (3), 1311–1332.
Hsu, W.C., Chang, H.C., Chang, K.T., Lin, E.K., Liu, J.K., Liou, Y.A., 2015. Observing land subsidence and revealing the factors that influence it using a multi-sensor approach in Yunlin County,Taiwan. Remote Sens. 7 (6), 8202–8223.
Hu, B., Chen, J.Y., Zhang, X.F., 2019a. Monitoring the land subsidence area in a coastal urban area with InSAR and GNSS. Sensors 19 (14), 19.
Hu, B.L., Chen, L., Zou, Y.F., Wu, X.X., Washaya, P., 2021. Methods for monitoring fast and large gradient subsidence in coal mining areas using SAR Images: a review. Ieee Access 9, 159018–159035.
Hu, L.Y., Dai, K., Xing, C.Q., Li, Z.H., Tomas, R., Clark, B., Shi, X.L., Chen, M., Zhang, R., Qiu, Q., Lu, Y.J., 2019b. Land subsidence in Beijing and its relationship with geological faults revealed by Sentinel-1 InSAR observations. Int. J. Appl. Earth Obs. Geoinf. 82, 10.
Hu, R., Yue, Z., Wang, L.U., Wang, S., 2004. Review on current status and challenging issues of land subsidence in China. Eng. Geol. 76 (1-2), 65–77.
Hu, Z., Ge, L.L., Li, X.J., Zhang, K., Zhang, L., 2013. An underground-mining detection system based on DInSAR. IEEE Trans. Geosci. Remote Sens. 51 (1), 615–625.
Hubatka, F., Pospisil, L., Lazecky, M., 2021. Identification of ground instability in the housing estate complex based on georadar and satellite radar interferometry. Acta Geodyn. Geomater. 18 (2), 231–240.
Hung, W.C., Hwang, C., Chen, Y.A., Chang, C.P., Yen, J.Y., Hooper, A., Yang, C.Y., 2011. Surface deformation from persistent scatterers SAR interferometry and fusion with leveling data: a case study over the Choushui River Alluvial Fan, Taiwan. Remote Sens. Environ. 115 (4), 957–967.
Ignatenko, V., Laurila, P., Radius, A., Lamentowski, L., Antropov, O., Muff, D., 2020. ICEYE Microsatellite SAR constellation status update: evaluation of first commercial imaging modes. In: IGARSS 2020-2020 IEEE International Geoscience and Remote Sensing Symposium. IEEE, pp. 3581–3584.
Intrieri, E., Gigli, G., Nocentini, M., Lombardi, L., Mugnai, F., Fidolini, F., Casagli, N., 2015. Sinkhole monitoring and early warning: an experimental and successful GB-InSAR application. Geomorphology 241, 304–314.
Ishwar, S.G., Kumar, D., 2017. Application of DInSAR in mine surface subsidence monitoring and prediction. Curr. Sci. 112 (1), 46–51.
Iwahana, G., Uchida, M., Liu, L., Gong, W.Y., Meyer, F.J., Guritz, R., Yamanokuchi, T., Hinzman, L., 2016. InSAR detection and field evidence for thermokarst after a Tundra Wildfire, using ALOS-PALSAR. Remote Sens. 8 (3), 18.
Jacome, M.C., Martinez-Grana, A.M., Valdes, V., 2020. Detection of terrain deformations using InSAR techniques in relation to results on Terrain subsidence (Ciudad de Zaruma, Ecuador). Remote Sens. 12 (10), 22.
Jeanne, P., Farr, T.G., Rutqvist, J., Vasco, D.W., 2019. Role of agricultural activity on land subsidence in the San Joaquin Valley, California. J. Hydrol. 569, 462–469.
Jha, B., Bottazzi, F., Wojcik, R., Coccia, M., Bechor, N., McLaughlin, D., Herring, T., Hager, B.H., Mantica, S., Juanes, R., 2015. Reservoir characterization in an underground gas storage field using joint inversion of flow and geodetic data. Int. J. Numer. Anal. Methods Geomech. 39 (14), 1619–1638.
Jiang, C., Wang, L., Yu, X.X., Chi, S.S., Wei, T., Wang, X.L., 2021. DPIM-based InSAR phase unwrapping model and a 3D mining-induced surface deformation extracting method: a case of Huainan mining area. Ksce J. Civ. Eng. 25 (2), 654–668.
Jiang, L.M., Lin, H., Ma, J.W., Kong, B., Wang, Y., 2011. Potential of small-baseline SAR interferometry for monitoring land subsidence related to underground coal fires: Wuda (Northern China) case study. Remote Sens. Environ. 115 (2), 257–268.
Jung, H.C., Kim, S.W., Jung, H.S., Min, K.D., Won, J.S., 2007. Satellite observation of coal mining subsidence by persistent scatterer analysis. Eng. Geol. 92 (1–2), 1–13.
Kalia, A.C., Frei, M., Lege,, T., 2014. Preparation of a national Copernicus-service for detection and monitoring of land subsidence and mass movements in the context of remote sensing assisted hazard mitigation. In: Earth Resources and Environmental Remote Sensing/GIS Applications V, 9245. SPIE, pp. 24–29.
Kampes, B., Usai, S., 1999. Doris: The delft object-oriented radar interferometric software. In: Proceedings of the 2nd International Symposium on Operationalization of Remote Sensing, Enschede, The Netherlands.
Karanam, V., Motagh, M., Garg, S., Jain, K., 2021. Multi-sensor remote sensing analysis of coal fire induced land subsidence in Jharia Coalfields, Jharkhand, India. Int. J. Appl. Earth Obs. Geoinf. 102, 15.
Karila, K., Karjalainen, M., Hyyppä, J., Koskinen, J., Saaranen, V., Rouhiainen, P., 2013. A comparison of precise leveling and persistent scatterer SAR interferometry for building subsidence rate measurement. ISPRS Int. J. Geo Inf. 2 (3), 797–816.
Keiding, M., Arnadottir, T., Jonsson, S., Decriem, J., Hooper, A., 2010. Plate boundary deformation and man-made subsidence around geothermal fields on the Reykjanes Peninsula, Iceland. J. Volcanol. Geotherm. Res. 194 (4), 139–149.
Khakim, M.Y.N., Tsuji, T., Matsuoka, T., 2014. Lithology-controlled subsidence and seasonal aquifer response in the Bandung basin, Indonesia, observed by synthetic aperture radar interferometry. Int. J. Appl. Earth Obs. Geoinf. 32, 199–207.
Khan, S.D., Huang, Z., Karacay, A., 2014. Study of ground subsidence in Northwest Harris county using GPS, LiDAR, and InSAR techniques. Nat. Hazards 73 (3), 1143–1173.
Khorrami, M., Alizadeh, B., Tousi, E.G., Shakerian, M., Maghsoudi, Y., Rahgozar, P., 2019. How groundwater level fluctuations and geotechnical properties lead to asymmetric subsidence: a PSInSAR analysis of land deformation over a transit corridor in the Los Angeles Metropolitan Area. Remote Sens. 11 (4), 22.
Kim, J.-S., Kim, D.-J., Kim, S.-W., Won, J.-S., Moon, W.M., 2007. Monitoring of urban land surface subsidence using PSInSAR. Geosci. J. 11 (1), 59–73.
Kim, J.W., Lu, Z., Jia, Y.Y., Shum, C.K., 2015. Ground subsidence in Tucson, Arizona, monitored by time-series analysis using multi-sensor InSAR datasets from 1993 to 2011. ISPRS J. Photogramm. Remote Sens. 107, 126–141.
Kim, J.W., Lu, Z., Kaufmann, J., 2019. Evolution of sinkholes over Wink, Texas, observed by high-resolution optical, and SAR imagery. Remote Sens. Environ. 222, 119–132.
Kim, S.W., Kim, C.O., Won, J.S., Lee, D.C., Kim, J.W., Ieee, 2005. Surface deformation in Mokpo area observed with synthetic aperture radar interferometry. In: 25th IEEE International Geoscience and Remote Sensing Symposium (IGARSS 2005). IEEE International Symposium on Geoscience and Remote Sensing (IGARSS). Ieee, Seoul, SOUTH KOREA, pp. 234–236.
Kim, S.W., Lee, C.W., Song, K.Y., Min, K.D., Won, J.S., 2005b. Application of L-band differential SAR interferometry to subsidence rate estimation in reclaimed coastal land. Int. J. Remote Sens. 26 (7), 1363–1381.
Kim, S.W., Wdowinski, S., Dixon, T.H., Amelung, F., Kim, J.W., Won, J.S., 2010. Measurements and predictions of subsidence induced by soil consolidation using persistent scatterer InSAR and a hyperbolic model. Geophys. Res. Lett. 37, 5.

Kim, S.W., Wdowinski, S., Dixon, T.H., Amelung, F., Won, J.S., Kim, J.W., 2008. InSAR-based mapping of surface subsidence in Mokpo City, Korea, using JERS-1 and ENVISAT SAR data. Earth Planets Space 60 (5), 453–461.
Koros, W.K., Agustin, F., 2017. Subsidence surveys at Olkaria geothermal field,Kenya. J. Spat. Sci. 62 (1), 195–205.
Lanari, R., Lundgren, P., Sansosti, E., 1998. Dynamic deformation of Etna volcano observed by satellite radar interferometry. Geophys. Res. Lett. 25 (10), 1541–1544.
Le, T.S., Chang, C.P., Nguyen, X.T., Yhokha, A., 2016. TerraSAR-X Data for high-precision land subsidence monitoring: a case study in the historical centre of Hanoi, Vietnam. Remote Sens. 8 (4), 23.
Lee, S.-R., 2010. Overview of KOMPSAT-5 program, mission, and system. In: 2010 IEEE international geoscience and remote sensing symposium. IEEE, pp. 797–800.
Lei, K.C., Chen, B.B., Jia, S.M., Wang, S.F., Luo, Y., 2014. Primary investigation of formation and genetic mechanism of land subsidence based on PS-InSAR technology in Beijing. Spectrosc. Spectr. Anal. 34 (8), 2185–2189.
Levy, M.C., Neely, W.R., Borsa, A.A., Burney, J.A., 2020. Fine-scale spatiotemporal variation in subsidence across California's San Joaquin Valley explained by groundwater demand. Environ. Res. Lett. 15 (10), 13.
Li, H.J., Zhu, L., Dai, Z.X., Gong, H.L., Guo, T., Guo, G.X., Wang, J.B., Teatini, P., 2021a. Spatiotemporal modeling of land subsidence using a geographically weighted deep learning method based on PS-InSAR. Sci. Total Environ. 799, 13.
Li, J.C., Gao, F., Lu, J.G., 2019. An application of InSAR time-series analysis for the assessment of mining-induced structural damage in Panji Mine,China. Nat. Haz. 97 (1), 243–258.
Li, J.H., Zhou, L., Ren, C., Liu, L.L., Zhang, D., Ma, J., Shi, Y.J., 2021b. Spatiotemporal inversion and mechanism analysis of surface subsidence in Shanghai area based on time-series InSAR. Appl. Sci. Basel 11 (16), 22.
Li, L.P., Zhang, M.J., Katzenstein, K., 2017. Calibration of a land subsidence model using InSAR data via the Ensemble Kalman Filter. Groundwater 55 (6), 871–878.
Li, Y.S., Zhang, J.F., Li, Z.H., Luo, Y., Jiang, W.L., Tian, Y.F., 2016. Measurement of subsidence in the Yangbajing geothermal fields, Tibet, from TerraSAR-X InSAR time series analysis. Int. J. Digital Earth 9 (7), 697–709.
Li, Z.W., Yang, Z.F., Zhu, J.J., Hu, J., Wang, Y.J., Li, P.X., Chen, G.L., 2015. Retrieving three-dimensional displacement fields of mining areas from a single InSAR pair. J. Geod. 89 (1), 17–32.
Liu, G., Jia, H., Zhang, R., Zhang, H., Jia, H., Yu, B., Sang, M., 2010. Exploration of subsidence estimation by persistent scatterer InSAR on time series of high resolution TerraSAR-X images. IEEE J. Select. Top. Appl. Earth Observ.Remote Sens. 4 (1), 159–170.
Liu, G.X., Luo, X.J., Chen, Q., Huang, D.F., Ding, X.L., 2008. Detecting land subsidence in Shanghai by PS-networking SAR interferometry. Sensors 8 (8), 4725–4741.
Liu, L., Jafarov, E.E., Schaefer, K.M., Jones, B.M., Zebker, H.A., Williams, C.A., Rogan, J., Zhang, T.J., 2014a. InSAR detects increase in surface subsidence caused by an Arctic tundra fire. Geophys. Res. Lett. 41 (11), 3906–3913.
Liu, L., Schaefer, K.M., Chen, A.C., Gusmeroli, A., Zebker, H.A., Zhang, T., 2015. Remote sensing measurements of thermokarst subsidence using InSAR. J. Geophys. Res. Earth Surf. 120 (9), 1935–1948.
Liu, P., Chen, X.F., Li, Z.H., Zhang, Z.G., Xu, J.K., Feng, W.P., Wang, C.S., Hu, Z.W., Tu, W., Li, H., 2018. Resolving surface displacements in shenzhen of china from time series InSAR. Remote Sens. 10 (7), 26.
Liu, Y.L., Huang, H.J., Liu, Y.X., Bi, H.B., 2016. Linking land subsidence over the Yellow River delta, China, to hydrocarbon exploitation using multi-temporal InSAR. Nat. Hazards 84 (1), 271–291.
Liu, Z., Liu, P.W., Massoud, E., Farr, T.G., Lundgren, P., Famiglietti, J.S., 2019. Monitoring groundwater change in California's central valley using Sentinel-1 and GRACE observations. Geosciences 9 (10), 21.
Liu, Z.G., Bian, Z.F., Lei, S.G., Liu, D.L., Sowter, A., 2014b. Evaluation of PS-DInSAR technology for subsidence monitoring caused by repeated mining in mountainous area. Trans. Nonferrous Metals Soc. China 24 (10), 3309–3315.
Long, Z., Yumei, L., Yong, L., Jiurong, L., Wenjun, C., Youquan, Z., Kunchao, L., Fang, T., Zhantao, H., He, L., 2021. An extension-dominant 9-km-long ground failure along a buried geological fault on the eastern Beijing Plain,China. Eng. Geol. 289, 106168.
Lopez-Quiroz, P., Doin, M.P., Tupin, F., Briole, P., Nicolas, J.M., 2009. Time series analysis of Mexico City subsidence constrained by radar interferometry. J. Appl. Geophys. 69 (1), 1–15.
Lubis, A.M., Sato, T., Tomiyama, N., Isezaki, N., Yamanokuchi, T., 2011. Ground subsidence in Semarang-Indonesia investigated by ALOS-PALSAR satellite SAR interferometry. J. Asian Earth Sci. 40 (5), 1079–1088.
Luo, Q.L., Perissin, D., Lin, H., Zhang, Y.Z., Wang, W., 2014a. Subsidence monitoring of Tianjin suburbsby TerraSAR-X persistent scatterers interferometry. Ieee J.Select.Top. Appl. Earth Observ. Remote Sens. 7 (5), 1642–1650.
Luo, Q.L., Perissin, D., Zhang, Y.Z., Jia, Y.L., 2014b. L-and X-band multi-temporal InSAR analysis of Tianjin subsidence. Remote Sens. 6 (9), 7933–7951.
Luo, Q.L., Zhou, G.Q., Perissin, D., 2017. Monitoring of subsidence along Jingjin inter-city railway with high-resolution TerraSAR-X MT-InSAR analysis. Remote Sens. 9 (7), 14.
Luo, X.G., Wang, J.J., Xu, Z.Y., Zhu, S., Meng, L.S., Liu, J.K., Cui, Y., 2018. Dynamic analysis of urban ground subsidence in Beijing based on the permanent scattering InSAR technology. J. Appl. Remote. Sens. 12 (2), 18.
Ma, C., Cheng, X.G., Yang, Y.L., Zhang, X.K., Guo, Z.Z., Zou, Y.F., 2016. Investigation on mining subsidence based on multi-temporal InSAR and time-series analysis of the small baseline subset-case study of working faces 22201–1/2 in Bu'ertai Mine, Shendong Coalfield, China. Remote Sens. 8 (11), 25.
Ma, G.Y., Yang, T.L., Zhao, Q., Kubanek, J.L., Pepe, A., Dong, H.B., Sun, Z.B., 2017. Potential inundated coastal area estimation in Shanghai with multi-platform SAR and altimetry data. In: Conference on Remote Sensing and Modeling of Ecosystems for Sustainability XIV. Proceedings of SPIE. Spie-Int Soc Optical Engineering, San Diego, CA.
Ma, P.F., Wang, W.X., Zhang, B.W., Wang, J.L., Shi, G.Q., Huang, G.Q., Chen, F.L., Jiang, L.M., Lin, H., 2019. Remotely sensing large- and small-scale ground subsidence: a case study of the Guangdong-Hong Kong-Macao Greater Bay Area of China. Remote Sens. Environ. 232, 18.
Maleki, H., McKenzie, J., 2021. Review of US subsidence monitoring using conventional and satellite based methods. In: IOP Conference Series: Earth and Environmental Science. IOP Publishing, p. 012154.
Malinowska, A.A., Witkowski, W.T., Guzy, A., Hejmanowski, R., 2018. Mapping ground movements caused by mining-induced earthquakes applying satellite radar interferometry. Eng. Geol. 246, 402–411.
Mallorqui, J.J., Blanco, P., Broquetas, A., Mora, O., Ieee, 2003. In: Phase statistics and quality evaluation of deformation maps with multiple-image differential interferometry, 23rd International Geoscience and Remote Sensing Symposium (IGARSS 2003). IEEE International Symposium on Geoscience and Remote Sensing IGARSS. Ieee, Toulouse, France, pp. 4344–4346.
Marshall, C., Large, D.J., Athab, A., Evers, S.L., Sowter, A., Marsh, S., Sjogersten, S., 2018. Monitoring tropical peat related settlement using ISBAS InSAR, Kuala Lumpur International Airport (KLIA). Eng. Geol. 244, 57–65.
Massonnet, D., Feigl, K.L., 1995. Discrimination of geophysical phenomena in satellite radar interferograms. Geophys. Res. Lett. 22 (12), 1537–1540.
Massonnet, D., Feigl, K.L., 1998. Radar interferometry and its application to changes in the Earth's surface. Rev. Geophys. 36 (4), 441–500.
Massonnet, D., Holzer, T., Vadon, H., 1997. Land subsidence caused by the East Mesa geothermal field, California, observed using SAR interferometry. Geophys. Res. Lett. 24 (8), 901–904.
Massonnet, D., Rossi, M., Carmona, C., Adragna, F., Peltzer, G., Feigl, K., Rabaute, T., 1993. The displacement field of the Landers earthquake mapped by radar interferometry. Nature 364 (6433), 138–142.
Matano, F., Sacchi, M., Vigliotti, M., Ruberti, D., 2018. Subsidence trends of Volturno River Coastal Plain (Northern Campania, Southern Italy) inferred by SAR interferometry data. Geosciences 8 (1), 22.
Meisina, C., Zucca, F., Fossati, D., Ceriani, M., Allievi, J., 2006. Ground deformation monitoring by using the permanent scatterers technique: the example of the Oltrepo Pavese (Lombardia, Italy). Eng. Geol. 88 (3–4), 240–259.
Meisina, C., Zucca, F., Notti, D., Colombo, A., Cucchi, A., Savio, G., Giannico, C., Bianchi, M., 2008. Geological Interpretation of PSInSAR Data at Regional Scale. Sensors 8 (11), 7469–7492.
Melet, A., Buontempo, C., Mattiuzzi, M., Salamon, P., Bahurel, P., Breyiannis, G., Burgess, S., Crosnier, L., Le Traon, P-Y., Mentaschi, L., Nicolas, J., Solari, L., Vamborg, F., Voukouvalas, E., 2021. European Copernicus Services to Inform on Sea-Level Rise Adaptation: Current Status and Perspectives. Front. Mar. Sci. 8, 1–8.
Milillo, P., Giardina, G., DeJong, M.J., Perissin, D., Milillo, G., 2018. Multi-temporal InSAR structural damage assessment: the London Crossrail Case Study. Remote Sens. 10 (2), 11.
Miller, M.M., Jones, C.E., Sangha, S.S., Bekaert, D.P., 2020. Rapid drought-induced land subsidence and its impact on the California aqueduct. Remote Sens. Environ. 251, 15.
Miller, M.M., Shirzaei, M., 2015. Spatiotemporal characterization of land subsidence and uplift in Phoenix using InSAR time series and wavelet transforms. J. Geophys.Res. Solid Earth 120 (8), 5822–5842.
Miller, M.M., Shirzaei, M., 2019. Land subsidence in Houston correlated with flooding from Hurricane Harvey. Remote Sens. Environ. 225, 368–378.
Miller, M.M., Shirzaei, M., 2021. Assessment of future flood hazards for Southeastern Texas: synthesizing subsidence, sea-level rise, and storm surge scenarios. Geophys. Res. Lett. 48 (8), 12.
Miller, M.M., Shirzaei, M., Argus, D., 2017. Aquifer mechanical properties and decelerated compaction in Tucson,Arizona. J. Geophys. Res. Solid Earth 122 (10), 8402–8416.
Minderhoud, P.S.J., Coumou, L., Erban, L.E., Middelkoop, H., Stouthamer, E., Addink, E. A., 2018. The relation between land use and subsidence in the Vietnamese Mekong delta. Sci. Total Environ. 634, 715–726.
Minh, D.H.T., Van Trung, L., Toan, T.L., 2015. Mapping ground subsidence phenomena in Ho Chi Minh City through the radar interferometry technique using ALOS PALSAR data. Remote Sens. 7 (7), 8543–8562.
Mirzadeh, S.M.J., Jin, S.G., Parizi, E., Chaussard, E., Burgmann, R., Blasco, J.M.D., Amani, M., Bao, H., Mirzadeh, S.H., 2021. Characterization of irreversible land subsidence in the Yazd-Ardakan Plain, Iran from 2003 to 2020 InSAR time series. J. Geophys. Res.Solid Earth 126 (11), 22.
Modeste, G., Doubre, C., Masson, F., 2021. Time evolution of mining-related residual subsidence monitored over a 24-year period using InSAR in southern Alsace, France. Int. J. Appl. Earth Obs. Geoinf. 102, 11.
Moghaddam, N.F., Sahebi, M.R., Matkan, A.A., Roostaei, M., 2013. Subsidence rate monitoring of Aghajari oil field based on differential SAR interferometry. Adv. Space Res. 51 (12), 2285–2296.
Mondini, A.C., Guzzetti, F., Chang, K.-T., Monserrat, O., Martha, T.R., Manconi, A., 2021. Landslide failures detection and mapping using Synthetic Aperture Radar: past, present and future. Earth Sci. Rev. 103574.
Mongeon, P., Paul-Hus, A., 2016. The journal coverage of Web of Science and Scopus: a comparative analysis. Scientometrics 106 (1), 213–228.
Montuori, A., Anderlini, L., Palano, M., Albano, M., Pezzo, G., Antoncecchi, I., Chiarabba, C., Serpelloni, E., Stramondo, S., 2018. Application and analysis of geodetic protocols for monitoring subsidence phenomena along on-shore hydrocarbon reservoirs. Int. J. Appl. Earth Obs. Geoinf. 69, 13–26.

Mora, O., Lanari, R., Mallorqui, J.J., Berardino, P., Sansosti, E., 2002. A new algorithm for monitoring localized deformation phenomena based on small baseline differential SAR interferograms, IEEE International Geoscience and Remote Sensing Symposium. IEEE 1237–1239.
Morishita, Y., Lazecky, M., Wright, T.J., Weiss, J.R., Elliott, J.R., Hooper, A., 2020. LiCSBAS: an open-source InSAR time series analysis package integrated with the LiCSAR automated Sentinel-1 InSAR processor. Remote Sens. 12 (3), 29.
Motagh, M., Djamour, Y., Walter, T.R., Wetzel, H.-U., Zschau, J., Arabi, S., 2007. Land subsidence in Mashhad Valley, Northeast Iran: results from InSAR, levelling and GPS. Geophys. J. Int. 168 (2), 518–526.
Motagh, M., Shamshiri, R., Haghighi, M.H., Wetzel, H.U., Akbari, B., Nahavandchi, H., Roessner, S., Arabi, S., 2017. Quantifying groundwater exploitation induced subsidence in the Rafsanjan plain, southeastern Iran, using InSAR time-series and in situ measurements. Eng. Geol. 218, 134–151.
Murgia, F., Bignami, C., Brunori, C.A., Tolomei, C., Pizzimenti, L., 2019. Ground deformations controlled by hidden faults: multi-frequency and multitemporal InSAR techniques for urban hazard monitoring. Remote Sens. 11 (19), 17.
Nadiri, A.A., Khatibi, R., Khalifi, P., Feizizadeh, B., 2020. A study of subsidence hotspots by mapping vulnerability indices through innovatory 'ALPRIFT' using artificial intelligence at two levels. Bull. Eng. Geol. Environ. 79 (8), 3989–4003.
Nadiri, A.A., Taheri, Z., Khatibi, R., Barzegari, G., Dideban, K., 2018. Introducing a new framework for mapping subsidence vulnerability indices (SVIs): ALPRIFT. Sci. Total Environ. 628–629, 1043–1057.
Nappo, N., Peduto, D., Polcari, M., Livio, F., Ferrario, M.F., Comerci, V., Stramondo, S., Michetti, A.M., 2021. Subsidence in Como historic Centre (northern Italy): assessment of building vulnerability combining hydrogeological and stratigraphic features, Cosmo-SkyMed InSAR and damage data. Int. J. Disast. Risk Reduct. 56, 16.
Navarro-Hernandez, M.I., Tomas, R., Lopez-Sanchez, J.M., Cardenas-Tristan, A., Mallorqui, J.J., 2020. Spatialanalysis of land subsidence in the San Luis Potosi Valley induced by aquifer overexploitation using the Coherent Pixels Technique (CPT) and Sentinel-1 InSAR Observation. Remote Sens. 12 (22), 23.
Navarro-Sanchez, V.D., Lopez-Sanchez, J.M., 2012. Improvement of persistent-scatterer interferometry performance by means of a polarimetric optimization. IEEE Geosci. Remote Sens. Lett. 9 (4), 609–613.
Navarro-Sanchez, V.D., Lopez-Sanchez, J.M., 2014. Spatial adaptive speckle filtering driven by temporal polarimetric statistics and its application to PSI. IEEE Trans. Geosci. Remote Sens. 52 (8), 4548–4557.
Navarro-Sanchez, V.D., Lopez-Sanchez, J.M., Ferro-Famil, L., 2014. Polarimetric approaches for persistent scatterers interferometry. IEEE Trans. Geosci. Remote Sens. 52 (3), 1667–1676.
Neely, W.R., Borsa, A.A., Silverii, F., 2020. GInSAR: a cGPS correction for enhanced InSAR time series. IEEE Trans. Geosci. Remote Sens. 58 (1), 136–146.
Ng, A.H.M., Chang, H.C., Ge, L.L., Rizos, C., Omura, M., 2009. Assessment of radar interferometry performance for ground subsidence monitoring due to underground mining. Earth Planets Space 61 (6), 733–745.
Ng, A.H.M., Chang, H.C., Zhang, K., Ge, L.L., Rizos, C., 2007. Land subsidence monitoring in Australia and China using satellite interferometry. In: General Assembly of the International-Association-of-Geodesy/24th General Assembly of the International-Union-of-Geodesy-and-Geophysics. International Association of Geodesy Symposia. Springer-Verlag Berlin, Perugia, ITALY, pp. 743–750.
Ng, A.H.M., Ge, L.L., 2007. Application of Persistent Scatterer InSAR and GIS for urban subsidence monitoring. In: IEEE International Geoscience and Remote Sensing Symposium (IGARSS). IEEE International Symposium on Geoscience and Remote Sensing IGARSS. Ieee, Barcelona, SPAIN, pp. 1091–1094.
Ng, A.H.M., Ge, L.L., Du, Z.Y., Wang, S.R., Ma, C., 2017. Satellite radar interferometry for monitoring subsidence induced by longwall mining activity using Radarsat-2, Sentinel-1 and ALOS-2 data. Int. J. Appl. Earth Obs. Geoinf. 61, 92–103.
Ng, A.H.M., Ge, L.L., Li, X.J., Abidin, H.Z., Andreas, H., Zhang, K., 2012a. Mapping land subsidence in Jakarta, Indonesia using persistent scatterer interferometry (PSI) technique with ALOS PALSAR. Int. J. Appl. Earth Obs. Geoinf. 18, 232–242.
Ng, A.H.M., Ge, L.L., Li, X.J., Zhang, K., 2012b. Monitoring ground deformation in Beijing, China with persistent scatterer SAR interferometry. J. Geod. 86 (6), 375–392.
Ng, A.H.M., Ge, L.L., Yan, Y.G., Li, X.J., Chang, H.C., Zhang, K., Rizos, C., 2010. Mapping accumulated mine subsidence using small stack of SAR differential interferograms in the Southern coalfield of New South Wales,Australia. Eng. Geol. 115 (1–2), 1–15.
Nicholls, R.J., Cazenave, A., 2010. Sea-level rise and its impact on coastal zones. Science 328 (5985), 1517–1520.
Nikos, S., Ioannis, P., Constantinos, L., Paraskevas, T., Anastasia, K., Charalambos, K., 2016. Land subsidence rebound detected via multi-temporal InSAR and ground truth data in Kalochori and Sindos regions, Northern Greece. Eng. Geol. 209, 175–186.
Nof, R.N., Abelson, M., Raz, E., Magen, Y., Atzori, S., Salvi, S., Baer, G., 2019. SAR interferometry for sinkhole early warning and susceptibility assessment along the Dead Sea,Israel. Remote Sens. 11 (1), 19.
Norris, M., Oppenheim, C., 2007. Comparing alternatives to the Web of Science for coverage of the social sciences' literature. J. Inform. 1 (2), 161–169.
Notti, D., Calo, F., Cigna, F., Manunta, M., Herrera, G., Berti, M., Meisina, C., Tapete, D., Zucca, F., 2015. A user-oriented methodology for DInSAR. Pure Appl. Geophys. 172 (11), 3081–3105.
Notti, D., Mateos, R.M., Monserrat, O., Devanthery, N., Peinado, T., Roldan, F.J., Fernandez-Chacon, F., Galve, J.P., Lamas, F., Azanon, J.M., 2016. Lithological control of land subsidence induced by groundwater withdrawal in new urban AREAS (Granada Basin, SE Spain). Multiband DInSAR monitoring. Hydrol. Process. 30 (13), 2317–2331.
Ojha, C., Shirzaei, M., Werth, S., Argus, D.F., Farr, T.G., 2018. Sustained groundwater loss in California's central valley exacerbated by intense drought periods. Water Resour. Res. 54 (7), 4449–4460.
Ojha, C., Werth, S., Shirzaei, M., 2020. Recovery of aquifer-systems in Southwest US following 2012–2015 drought: evidence from InSAR, GRACE and groundwater level data. J. Hydrol. 587, 16.
Osmanoglu, B., Dixon, T.H., Wdowinski, S., Cabral-Cano, E., Jiang, Y., 2011. Mexico City subsidence observed with persistent scatterer InSAR. Int. J. Appl. Earth Obs. Geoinf. 13 (1), 1–12.
Othman, A., 2018. Measuring and monitoring land subsidence and earth fissures in Al-Qassim Region, Saudi Arabia: inferences from InSAR. In: 1st Springer Conference of the Arabian-Journal-of-Geosciences (CAJG). Advances in Science Technology & Innovation. Springer International Publishing Ag, Hammamet, TUNISIA, pp. 287–291.
Othman, A., Abotalib, A.Z., 2019. Land subsidence triggered by groundwater withdrawal under hyper-arid conditions: case study from Central Saudi Arabia. Environ. Earth Sci. 78 (7), 8.
Ou, D.P., Tan, K., Du, Q., Chen, Y., Ding, J.W., 2018. Decision fusion of D-InSAR and pixel offset tracking for coal mining deformation monitoring. Remote Sens. 10 (7), 18.
Pacheco-Martinez, J., Cabral-Cano, E., Wdowinski, S., Hernandez-Marin, M., Ortiz-Lozano, J.A., Zermeno-de-Leon, M.E., 2015. Application of InSAR and gravimetry for land subsidence hazard zoning in Aguascalientes,Mexico. Remote Sens. 7 (12), 17035–17050.
Paine, J.G., Buckley, S.M., Collins, E.W., Wilson, C.R., 2010. Assessing collapse risk in evaporite sinkhole-prone areas using gravimetry and radar interferometry. In: 4th International Conference on Environmental and Engineering Geophysics. Science Press USA Inc, Chengdu Univ Technol, Chengdu, PEOPLES R CHINA, pp. 753–763.
Papoutsis, I., Kontoes, C., Paradissis, D., 2017. Multi-stack persistent scatterer interferometry analysis in Wider Athens,Greece. Remote Sens. 9 (3), 20.
Parcharidis, I., Foumelis, M., Kourkouli, P., Wegmuller, U., 2009. Persistent Scatterers InSAR to detect ground deformation over Rio-Antirio area (Western Greece) for the period 1992–2000. J. Appl. Geophys. 68 (3), 348–355.
Parcharidis, I., Kourkouli, P., Karymbalis, E., Foumelis, M., Karathanassi, V., 2013. Time series synthetic aperture radar interferometry for ground deformation monitoring over a small scale tectonically active deltaic environment (Mornos, Central Greece). J. Coast. Res. 29 (2), 325–338.
Parcharidis, I., Lagios, E., Sakkas, V., Raucoules, D., Feurer, D., Le Mouelic, S., King, C., Carnec, C., Novali, F., Ferretti, A., Capes, R., Cooksley, G., 2006. Subsidence monitoring within the Athens Basin (Greece) using space radar interferometric techniques. Earth Planets Space 58 (5), 505–513.
Parker, A.L., Filmer, M.S., Featherstone, W.E., 2017. First results from Sentinel-1A InSAR over Australia: application to the Perth Basin. Remote Sens. 9 (3), 19.
Parks, M., Sigmundsson, F., Sigurdsson, O., Hooper, A., Hreinsdottir, S., Ofeigsson, B., Michalczewska, K., 2020. Deformation due to geothermal exploitation at Reykjanes, Iceland. J. Volcanol. Geotherm. Res. 391, 12.
Peduto, D., Cascini, L., Arena, L., Ferlisi, S., Fornaro, G., Reale, D., 2015. A general framework and related procedures for multiscale analyses of DInSAR data in subsiding urban areas. ISPRS J. Photogramm. Remote Sens. 105, 186–210.
Peltzer, G., Rosen, P., 1995. Surface displacement of the 17 May 1993 Eureka Valley, California, earthquake observed by SAR interferometry. Science 268 (5215), 1333–1336.
Peng, M.M., Zhao, C.Y., Zhang, Q., Lu, Z., Li, Z.S., 2019. Research on spatiotemporal land deformation (2012–2018) over Xi'an, China, with multi-sensor SAR datasets. Remote Sens. 11 (6), 21.
Perissin, D., Wang, Z., Wang, T., 2011. The SARPROZ InSAR tool for urban subsidence/manmade structure stability monitoring in China. In: Proceedings of the ISRSE, Sidney, Australia, p. 1015.
Perski, Z., Hanssen, R., Wojcik, A., Wojciechowski, T., 2009. InSAR analyses of terrain deformation near the Wieliczka Salt Mine,Poland. Eng. Geol. 106 (1–2), 58–67.
Pierdicca, N., Davidson, M., Chini, M., Dierking, W., Djavidnia, S., Haarpaintner, J., Hajduch, G., Laurin, G.V., Lavalle, M., López-Martínez, C., 2019. The copernicus L-band SAR mission ROSE-L (Radar Observing System for Europe)(conference presentation). In: Active and Passive Microwave Remote Sensing for Environmental Monitoring III. International Society for Optics and Photonics, p. 111540E.
Plattner, C., Wdowinski, S., Dixon, T.H., Biggs, J., 2010. Surface subsidence induced by the Crandall Canyon Mine (Utah) collapse: InSAR observations and elasto-plastic modelling. Geophys. J. Int. 183 (3), 1089–1096.
Poitevin, C., Woppelmann, G., Raucoules, D., Le Cozannet, G., Marcos, M., Testut, L., 2019. Vertical land motion and relative sea level changes along the coastline of Brest (France) from combined space-borne geodetic methods. Remote Sens. Environ. 222, 275–285.
Polcari, M., Albano, M., Saroli, M., Tolomei, C., Lancia, M., Moro, M., Stramondo, S., 2014. Subsidence detected by multi-pass differential SAR interferometry in the Cassino Plain (Central Italy): joint effect of Geological and Anthropogenic Factors? Remote Sens. 6 (10), 9676–9690.
Poreh, D., Iodice, A., Riccio, D., Ruello, G., 2016. Railways' stability observed in Campania (Italy) by InSAR data. Eur. J. Remote Sens. 49, 417–431.
Poreh, D., Pirasteh, S., Cabral-Cano, E., 2021. Assessing subsidence of Mexico City from InSAR and LandSat ETM plus with CGPS and SVM. Geoenviron. Disasters 8 (1), 19.
Przylucka, M., Herrera, G., Graniczny, M., Colombo, D., Bejar-Pizarro, M., 2015. Combination of conventional and Advanced DInSAR to monitor very fast mining subsidence with TerraSAR-X data: Bytom City (Poland). Remote Sens. 7 (5), 5300–5328.
Pu, C.H., Xu, Q., Zhao, K.Y., Jiang, Y.N., Hao, L.N., Liu, J.L., Chen, W.L., Kou, P.L., 2021. Characterizing the topographic changes and land subsidence associated with the

mountain excavation and city construction on the Chinese Loess Plateau. Remote Sens. 13 (8), 20.
Pulido-Bosch, A., Delgado, J., Sola, F., Vallejos, A., Vicente, F., Lopez-Sanchez, J.M., Mallorqui, J.J., 2012. Identification of potential subsidence related to pumping in the Almeria basin (SE Spain). Hydrol. Process. 26 (5), 731–740.
Qu, F.F., Lu, Z., Zhang, Q., Bawden, G.W., Kim, J.W., Zhao, C.Y., Qu, W., 2015. Mapping ground deformation over Houston-Galveston, Texas using multi-temporal InSAR. Remote Sens. Environ. 169, 290–306.
Qu, F.F., Zhang, Q., Lu, Z., Zhao, C.Y., Yang, C.S., Zhang, J., 2014. Land subsidence and ground fissures in Xi'an, China 2005–2012 revealed by multi-band InSAR time-series analysis. Remote Sens. Environ. 155, 366–376.
Radman, A., Akhoondzadeh, M., Hosseiny, B., 2021. Integrating InSAR and deep-learning for modeling and predicting subsidence over the adjacent area of Lake Urmia,Iran. Gisci. Remote Sens. 58 (8), 1413–1433.
Radutu, A., Nedelcu, I., Gogu, C.R., 2017. An overview of ground surface displacements generated by groundwater dynamics, revealed by InSAR techniques. In: Urban Subsurface Planning and Management Week (SUB-URBAN). Procedia Engineering. Elsevier, Tech Univ Civil Engn Bucharest, Groundwater Engn Res Ctr, Bucharest, ROMANIA, pp. 119–126.
Rahmani, Y., Ahmadi, F.F., 2018. Application of InSAR in measuring Earth's surface deformation caused by groundwater extraction and modeling its behavior using time series analysis by artificial neural networks. Acta Geophysica 66 (5), 1171–1184.
Ramos, F.L.G., de Miranda, F.P., Trouve, E., Soler, L., Ieee, 2014. Urban subsidence as a local response of Amazonas river flooding observed by satellite SAR interferometry. In: IEEE Joint International Geoscience and Remote Sensing Symposium (IGARSS) / 35th Canadian Symposium on Remote Sensing. IEEE International Symposium on Geoscience and Remote Sensing IGARSS. Ieee, Quebec City, CANADA, pp. 628–631.
Ranjgar, B., Razavi-Termeh, S.V., Foroughnia, F., Sadeghi-Niaraki, A., Perissin, D., 2021. Land subsidence susceptibility mapping using persistent Scatterer SAR interferometry technique and optimized hybrid machine learning algorithms. Remote Sens. 13 (7), 24.
Raspini, F., Bianchini, S., Ciampalini, A., Del Soldato, M., Montalti, R., Solari, L., Tofani, V., Casagli, N., 2019. Persistent scatterers continuous streaming for landslide monitoring and mapping: the case of the Tuscany region (Italy). Landslides 16 (10), 2033–2044.
Raspini, F., Bianchini, S., Ciampalini, A., Del Soldato, M., Solari, L., Novali, F., Del Conte, S., Rucci, A., Ferretti, A., Casagli, N., 2018. Continuous, semi-automatic monitoring of ground deformation using Sentinel-1 satellites. Sci. Rep. 8.
Raspini, F., Bianchini, S., Moretti, S., Loupasakis, C., Rozos, D., Duro, J., Garcia, M., 2016. Advanced interpretation of interferometric SAR data to detect, monitor and model ground subsidence: outcomes from the ESA-GMES Terrafirma project. Nat. Hazards 83, S155–S181.
Raspini, F., Cigna, F., Moretti, S., 2012. Multi-temporal mapping of land subsidence at basin scale exploiting Persistent Scatterer Interferometry: case study of Gioia Tauro plain (Italy). J. Maps 8 (4), 514–524.
Raspini, F., Loupasakis, C., Rozos, D., Adam, N., Moretti, S., 2014. Ground subsidence phenomena in the Delta municipality region (Northern Greece): geotechnical modeling and validation with Persistent Scatterer Interferometry. Int. J. Appl. Earth Obs. Geoinf. 28, 78–89.
Raspini, F., Loupasakis, C., Rozos, D., Moretti, S., 2013. Advanced interpretation of land subsidence by validating multi-interferometric SAR data: the case study of the Anthemountas basin (Northern Greece). Nat. Hazards Earth Syst. Sci. 13 (10), 2425–2440.
Rateb, A., Hermas, E., 2020. The 2018 long rainy season in Kenya: hydrological changes and correlated land subsidence. Remote Sens. 12 (9), 16.
Raucoules, D., Bourgine, B., de Michele, M., Le Cozannet, G., Closset, L., Bremmer, C., Veldkamp, H., Tragheim, D., Bateson, L., Crosetto, M., Agudo, M., Engdahl, M., 2009. Validation and intercomparison of Persistent Scatterers Interferometry: PSIC4 project results. J. Appl. Geophys. 68 (3), 335–347.
Raucoules, D., Cartannaz, C., Mathieu, F., Midot, D., 2013a. Combined use of space-borne SAR interferometric techniques and ground-based measurements on a 0.3 km (2) subsidence phenomenon. Remote Sens. Environ. 139, 331–339.
Raucoules, D., Colesanti, C., Carnec, C., 2007. Use of SAR interferometry for detecting and assessing ground subsidence. Compt. Rendus Geosci. 339 (5), 289–302.
Raucoules, D., Le Cozannet, G., Woppelmann, G., de Michele, M., Gravelle, M., Daag, A., Marcos, M., 2013b. High nonlinear urban ground motion in Manila (Philippines) from 1993 to 2010 observed by DInSAR: implications for sea-level measurement. Remote Sens. Environ. 139, 386–397.
Raucoules, D., Le Mouelic, S., Carnec, C., Maisons, C., King, C., 2003a. Urban subsidence in the city of Prato (Italy) monitored by satellite radar interferometry. Int. J. Remote Sens. 24 (4), 891–897.
Raucoules, D., Maisons, C., Camec, C., Le Mouelic, S., King, C., Hosford, S., 2003b. Monitoring of slow ground deformation by ERS radar interferometry on the Vauvert salt mine (France) - Comparison with ground-based measurement. Remote Sens. Environ. 88 (4), 468–478.
Raymond, D., Rudant, J.P., 1997. ERS-1-SAR interferometry: potential and limits for mining subsidence detection. In: 3rd ERS Symposium on Space at the Service of Our Environment. Esa Special Publications. European Space Agency, Florence, Italy, pp. 541–544.
Reichenbach, P., Rossi, M., Malamud, B.D., Mihir, M., Guzzetti, F., 2018. A review of statistically-based landslide susceptibility models. Earth Sci. Rev. 180, 60–91.
Roa, Y., Rosell, P., Solarte, A., Euillades, L., Carballo, F., García, S., Euillades, P., 2021. First assessment of the interferometric capabilities of SAOCOM-1A: new results over the Domuyo Volcano, Neuquén Argentina. J. S. Am. Earth Sci. 106, 102882.
Robson, G., Treitz, P., Lamoureux, S.F., Murnaghan, K., Brisco, B., 2021. Seasonal surface subsidence and frost heave detected by C-band DInSAR in a High Arctic Environment, Cape Bounty, Melville Island, Nunavut, Canada. Remote Sens. 13 (13), 21.
Roccheggiani, M., Piacentini, D., Tirincanti, E., Perissin, D., Menichetti, M., 2019. Detection and monitoring of tunneling induced ground movements using Sentinel-1 SAR Interferometry. Remote Sens. 11 (6), 14.
Rosen, P., Hensley, S., Shaffer, S., Edelstein, W., Kim, Y., Kumar, R., Misra, T., Bhan, R., Sagi, R., 2017. The NASA-ISRO SAR (NISAR) mission dual-band radar instrument preliminary design. In: 2017 IEEE international geoscience and remote sensing symposium (IGARSS). IEEE, pp. 3832–3835.
Rosen, P.A., Gurrola, E., Sacco, G.F., Zebker, H., 2012. The InSAR scientific computing environment, EUSAR 2012. In: 9th European conference on synthetic aperture radar. VDE, pp. 730–733.
Rosen, P.A., Hensley, S., Peltzer, G., Simons, M., 2004. Updated repeat orbit interferometry package released. Eos, Trans. Am. Geophys. Union 85 (5), 47.
Rosi, A., Agostini, A., Tofani, V., Casagli, N., 2014. A procedure to map subsidence at the regional scale using the persistent scatterer interferometry (PSI) technique. Remote Sens. 6 (11), 10510–10522.
Rosi, A., Tofani, V., Agostini, A., Tanteri, L., Tacconi Stefanelli, C., Catani, F., Casagli, N., 2016. Subsidence mapping at regional scale using persistent scatters interferometry (PSI): the case of Tuscany region (Italy). Int.J. Appl. Earth Observ. Geoinform. 52, 328–337.
Rotter, P., Muron, W., 2021. Automatic detection of subsidence troughs in SAR. IEEE Geosci. Remote Sens. Lett. 18 (1), 82–86.
Rouyet, L., Lauknes, T.R., Christiansen, H.H., Strand, S.M., Larsen, Y., 2019. Seasonal dynamics of a permafrost landscape, Adventdalen, Svalbard, investigated by InSAR. Remote Sens. Environ. 231, 17.
Ruiz-Constan, A., Ruiz-Armenteros, A.M., Galindo-Zaldivar, J., Lamas-Fernandez, F., Sousa, J.J., de Galdeano, C.S., Pedrera, A., Martos-Rosillo, S., Cuenca, M.C., Delgado, J.M., Hanssen, R.F., Gil, A.J., 2017. Factors determining subsidence in urbanized floodplains: evidence from MT-InSAR in Seville (southern Spain). Earth Surf. Process. Landf. 42 (14), 2484–2497.
Sadeghi, Z., Zoej, M.J.V., Dehghani, M., Chang, N.B., 2012. Enhanced algorithm based on persistent scatterer interferometry for the estimation of high-rate land subsidence. J. Appl. Remote. Sens. 6, 15.
Samsonov, S., d'Oreye, N., Smets, B., 2013. Ground deformation associated with post-mining activity at the French-german border revealed by novel InSAR time series method. Int. J. Appl. Earth Obs. Geoinf. 23, 142–154.
Samsonov, S.V., d'Oreye, N., Gonzalez, P.J., Tiampo, K.F., Ertolahti, L., Clague, J.J., 2014. Rapidly accelerating subsidence in the Greater Vancouver region from two decades of ERS-ENVISAT-RADARSAT-2 DInSAR measurements. Remote Sens. Environ. 143, 180–191.
Samsonov, S.V., Feng, W.P., Fialko, Y., 2017. Subsidence at Cerro Prieto Geothermal Field and postseismic slip along the Indiviso fault from 2011 to 2016 RADARSAT-2 DInSAR time series analysis. Geophys. Res. Lett. 44 (6), 2716–2724.
Sanabria, M.P., Guardiola-Albert, C., Tomas, R., Herrera, G., Prieto, A., Sanchez, H., Tessitore, S., 2014. Subsidence activity maps derived from DInSAR data: Orihuela case study. Nat. Hazards Earth Syst. Sci. 14 (5), 1341–1360.
Sandwell, D., Mellors, R., Tong, X., Wei, M., Wessel, P., 2011. Open Radar Interferometry Software for Mapping Surface Deformation. Wiley Online Library.
Sarychikhina, O., Glowacka, E., Mellors, R., Vidal, F.S., 2011. Land subsidence in the Cerro Prieto Geothermal Field, Baja California, Mexico, from 1994 to 2005 an integrated analysis of DInSAR, leveling and geological data. J. Volcanol. Geotherm. Res. 204 (1–4), 76–90.
Sarychikhina, O., Glowacka, E., Suarez-Vidal, F., Mellors, R., 2010. DInSAR analysis of land subsidence caused by geothermal fluid exploitation in the Mexicali Valley, BC, Mexico. In: 8th International Symposium on Land Subsidence. IAHS Publication. Int Assoc Hydrological Sciences, Natl Autonomous Univ Mexico, Santiago de Queretaro, MEXICO, 268-+.
Schaefer, L., Wang, T., Escobar-Wolf, R., Oommen, T., Lu, Z., Kim, J., Lundgren, P., Waite, G., 2017. Three-dimensional displacements of a large volcano flank movement during the May 2010 eruptions at Pacaya Volcano,Guatemala. Geophys. Res. Lett. 44 (1), 135–142.
Schmidt, D.A., Bürgmann, R., 2003. Time-dependent land uplift and subsidence in the Santa Clara valley, California, from a large interferometric synthetic aperture radar data set. J. Geophys.Res.Solid Earth 108 (B9).
Scoular, J., Ghail, R., Mason, P., Lawrence, J., Bellhouse, M., Holley, R., Morgan, T., 2020. Retrospective InSAR analysis of East London during the construction of the Lee Tunnel. Remote Sens. 12 (5), 19.
Semple, A.G., Pritchard, M.E., Lohman, R.B., 2017. An incomplete inventory of suspected human-induced surface deformation in North America detected by Satellite Interferometric Synthetic-Aperture Radar. Remote Sens. 9 (12), 26.
Shi, L.Y., Gong, H.L., Chen, B.B., Zhou, C.F., 2020a. Land subsidence prediction induced by multiple factors using machine learning method. Remote Sens. 12 (24), 17.
Shi, W., Chen, G., Meng, X.M., Jiang, W.Y., Chong, Y., Zhang, Y., Dong, Y., Zhang, M.S., 2020b. Spatial-temporal evolution of land subsidence and rebound over Xi'an in Western China revealed by SBAS-InSAR analysis. Remote Sens. 12 (22), 21.
Shi, X.G., Zhang, S.C., Jiang, M., Pei, Y.Y., Qu, T.T., Xu, J.H., Yang, C., 2021. Spatial and temporal subsidence characteristics in Wuhan (China), during 2015–2019, inferred from Sentinel-1 synthetic aperture radar (SAR) interferometry. Nat. Hazards Earth Syst. Sci. 21 (8), 2285–2297.
Shi, Y., Tang, Y.M., Lu, Z., Kim, J.W., Peng, J.H., 2019. Subsidence of sinkholes in Wink, Texas from 2007 to 2011 detected by time-series InSAR analysis. Geomat. Nat. Haz. Risk 10 (1), 1125–1138.
Shirzaei, M., Bürgmann, R., 2018. Global climate change and local land subsidence exacerbate inundation risk to the San Francisco Bay Area. Sci. Adv. 4 (3), eaap9234.

Showstack, R., 2014. Sentinel satellites initiate new era in earth observation. Eos, Trans. Am.Geophys.Union 95 (26), 239–240.
Shviro, M., Haviv, I., Baer, G., 2017. High-resolution InSAR constraints on flood-related subsidence and evaporite dissolution along the Dead Sea shores: interplay between hydrology and rheology. Geomorphology 293, 53–68.
Sillerico, E., Ezquerro, P., Marchamalo, M., Herrera, G., Duro, J., Martinez, R., 2015. Monitoring ground subsidence in urban environments: M-30 tunnels under Madrid City (Spain). Ingenieria E Investigacion 35 (2), 30–35.
Simmons, B.S., Wempen, J.M., 2021. Quantifying relationships between subsidence and longwall face advance using DInSAR. Int. J. Min. Sci. Technol. 31 (1), 91–94.
Smith, L.C., 2002. Emerging applications of interferometric synthetic aperture radar (InSAR) in geomorphology and hydrology. Ann. Assoc. Am. Geogr. 92 (3), 385–398.
Smith, R., Knight, R., 2019. Modeling land subsidenceusing InSAR and. Water Resour. Res. 55 (4), 2801–2819.
Smith, R., Li, J.W., 2021. Modeling elastic and inelastic pumping-induced deformation with incomplete water level records in Parowan Valley,Utah. J. Hydrol. 601, 9.
Smith, R.G., Knight, R., Chen, J., Reeves, J.A., Zebker, H.A., Farr, T., Liu, Z., 2017. Estimating the permanent loss of groundwater storage in the southern San Joaquin Valley,California. Water Resour. Res. 53 (3), 2133–2148.
Solari, L., Ciampalini, A., Raspini, F., Bianchini, S., Moretti, S., 2016. PSInSAR analysis in the Pisa Urban Area (Italy): a case study of subsidence related to stratigraphical factors and urbanization. Remote Sens. 8 (2), 120.
Solari, L., Ciampalini, A., Raspini, F., Bianchini, S., Zinno, I., Bonano, M., Manunta, M., Moretti, S., Casagli, N., 2017. Combined use of C-and X-Band SAR data for subsidence monitoring in an. Geosciences 7 (2), 21.
Solari, L., Del Soldato, M., Bianchini, S., Ciampalini, A., Ezquerro, P., Montalti, R., Raspini, F., Moretti, S., 2018. From ERS 1/2 to Sentinel-1: subsidence monitoring in Italy in the last two decades. Front. Earth Sci. 6, 149.
Solari, L., Del Soldato, M., Raspini, F., Barra, A., Bianchini, S., Confuorto, P., Casagli, N., Crosetto, M., 2020. Review of satellite interferometry for landslide detection in Italy. Remote Sens. 12 (8), 1351.
Sowter, A., Amat, M.B., Cigna, F., Marsh, S., Athab, A., Alshammari, L., 2016. Mexico City land subsidence in 2014–2015 with Sentinel-1 IW TOPS: results using the Intermittent SBAS (ISBAS) technique. Int. J. Appl. Earth Obs. Geoinf. 52, 230–242.
Stow, R.J., Wright, P., 1997. Mining subsidence land survey by SAR interferometry. In: 3rd ERS Symposium on Space at the Service of Our Environment. Esa Special Publications. European Space Agency, Florence, Italy, pp. 525–530.
Stramondo, S., Bozzano, F., Marra, F., Wegmuller, U., Cinti, F.R., Moro, M., Saroli, M., 2008. Subsidence induced by urbanisation in the city of Rome detected by advanced InSAR technique and geotechnical investigations. Remote Sens. Environ. 112 (6), 3160–3172.
Stramondo, S., Saroli, M., Tolomei, C., Moro, M., Doumaz, F., Pesci, A., Loddo, F., Baldi, P., Boschi, E., 2007. Surface movements in Bologna (Po Plain-Italy) detected by multitemporal DInSAR. Remote Sens. Environ. 110 (3), 304–316.
Strassberg, G., Scanlon, B.R., Chambers, D., 2009. Evaluation of groundwater storage monitoring with the GRACE satellite: case study of the High Plains aquifer, Central United States. Water Resour. Res. 45 (5).
Strozzi, T., Antonova, S., Gunther, F., Matzler, E., Vieira, G., Wegmuller, U., Westermann, S., Bartsch, A., 2018. Sentinel-1 SAR interferometry for surface deformation monitoring in low-land permafrost areas. Remote Sens. 10 (9), 20.
Strozzi, T., Caduff, R., Wegmuller, U., Raetzo, H., Hauser, M., 2017. Widespread surface subsidence measured with satellite SAR interferometry in the swiss alpine range associated with the construction of the Gotthard Base Tunnel. Remote Sens. Environ. 190, 1–12.
Strozzi, T., Delaloye, R., Poffet, D., Hansmann, J., Loew, S., 2011. Surface subsidence and uplift above a headrace tunnel in metamorphic basement rocks of the Swiss Alps as detected by satellite SAR interferometry. Remote Sens. Environ. 115 (6), 1353–1360.
Strozzi, T., Farina, P., Corsini, A., Ambrosi, C., Thuring, M., Zilger, J., Wiesmann, A., Wegmuller, U., Werner, C., 2005. Survey and monitoring of landslide displacements by means of L-band satellite SAR interferometry. Landslides 2 (3), 193–201.
Strozzi, T., Kääb, A., Frauenfelder, R., 2004. Detecting and quantifying mountain permafrost creep from in situ inventory, space-borne radar interferometry and airborne digital photogrammetry. Int. J. Remote Sens. 25 (15), 2919–2931.
Strozzi, T., Teatini, P., Tosi, L., Wegmuller, U., Werner, C., 2013. Land subsidence of natural transitional environments by satellite radar interferometry on artificial reflectors. J. Geophys.Res.Earth Surf. 118 (2), 1177–1191.
Strozzi, T., Tosi, L., Teatini, P., Werner, C., Wegmuller, U., 2009. Monitoring land subsidence within the Venice lagoon with SAR interferometry on thrihedral cornel reflector. In: IEEE International Geoscience and Remote Sensing Symposium. IEEE International Symposium on Geoscience and Remote Sensing IGARSS. Ieee, Cape Town, SOUTH AFRICA.
Strozzi, T., Wegmuller, U., Tosi, L., Bitelli, G., Spreckels, V., 2001. Land subsidence monitoring with differential SAR interferometry. Photogramm. Eng. Remote. Sens. 67 (11), 1261–1270.
Strozzi, T., Wegmuller, U., Werner, C.L., Wiesmann, A., Spreckels, V., 2003. JERS SAR interferometry for land subsidence monitoring. IEEE Trans. Geosci. Remote Sens. 41 (7), 1702–1708.
Suganthi, S., Elango, L., Subramanian, S.K., 2017. Microwave D-InSAR technique for assessment of land subsidence in Kolkata city,India, 10 (21), 10.
Sun, H., Zhang, Q., Zhao, C.Y., Yang, C.S., Sun, Q.F., Chen, W.R., 2017. Monitoring land subsidence in the southern part of the lower Liaohe plain, China with a multi-track PS-InSAR technique. Remote Sens. Environ. 188, 73–84.
Sun, Q.S., Jiang, L.M., Jiang, M., Lin, H., Ma, P.F., Wang, H.S., 2018. Monitoring coastal reclamation subsidence in Hong Kong with distributed scatterer interferometry. Remote Sens. 10 (11), 23.
Suresh, D., Yarrakula, K., 2018. Subsidence monitoring techniques in coal mining: Indian scenario. Ind. J. Geo-Marine Sci. 47 (10), 1918–1933.
Takeuchi, S., Yamada, S., 2002. Comparison of InSAR capability for land subsidence detection between C-band and L-band SAR. In: IEEE International Geoscience and Remote Sensing Symposium (IGARSS 2002)/24th Canadian Symposium on Remote Sensing. IEEE International Symposium on Geoscience and Remote Sensing (IGARSS). Ieee, Toronto, Canada, pp. 2379–2381.
Tang, W., Liao, M.S., Yuan, P., 2016. Atmospheric correction in time-series SAR interferometry for land surface deformation mapping - a case study of Taiyuan, China. Adv. Space Res. 58 (3), 310–325.
Tang, W., Yuan, P., Liao, M.S., Balz, T., 2018. Investigation of ground deformation in Taiyuan Basin, China from 2003 to 2010, with atmosphere-corrected time series InSAR. Remote Sens. 10 (9), 22.
Tang, W., Zhan, W., Jin, B.W., Motagh, M., Xu, Y.B., 2021. Spatial variability of relative sea-level rise in Tianjin, China: insight from InSAR, GPS, and Tide-Gauge observations. Ieee J. Select. Top. Appl. Earth Observ. Remote Sens. 14, 2621–2633.
Taravatrooy, N., Nikoo, M.R., Sadegh, M., Parvinnia, M., 2018. A hybrid clustering-fusion methodology for land subsidence estimation. Nat. Hazards 94 (2), 905–926.
Teatini, P., Tosi, L., Strozzi, T., Carbognin, L., Cecconi, G., Rosselli, R., Libardo, S., 2012. Resolving land subsidence within the Venice Lagoon by persistent scatterer SAR interferometry. Phys. Chem. Earth 40–41, 72–79.
Teatini, P., Tosi, L., Strozzi, T., Carbognin, L., Wegmüller, U., Rizzetto, F., 2005. Mapping regional land displacements in the Venice coastland by an integrated monitoring system. Remote Sens. Environ. 98 (4), 403–413.
Temtime, T., Biggs, J., Lewi, E., Hamling, I., Wright, T., Ayele, A., 2018. Spatial and temporal patterns of deformation at the Tendaho geothermal prospect, Ethiopia. J. Volcanol. Geotherm. Res. 357, 56–67.
Terranova, C., Ventura, G., Vilardo, G., 2015. Multiple causes of ground deformation in the Napoli metropolitan area (Italy) from integrated Persistent Scatterers DinSAR, geological, hydrological, and urban infrastructure data. Earth Sci. Rev. 146, 105–119.
Terzaghi, K., Peck, R.B., Mesri, G., 1996. Soil Mechanics in Engineering Practice. John Wiley & Sons.
Tesauro, M., Berardino, P., Lanari, R., Sansosti, E., Fornaro, G., Franceschetti, G., 2000. Urban subsidence inside the city of Napoli (Italy) observed by satellite radar interferometry. Geophys. Res. Lett. 27 (13), 1961–1964.
Tessitore, S., Fernandez-Merodo, J., Herrera, G., Tomas, R., Ramondini, M., Sanabria, M., Duro, J., Mulas, J., Calcaterra, D., 2016. Comparison of water-level, extensometric, DInSAR and simulation data for quantification of subsidence in Murcia City (SE Spain). Hydrogeol. J. 24 (3), 727–747.
Tomás, R., Garcia-Barba, J., Cano, M., Sanabria, M.P., Ivorra, S., Duro, J., Herrera, G., 2012. Subsidence damage assessment of a gothic church using Differential Interferometry and field data. Struct. Health Monit. 11 (6), 751–762.
Tomas, R., Herrera, G., Delgado, J., Lopez-Sanchez, J.M., Mallorqui, J.J., Mulas, J., 2010a. A ground subsidence study based on DInSAR data: calibration of soil parameters and subsidence prediction in Murcia City (Spain). Eng. Geol. 111 (1–4), 19–30.
Tomas, R., Herrera, G., Lopez-Sanchez, J.M., Vicente, F., Cuenca, A., Mallorqui, J.J., 2010b. Study of the land subsidence in Orihuela City (SE Spain) using PSI data: distribution, evolution and correlation with conditioning and triggering factors. Eng. Geol. 115 (1–2), 105–121.
Tomas, R., Herrera, G.H., Cooksley, G., Mulas, J., 2011. Persistent Scatterer Interferometry subsidence data exploitation using spatial tools: the Vega Media of the Segura River Basin case study. J. Hydrol. 400 (3–4), 411–428.
Tomás, R., Li, Z., 2017. Earth Observations for Geohazards: Present and Future Challenges. Multidisciplinary Digital Publishing Institute.
Tomás, R., Márquez, Y., Lopez-Sanchez, J.M., Delgado, J., Blanco, P., Mallorquí, J.J., Martínez, M., Herrera, G., Mulas, J., 2005. Mapping ground subsidence induced by aquifer overexploitation using advanced differential SAR interferometry: Vega Media of the Segura River (SE Spain) case study. Remote Sens. Environ. 98 (2), 269–283.
Tomás, R., Romero, R., Mulas, J., Marturià, J.J., Mallorquí, J.J., Lopez-Sanchez, J.M., Herrera, G., Gutiérrez, F., González, P.J., Fernández, J., 2014. Radar interferometry techniques for the study of ground subsidence phenomena: a review of practical issues through cases in Spain. Environ. Earth Sci. 71 (1), 163–181.
Tosi, L., Da Lio, C., Strozzi, T., Teatini, P., 2016. Combining L-and X-band SAR interferometry to assess ground displacements in heterogeneous coastal environments: the Po River Delta and Venice Lagoon,Italy. Remote Sens. 8 (4), 308.
Tosi, L., Da Lio, C., Teatini, P., Strozzi, T., 2018. Land subsidence in coastal environments: knowledge advance in the Venice Coastland by TerraSAR-X PSI. Remote Sens. 10 (8), 17.
Tosi, L., Strozzi, T., Da Lio, C., Teatini, P., 2015. Regional and local land subsidence at the Venice coastland by TerraSAR-X PSI, Prevention and Mitigation of Natural and Anthropogenic Hazards due to Land Subsidence. In: Proceedings of the International Association of Hydrological Sciences (IAHS). Copernicus Gesellschaft Mbh, Nagoya, JAPAN, pp. 199–205.
Trenberth, K.E., 2011. Changes in precipitation with climate change. Clim. Res. 47 (1–2), 123–138.
Tung, H., Hu, J.C., 2012. Assessments of serious anthropogenic land subsidence in Yunlin County of Central Taiwan from 1996 to 1999 by Persistent Scatterers InSAR. Tectonophysics 578, 126–135.
Umarhadi, D.A., Avtar, R., Widyatmanti, W., Johnson, B.A., Yunus, A.P., Khedher, K.M., Singh, G., 2021. Use of multifrequency (C-band and L-band) SAR data to monitor peat subsidence based on time-series SBAS InSAR technique. Land Degrad. Dev. 32 (16), 4779–4794.

Unlu, T., Akcin, H., Yilmaz, O., 2013. An integrated approach for the prediction of subsidence for coal mining basins. Eng. Geol. 166, 186–203.
US National Research Council, 1991. Mitigating Losses From Land Subsidence in the United States. National Academy Press, Washington DC.
Ustun, A., Tusat, E., Yalvac, S., Ozkan, I., Eren, Y., Ozdemir, A., Bildirici, I.O., Ustuntas, T., Kirtiloglu, O.S., Mesutoglu, M., Doganalp, S., Canaslan, F., Abbak, R.A., Avsar, N.B., Simsek, F.F., 2015. Land subsidence in Konya Closed Basin and its spatio-temporal detection by GPS and DInSAR. Environ. Earth Sci. 73 (10), 6691–6703.
Vadivel, S.K.P., Kim, D.J., Jung, J., Cho, Y.K., Han, K.J., Jeong, K.Y., 2019. Sinking Tide Gauge revealed by space-borne InSAR: implications for sea level acceleration at PohangSouth Korea. Remote Sens. 11 (3), 13.
van der Horst, T., Rutten, M.M., van de Giesen, N.C., Hanssen, R.F., 2018. Monitoring land subsidence in Yangon, Myanmar using Sentinel-1 persistent scatterer interferometry and assessment of driving mechanisms. Remote Sens. Environ. 217, 101–110.
van Thienen-Visser, K., Breunese, J.J.T.L.E., 2015. Induced seismicity of the Groningen gas field. History and recent developments. 34 (6), 664–671.
Vervoort, A., Declercq, P.Y., 2017. Surface movement above old coal longwalls after mine closure. Int. J. Min. Sci. Technol. 27 (3), 481–490.
Vervoort, A., Declercq, P.Y., 2018. Upward surface movement above deep coal mines after closure and flooding of underground workings. Int. J. Min. Sci. Technol. 28 (1), 53–59.
Vieira, E., Gomes, J., 2009. A comparison of Scopus and Web of Science for a typical university. Scientometrics 81 (2), 587–600.
Wang, A.G., Sun, Z.Y., 2014. Multi-geodesy techniques data fusing and analyzing for land subsidence monitoring. In: 3rd International Workshop on Earth Observation and Remote Sensing Applications (EORSA). International Workshop on Earth Observation and Remote Sensing Applications. Ieee, Changsha, PEOPLES R CHINA.
Wang, H., Wright, T.J., Yu, Y.P., Lin, H., Jiang, L.L., Li, C.H., Qiu, G.X., 2012. InSAR reveals coastal subsidence in the Pearl River Delta,China. Geophys. J. Int. 191 (3), 1119–1128.
Wang, H.Q., Feng, G.C., Xu, B., Yu, Y.P., Li, Z.W., Du, Y.A., Zhu, J.J., 2017. Deriving spatio-temporal development of ground subsidence due to subway construction and operation in delta regions with PS-InSAR Data: a Case Study in Guangzhou,China. Remote Sens. 9 (10), 19.
Wang, L., Jiang, K.G., Wei, T., 2021a. Development of a new inversion method for detecting spatiotemporal characteristics of coal mines based on earth observation technology. Int. J. Appl. Earth Obs. Geoinf. 100, 10.
Wang, L., Li, N., Zhang, X.N., Wei, T., Chen, Y.F., Zha, J.F., 2018. Full parameters inversion model for mining subsidence prediction using simulated annealing based on single line of sight D-InSAR. Environ. Earth Sci. 77 (5), 11.
Wang, L., Teng, C.Q., Jiang, K.G., Jiang, C., Zhu, S.J., 2022. D-InSAR monitoring method of mining subsidence based on Boltzmann and its application in building mining damage assessment. KSCE J. Civ. Eng. 26 (1), 353–370.
Wang, Z.Y., Li, L., Yu, Y.R., Wang, J., Li, Z.J., Liu, W., 2021b. A novel phase unwrapping method used for monitoring the land subsidence in coal mining area based on U-Net Convolutional Neural Network. Front. Earth Sci. 9, 13.
Watson, K.M., Bock, Y., Sandwell, D.T., 2002. Satellite interferometric observations of displacements associated with seasonal groundwater in the Los Angeles basin. J. Geophys. Res. Solid Earth 107 (B4), 17.
Wegmuller, U., Werner, C., Strozzi, T., Wiesmann, A., ieee, 2004. Monitoring mining induced surface deformation. In: IEEE International Geoscience and Remote Sensing Symposium. IEEE International Symposium on Geoscience and Remote Sensing IGARSS. Ieee, Anchorage, AK, pp. 1933–1935.
Wei, M., Chao, M., 2018. Soil moisture retrievals in aeolian sand mining areas using temporal, single-polarization, high-resolution SAR. Frequenz 72 (11–12), 547–560.
Wempen, J.M., McCarter, M.K., 2017. Comparison of L-band and X-band differential interferometric synthetic aperture radar for mine subsidence monitoring in Central Utah. Int. J. Min. Sci. Technol. 27 (1), 159–163.
Werner, C., Wegmuller, U., Strozzi, T., Wiesmann, A., 2003. In: Interferometric point target analysis for deformation mapping, Geoscience and Remote Sensing Symposium, 2003. IGARSS'03. Proceedings. 2003 IEEE International. IEEE, pp. 4362–4364.
Werner, C., Wegmüller, U., Strozzi, T., Wiesmann, A., 2000. In: Gamma SAR and interferometric processing software, Proceedings of the ers-envisat symposium, gothenburg, sweden. Citeseer, p. 1620.
Wnuk, K., Walton, G., Zhou, W., 2019. Four-dimensional filtering of InSAR persistent scatterers elucidates subsidence induced by tunnel excavation in the Sri Lankan highlands. J. Appl. Remote. Sens. 13 (3), 16.
Woo, K.S., Eberhardt, E., Rabus, B., Stead, D., Vyazmensky, A., 2012. Integration of field characterisation, mine production and InSAR monitoring data to constrain and calibrate 3-D numerical modelling of block caving-induced subsidence. Int. J. Rock Mech. Min. Sci. 53, 166–178.
Woppelmann, G., Le Cozannet, G., de Michele, M., Raucoules, D., Cazenave, A., Garcin, M., Hanson, S., Marcos, M., Santamaria-Gomez, A., 2013. Is land subsidence increasing the exposure to sea level rise in Alexandria, Egypt? Geophys. Res. Lett. 40 (12), 2953–2957.
Xing, X.M., Zhu, J.J., Wang, Y.Z., Yang, Y.F., Ieee, 2010. A new method of CRInSAR and PSInSAR combined calculation. In: 6th International Conference on Wireless Communications, Networking and Mobile Computing (WICOM). International Conference on Wireless Communications Networking and Mobile Computing-WiCOM. Ieee, Chengdu, PEOPLES R CHINA.
Xiuming, J., Chao, M., Anyuan, Z., 2008. Environmental investigation and evaluation of land subsidence in the Datong coalfield based on InSAR technology. Acta Geologica Sinica-English Edition 82 (5), 1035–1044.
Xu, B., Feng, G., Li, Z., Wang, Q., Wang, C., Xie, R., 2016. Coastal subsidence monitoring associated with land reclamation using the point target based SBAS-INSAR method: a case study of Shenzhen,China. Remote Sens. 8 (8), 652.
Xu, X.B., Ma, C., Lian, D.J., Zhao, D.Z., 2020. Inversion and analysis of mining subsidence by integrating DInSAR, offset tracking,and PIM technology. J. Sens. 2020, 15.
Xu, X.H., Sandwell, D.T., Tymofyeyeva, E., Gonzalez-Ortega, A., Tong, X.P., 2017. Tectonic and anthropogenic deformation at the cerro prieto geothermal step-over revealed by Sentinel-1A InSAR. IEEE Trans. Geosci. Remote Sens. 55 (9), 5284–5292.
Xu, X.Y., Liu, L., Schaefer, K., Michaelides, R., 2021. Comparison of surface subsidence measured by airborne and satellite InSAR over permafrost areas near Yellowknife Canada. Earth Space Sci. 8 (6), 15.
XunChun, W., Yue, Z., XingGe, J., Peng, Z., 2011. A dynamic prediction method of deep mining subsidence combines d-Insar technique. Procedia Environ. Sci. 10, 2533–2539.
Yalvac, S., 2020. Validating InSAR-SBAS results by means of different GNSS analysis techniques in medium- and high-grade deformation areas. Environ. Monit. Assess. 192 (2), 12.
Yan, Y.J., Doin, M.P., Lopez-Quiroz, P., Tupin, F., Fruneau, B., Pinel, V., Trouve, E., 2012. Mexico City subsidence measured by InSAR Time Series: jointanalysis using PS and SBAS Approaches. Ieee J. Select. Top. Appl. Earth Observ. Remote Sens. 5 (4), 1312–1326.
Yang, C.S., Lu, Z., Zhang, Q., Liu, R.C., Ji, L.Y., Zhao, C.Y., 2019. Ground deformation and fissure activity in Datong basin, China 2007–2010 revealed by multi-track InSAR. Geomatics Nat. Haz. Risk 10 (1), 465–482.
Yang, C.S., Zhang, Q., Zhao, C.Y., Wang, Q.L., Ji, L.Y., 2014. Monitoring land subsidence and fault deformation using the small baseline subset InSAR technique: a case study in the Datong Basin, China. J. Geodyn. 75, 34–40.
Yang, D.D., Qiu, H.J., Ma, S.Y., Liu, Z.J., Du, C., Zhu, Y.R., Cao, M.M., 2022. Slow surface subsidence and its impact on shallow loess landslides in a coal mining area. Catena 209, 15.
Yang, Q., Ke, Y.H., Zhang, D.Y., Chen, B.B., Gong, H.L., Lv, M.Y., Zhu, L., Li, X.J., 2018. Multi-scale analysis of the relationship between land subsidence and buildings: a case study in an Eastern Beijing urban areausing the PS-InSAR. Remote Sens. 10 (7), 20.
Yang, Z.F., Li, Z.W., Zhu, J.J., Preusse, A., Yi, H.W., Hu, J., Feng, G.C., Papst, M., 2017a. Retrieving 3-D large displacements of mining areas from a single amplitude pair of SAR using offset tracking. Remote Sens. 9 (4), 18.
Yang, Z.F., Li, Z.W., Zhu, J.J., Preusse, A., Yi, H.W., Wang, Y.J., Papst, M., 2017b. An extension of the InSAR-based probability integral method and its application for predicting 3-D. IEEE Trans. Geosci. Remote Sens. 55 (7), 3835–3845.
Yang, Z.F., Li, Z.W., Zhu, J.J., Yi, H.W., Hu, J., Feng, G.C., 2017c. Deriving dynamic subsidence of coal mining areas using InSAR and. Remote Sens. 9 (2), 19.
Yastika, P.E., Shimizu, N., Abidin, H.Z., 2019. Monitoring of long-term land subsidence from 2003 to 2017 in coastal area of Semarang, Indonesia by SBAS DInSAR analyses using Envisat-ASAR, ALOS-PALSAR, and Sentinel-1A SAR data. Adv. Space Res. 63 (5), 1719–1736.
Yerro, A., Corominas, J., Monells, D., Mallorqui, J.J., 2014. Analysis of the evolution of ground movements in a low densely urban area by means of DInSAR technique. Eng. Geol. 170, 52–65.
Yin, J., Zhao, Q., Yu, D.P., Lin, N., Kubanek, J., Ma, G.Y., Liu, M., Pepe, A., 2019. Long-term flood-hazard modeling for coastal areas using InSAR measurements and a hydrodynamic model: the case study of Lingang New City, Shanghai. J. Hydrol. 571, 593–604.
Yu, B., Liu, G.X., Li, Z.L., Zhang, R., Jia, H.G., Wang, X.W., Cai, G.L., 2013. Subsidence detection by TerraSAR-X interferometry on a network of natural persistent scatterers and artificial corner reflectors. Comput. Geosci. 58, 126–136.
Yu, W., Gong, H.L., Chen, B.B., Zhou, C.F., Zhang, Q.Q., 2021. Combined GRACE and MT-InSAR to assess the relationship between groundwater storage change and land subsidence in the Beijing-Tianjin-Hebei region. Remote Sens. 13 (18), 24.
Yuan, D.B., Geng, C.X., Zhang, L., Zhang, Z.C., 2021. Application of Gray-Markov. Ieee Access 9, 118716–118725.
Yunjun, Z., Fattahi, H., Amelung, F., 2019. Small baseline InSAR time series analysis: unwrapping error correction and noise reduction. Comput. Geosci. 133, 104331.
Zhang, B., Zhang, L.Z., Yang, H.L., Zhang, Z.J., Tao, J.L., 2016a. Subsidence prediction and susceptibility zonation for collapse above goaf with thick alluvial cover: a case study of the Yongcheng coalfield, Henan Province, China. Bull. Eng. Geol. Environ. 75 (3), 1117–1132.
Zhang, B.W., Wang, R., Deng, Y.K., Ma, P.F., Lin, H., Wang, J.L., 2019a. Mapping the Yellow River Delta land subsidence with multitemporal SAR interferometry by exploiting both persistent and distributed scatterers. ISPRS J. Photogramm. Remote Sens. 148, 157–173.
Zhang, J.Z., Huang, H.J., Bi, H.B., 2015a. Land subsidence in the modern Yellow River Delta based on InSAR time series analysis. Nat. Hazards 75 (3), 2385–2397.
Zhang, L., Lu, Z., Ding, X.L., Jung, H.S., Feng, G.C., Lee, C.W., 2012. Mapping ground surface deformation using temporarily coherent point SAR interferometry: application to Los Angeles Basin. Remote Sens. Environ. 117, 429–439.
Zhang, Q., Zhao, C.Y., Ding, X.L., Chen, Y.Q., Wang, L., Huang, G.W., Yang, C.S., Ding, X. G., Ma, J., 2009. Research on recent characteristics of spatio-temporal evolution and mechanism of Xi'an land subsidence and ground fissure by using GPS and InSAR techniques. Chin. J. Geophys. Chin. Ed. 52 (5), 1214–1222.
Zhang, S.Y., Li, T., Liu, J.N., Liu, Y.W., Shao, L.J., Xia, Y., Ieee, 2007. Urban subsidence observed by InSAR in Tianjin region. In: IEEE International Geoscience and Remote Sensing Symposium (IGARSS). IEEE International Symposium on Geoscience and Remote Sensing IGARSS. Ieee, Barcelona, SPAIN, 2078-+.

Zhang, T.X., Shen, W.B., Wu, W.H., Zhang, B., Pan, Y.J., 2019b. Recent surface deformation in the Tianjin area revealed by Sentinel-1A Data. Remote Sens. 11 (2), 25.
Zhang, X.F., Zhang, H., Wang, C., Tang, Y.X., Zhang, B., Wu, F., Wang, J., Zhang, Z.J., 2020. Active layer thickness retrieval over the Qinghai-Tibet Plateau using Sentinel-1 multitemporal InSAR Monitored Permafrost Subsidence and Temporal-Spatial Multilayer Soil moisture data. Ieee Access 8, 84336–84351.
Zhang, Y.H., Wu, H.A., Kang, Y.H., Zhu, C.G., 2016b. Ground subsidence in the Beijing-Tianjin-Hebei region from 1992 to 2014 revealed by multiple SAR stacks. Remote Sens. 8 (8), 17.
Zhang, Y.H., Zhang, J.X., Wu, H.A., Lu, Z., Sun, G.T., 2011. Monitoring of urban subsidence with SAR interferometric point target analysis: a case study in Suzhou, China. Int. J. Appl. Earth Obs. Geoinf. 13 (5), 812–818.
Zhang, Z.J., Wang, C., Tang, Y.X., Fu, Q.Y., Zhang, H., 2015b. Subsidence monitoring in coal area using time-series InSAR combining persistent scatterers and distributed scatterers. Int. J. Appl. Earth Obs. Geoinf. 39, 49–55.
Zhao, C.Y., Liu, C.J., Zhang, Q., Lu, Z., Yang, C.S., 2018. Deformation of Linfen-Yuncheng Basin (China) and its mechanisms revealed by Pi-RATE InSAR technique. Remote Sens. Environ. 218, 221–230.
Zhao, C.Y., Zhang, Q., Ding, X.L., Lu, Z., Yang, C.S., Qi, X.M., 2009a. Monitoring of land subsidence and ground fissures in Xian, China 2005–2006: mapped by SAR interferometry. Environ. Geol. 58 (7), 1533–1540.
Zhao, Q., Lin, H., Jiang, L.M., Chen, F.L., Cheng, S.L., 2009b. A study of ground deformation in the Guangzhou urban area with persistent scatterer interferometry. Sensors 9 (1), 503–518.
Zhao, R., Li, Z.-W., Feng, G.-C., Wang, Q.-J., Hu, J., 2016. Monitoring surface deformation over permafrost with an improved SBAS-InSAR algorithm: with emphasis on climatic factors modeling. Remote Sens. Environ. 184, 276–287.
Zhou, C.D., Gong, H.L., Zhang, Y.Q., Warner, T.A., Wang, C., 2018. Spatiotemporal evolution of land subsidence in the Beijing Plain 2003–2015 using persistent scatterer interferometry (PSI) with multi-source SAR data. Remote Sens. 10 (4), 20.
Zhou, C.F., Gong, H.L., Chen, B.B., Li, J.W., Gao, M.L., Zhu, F., Chen, W.F., Liang, Y., 2017a. InSAR time-series analysis of land subsidence under different land use types in the Eastern Beijing Plain,China. Remote Sens. 9 (4), 16.
Zhou, C.F., Gong, H.L., Chen, B.B., Zhu, F., Duan, G.Y., Gao, M.L., Lu, W., 2016. Land subsidence under different land use in the eastern Beijing plain, China 2005–2013 revealed by InSAR timeseries analysis. Gisci. Remote Sens. 53 (6), 671–688.
Zhou, L., Guo, J.M., Hu, J.Y., Li, J.W., Xu, Y.F., Pan, Y.J., Shi, M., 2017b. Wuhan surface subsidence analysis in 2015–2016 based on Sentinel-1A data by SBAS-InSAR. Remote Sens. 9 (10), 21.
Zhou, L.F., Zhang, D.R., Wang, J., Huang, Z.Q., Pan, D.L., 2013. Mapping land subsidence related to underground coal fires in the Wuda Coalfield (Northern China) using a small stack of ALOS PALSAR differential interferograms. Remote Sens. 5 (3), 1152–1176.
Zhou, Y., Stein, A., Molenaar, M., 2003. Integrating interferometric SAR data with levelling measurements of land subsidence using geostatistics. Int. J. Remote Sens. 24 (18), 3547–3563.
Zhu, L., Gong, H.L., Chen, Y., Wang, S.F., Ke, Y.H., Guo, G.X., Li, X.J., Chen, B.B., Wang, H.G., Teatini, P., 2020. Effects of Water Diversion Project on groundwater system and land subsidence in Beijing,China. Eng. Geol. 276, 12.
Zhu, L., Gong, H.L., Li, X.J., Wang, R., Chen, B.B., Dai, Z.X., Teatini, P., 2015. Land subsidence due to groundwater withdrawal in the northern Beijing plain, China. Eng. Geol. 193, 243–255.
Zhu, W., Zhang, Q., Ding, X.L., Zhao, C.Y., Yang, C.S., Qu, W., 2013. Recent ground deformation of Taiyuan basin (China) investigated with C-, L-, and X-bands SAR images. J. Geodyn. 70, 28–35.